THE FUNCTIONAL ROLE OF EXTRACELLULAR NUCLEOTIDES IN THE RENAL TUBULE

A thesis submitted

by

Renu M. Vekaria

For the degree of

Doctor of Philosophy

in Physiology

in the Faculty of Science

University of London

Department of Physiology,
Royal Free & University College
Medical School,
University College London,
Rowland Hill Street,
London,
NW3 2PF

ProQuest LLC
789 East Eisenhower Parkway
P.O. Box 1346
Ann Arbor, MI 48106-1346

ABSTRACT

There is increasing evidence that extracellular nucleotides (such as ATP, ADP, UTP and UDP), as well as the nucleoside adenosine, behave as autocrine or paracrine agents in most tissues including the kidney, acting on a group of receptors known as purinoceptors. Previous studies have shown that activation of these receptors by exogenous nucleotides can influence a variety of renal vascular and tubular functions.

Purinoceptors of various subtypes are present on basolateral and apical membranes of renal tubules. However, the extent to which apical receptors are stimulated by endogenous nucleotides is unknown. Using micropuncture, the first part of this study quantified endogenous ATP in the lumen of proximal and distal tubules of the rat *in vivo*, both under control conditions and during pathophysiological manoeuvres. The results showed that ATP levels were sufficiently high to activate some purinoceptor subtypes. To assess whether the intraluminal ATP was being secreted or merely filtered at the glomerulus, the ATP content of fluid from Bowman's space (in Munich-Wistar rats) was compared with that in proximal tubules. The conclusion was that tubular epithelial cells secrete ATP.

Using a proximal tubular epithelial cell line, the mechanism of ATP release was examined. Intracellular stores of ATP were visualised using a marker compound (quinacrine), and the fate of these stores was monitored following hypotonic stimulation of ATP release. The findings suggested that ATP is stored within the cytoplasm, possibly in vesicles, and is released by exocytosis.

In the final part of the investigation, using immunohistochemistry, the distribution of five nucleotide-hydrolysing ectonucleotidases, namely NTPDases 1-3, NPP3 and ecto-5'-nucleotidase, was examined along the rat nephron. These enzymes (which differ in their hydrolysis pathways) were found to be differentially expressed along the major segments of the nephron, suggesting that they may be strategically located to influence the activity of the different purinoceptor subtypes.

ACKNOWLEDGEMENTS

There are many people I would to thank for the construction of this thesis for a variety of reasons. First and foremost, I would like to thank my supervisor, Dr. David Shirley, without whom this thesis would not have been possible. I could not have imagined having a better mentor for my PhD. His continual enthusiastic supervision, support, constructive criticism and encouragement have been invaluable to the construction of this manuscript and original papers. Not only has he encouraged me in the subject of renal physiology but his admirable skills in tennis matches have led me to believe that anything is possible.

I also want to express my deep gratitude to Professor Robert Unwin, who has encouraged and supported new ideas to the course of the research and for his invaluable advice.

I would also like to thank the academic and support staff of the Royal Free and University College London, not only in the Physiology Department, but also the Autonomic Neuroscience Institute and the Molecular Biology Department, for allowing me to use their resources and for providing technical advice and support and in general for their words of wisdom.

I would also like to thank the National Kidney Research Fund and the Wellcome Trust for financially supporting this research, and Professor Jean Sévigny, Dr Michelle Maurice, Dr David Marples and Professor Ronco for their kind gifts in providing antibodies for this research.

Finally, but by no means least, I would like to thank my parents from whom I have drawn my inspiration and strength, and my family and friends for their never-ending support, understanding and encouragement when it was most required.

Renu Vekaria (2006).

DISCLAIMER

This thesis has been prepared and written by myself, and supervised by Dr David Shirley. Some collections of tubular fluid were performed by Dr David Shirley and some urinary analysis of Na^+ and K^+ as well as preparation and production of micropipettes was performed by Mr John Skinner. With the above exceptions and unless otherwise stated, all experiments described in this thesis have been performed by myself.

PUBLICATIONS ARISING FROM THE WORK IN THIS THESIS

Full papers

Vekaria RM, Shirley DG, Sevigny J, and Unwin RJ. (2006). Immunolocalization of ectonucleotidases along the rat nephron. *American Journal of Physiology; Renal Physiol* 290: F550–F560.

Vekaria RM, Unwin RJ and Shirley DG. Intraluminal ATP concentrations in rat renal tubules. *Journal of American Society of Nephrology*; in press.

Communications

Vekaria RM, Unwin RJ and Shirley DG. (2005). Luminal ATP concentrations in the renal proximal tubule of the rat following hypotensive haemorrhage. *J. Physiol.* 567P, C113.

Vekaria RM, Unwin RJ and Shirley DG. (2005). Is adenosine 5'-triphosphate secreted into the proximal tubular lumen? *Nephrol.Dial,Transplant.20* (suppl.5), SP030.

Shirley DG, Vekaria RM and Unwin RJ. Glomerular filtration and proximal tubular secretion of ATP in the rat. *Proceedings of the Renal Association*, Belfast meeting, April, 2005

Vekaria RM. (2004). Vesicular storage and release of ATP in a rat proximal tubule cell line. *J. Physiol.* 560P, C17.

Vekaria RM, Unwin RJ and Shirley DG. (2004). Endogenous ATP concentrations in proximal convoluted tubular fluid of the rat. *J. Physiol.* 552P, C25.

Vekaria RM, Shirley DG and Unwin RJ. (2003). Immunolocalisation of Ectonucleotidases in the renal tubule. *Journal of American Society of Nephrology,* 14, SU-PO 084.

Shirley DG, Vekaria RM and Unwin RJ. (2003). Proximal and distal tubular fluid ATP concentrations *in vivo. Journal of American Society of Nephrology,* 14, SU-PO 072.

Vekaria RM, Shirley DG and Unwin RJ. (2003). Proximal tubular and collecting duct ectonucleotidases in the rat kidney. *3rd FEPS Congress*, PO7-22, Nice, France

Vekaria RM, Shirley DG and Unwin RJ. Immunolocalisation of ecto-nucleotidases in the rat kidney. *NKRF Fellows day, Renal Association meeting*, Keele, April, 2003.

CONTENTS

CHAPTER 2
PURINOCEPTORS AND RENAL PHYSIOLOGY

CHAPTER 3
MICROPUNCTURE ASSESSMENT OF TUBULAR FLUID ATP CONCENTRATIONS

CHAPTER 4

VESICULAR STORAGE AND RELEASE OF ATP IN A RAT PROXIMAL TUBULE CELL LINE

CHAPTER 5

IMMUNOLOCALISATION OF ECTONUCLEOTIDASES ALONG THE RAT NEPHRON

LIST OF TABLES AND FIGURES

CHAPTER 1

CHAPTER 2

CHAPTER 3

CHAPTER 4

CHAPTER 5

CHAPTER 1

GENERAL RENAL PHYSIOLOGY

1.1 Introduction

The kidney has important physiological roles in regulating ion levels such as sodium, potassium, chloride, magnesium, calcium and phosphate, as well as maintaining acid-base balance and the overall osmolality (285-295 mosmol/kg H_2O) of the body fluids. By controlling sodium excretion, the kidney also regulates extracellular fluid volume and blood pressure. As well as the removal of drugs and toxins, the kidney is responsible for the excretion of urea (the end product of protein metabolism), uric acid (from purine metabolism) and creatinine (from muscle metabolism), and for the secretion of erythropoietin, 1, 25 dihydroxycholecalciferol and the enzyme renin.

1.2 Glomerulus

Together, the kidneys receive a renal blood flow of approximately 1000ml/min (in humans). Blood entering the glomerulus is filtered to produce an ultrafiltrate of plasma. The ultrafiltrate has an almost identical concentration of small molecules and ions such as glucose, amino acids, urea, sodium, potassium, etc., to that of the renal arterial plasma, but is virtually free of any large proteins. Small proteins (<69,000 daltons in MW) are freely, or partially, filtered. The ability to form this ultrafiltrate is governed by both the anatomical structure of the glomerulus and the physical forces, namely the Starling forces (hydrostatic and oncotic pressures), that control the movement of fluid across the glomerular capillary wall.

1.2.1 Anatomy of glomerulus

In moving from the glomerular capillaries to the Bowman's capsule, the filtrate must traverse three layers comprising (i) the endothelial cells lining the capillary; (ii) the glomerular basement membrane (non-cellular connective tissues) and (iii) the visceral epithelial cells (also known as podocytes) of the Bowman's capsule (see Fig 1.1).

The endothelial cells of the glomerular capillaries are thin and flattened and are separated by many circular pores or fenestrations of approximately 70-100 nm in diameter (in the human kidney). These fenestrations function as a sieve or filter that

allows the passage of molecules but prevents the passage of cells. A polyanionic surface glycoprotein provides the endothelial capillary surface with a negative charge. The next two layers, namely the basement membrane and the visceral epithelial cells, contribute significantly to the filtration barrier. The basement membrane lies directly beneath the endothelial cells and forms a continuous porous membrane composed of collagen IV, laminin, fibrinogen and polyanionic heparin sulphate proteoglygan, all of which are negatively charged. Directly below the basement membrane are visceral epithelial cells that have large cytoplasmic processes (foot processes) that extend to contact directly the basement membrane. The distance between adjacent processes can range between 25 and 60 nm, forming filtration slits. Each filtration slit is bridged by a membrane known as the slit diaphragm, composed of the protein nephrin, which also contains pores (4 - 14nm) to allow the passage of small molecules (Mathieson, 2004).

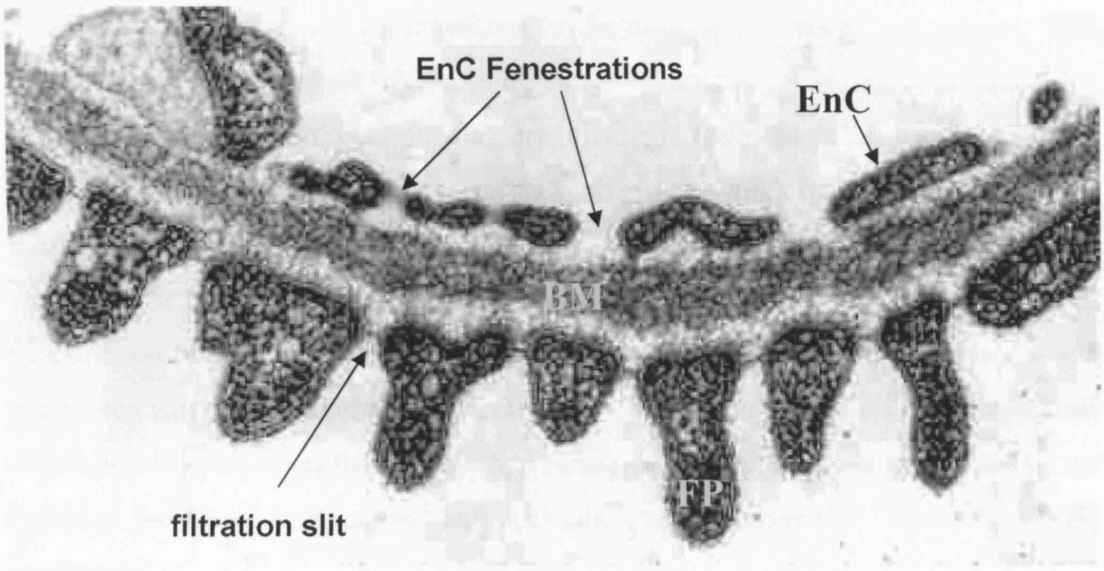

Fig. 1.1: Electron micrograph of a normal filtration barrier in the glomeruli. Endothelial fenestrations are formed between adjacent endothelial cells (EnC). The cytoplasmic foot processes (FP) of visceral epithelial cells are in direct contact with the basement membrane (BM) to form the filtration slit. Image taken from website: *http://www.nephrohus.org/uz/sm_semio_renale_folder/images_permselect_folder/Photo_filtration_barrier.html*.

The filtration barrier discriminates predominantly on the basis of size. However, large anions (such as proteins) are restricted additionally due to their negative charge, because the negatively charged glycoproteins found on each surface of the filtration barrier serve to hinder their passage. Abnormalities in the expression of these surface proteins have been shown to result in proteinuria (Mathieson, 2004).

1.2.2 Glomerular filtration rate (GFR) and autoregulation

The rate at which fluid crosses the glomerular membranes (glomerular filtration rate; GFR) is determined by the balance of the Starling pressures: the hydrostatic pressure in the glomerular capillaries, favouring filtration is opposed by the hydrostatic pressure in the Bowman's capsule and the oncotic pressure in the glomerular capillaries.

In order to avoid disastrous fluctuations in the excretion of water and solutes, GFR remains relatively constant over a wide range of arterial pressures, a phenomenon known as autoregulation. Although autoregulation in the kidneys has been recognized for many years, our understanding of how the autoregulatory mechanisms operate remains incomplete (Inscho, 2001). The key mechanism involves alterations in the resistance to blood flow in the afferent arteriole, whereby the vasoconstriction and vasodilation of this arteriole (which is also controlled through nervous, hormonal and paracrine systems) can increase or decrease preglomerular resistance. Two principal autoregulatory responses that occur when renal perfusion pressure is altered are (i) the myogenic control mechanism and (ii) the tubuloglomerular feedback (TGF) mechanism.

(i) The myogenic control mechanism

The myogenic control mechanism involves contraction and relaxation of the smooth muscle afferent arteriole wall in response to increases or decreases in vascular wall tension. A rise in perfusion pressure will result in the initial distension of the arteriole wall, followed by contraction, which increases pre-glomerular vascular resistance to ultimately normalize GFR. It is believed that the mechanism by which this occurs involves stretch-sensitive channels which, when activated, result in increased influx of

Ca^{2+}, causing depolarisation of the muscle and inducing contraction (Maddox and Brenner, 1991).

(ii) The tubuloglomerular feedback (TGF) mechanism

Increased arterial pressure results in a transient rise in renal blood flow, and glomerular capillary hydrostatic pressure, which results in a rise in GFR and increased tubular flow rate. This rise in tubular flow rate is monitored by increased sodium chloride delivery at the end of the thick ascending limb (TAL), by a group of specialised epithelial cells collectively known as the macula densa. The increased sodium chloride delivery to these cells initiates a sequence of events to increase preglomerular arteriolar resistance, thereby normalising renal blood flow, glomerular pressure and ultimately GFR. This response is possible because the macula densa of every nephron makes contact with its glomerulus of origin.

The signal from the macula densa that induces afferent arteriole vasoconstriction is not fully defined. Because there are no gap junctions between the cells of the macula densa and the smooth muscle arteriolar wall, the general consensus is that a chemical mediator is released from the macula densa to produce this TGF response. Adenosine and ATP are two strong candidates. With respect to adenosine, various studies using (i) mice deficient in adenosine A_1 receptors and (ii) acute blockade of A_1 receptors have shown that the TGF response is inhibited (Sun et al, 2001; Osswald et al, 1996). Further studies involving the inhibition of an enzyme involved in the conversion of AMP to adenosine, namely ecto-5' nucleotidase, has revealed that TGF efficiency is attenuated (Castrop et al, 2004; Thomson et al, 2000), demonstrating adenosine as a key mediator. With respect to ATP, Bell and colleagues (2003) were able to demonstrate the release of this nucleotide from the basolateral membrane of macula densa cells following elevations in luminal NaCl concentrations; the subsequent elevations in renal interstitial ATP concentrations were reported to increase vascular resistance of the afferent arteriole, an effect mediated by activation of P2X and/or $P2Y_2$ receptors (Komlosi et al, 2005). Overall, these studies strongly suggest that ATP released from the basolateral membrane of the macula densa cells acts on P2 receptors on the afferent arteriole to induce vasoconstriction; and that some extracellular ATP is hydrolysed by ectonucleotidases (including ecto-5' nucleotidase)

to produce adenosine, which, through the activation of A_1 receptors found on the same tissue, augments the response.

Ultimately, the rising levels of adenosine could lead to the activation of A_{2A} receptors also found on the afferent arteriole, which display lower sensitivity to activation than the A_1 receptors. Activation of the A_{2A} receptors acts to counteract and/or attenuate the vasoconstrictive response.

2.2.3 Mesangial cells

Surrounding the glomerular capillaries are mesangial cells, which, with their surrounding matrix, constitute the mesangium. The mesangium provides structural support to the glomerulus and prevents pernicious distension of the capillary wall following elevations in intracapillary hydrostatic pressure. It comprises an array of microfilaments containing actin and myosin that enable it to contract and relax. The mesangium may thus influence blood flow through capillaries, and the surface area available for filtration, through this ability to contract and relax in response to various paracrine/autocrine factors. Activation of purinoceptors on mesangial cells has been implicated in influencing the contraction and relaxation of the mesangium. In this context, pre-contracted glomeruli were found to relax in an ATP-dependent manner; an action which was reversed with time, assumed to be the result of increasing adenosine levels (from the hydrolysis of ATP) (Jankowski et al, 2001).

The information given in the remaining part of this chapter outlining tubular function has been taken from the following sources: Tisher and Madsen, 1991; Koeppen and Stanton, 2001 and Lote, 2000.

1.3 Proximal tubule

The proximal tubule consists of a convoluted segment known as the proximal convoluted tubule (~2/3 of the proximal tubular length) and a relatively straight segment known as the pars recta. Taken together, these segments may be further subdivided into three distinct segments: (i) the S1 segment, which comprises the

initial short section of the proximal convoluted tubule; (ii) the S2 segment, which makes up the remaining proximal convoluted tubule and the initial (cortical) portion of the pars recta; and (iii) the S3 segment, which consists of the medullary pars recta. Cells of the proximal tubule have a large number of mitochondria primarily located near the basolateral membrane and have a relatively permeable tight junction near the apical surface between adjacent cells. Cells of the proximal convoluted tubule (in particular the early regions), have very high rates of solute and water reabsorption. This is facilitated by the apical membrane having numerous microvilli, and the basolateral membrane having large invaginations increasing the surface area available for reabsorption to occur.

From the filtered load, the proximal convoluted tubule is responsible for reabsorbing ~15% magnesium; ~ 45% chloride, potassium and urea; ~ 50% sodium, calcium and water; ~ 80% bicarbonate and phosphate; and ~ 100% glucose, amino acids and proteins. Much of this solute reabsorption occurs against electrochemical gradients and is achieved through the coupled transport of Na^+ moving into the cell down its concentration gradient created by the Na^+-K^+ATPase located on the basolateral membrane (see Fig. 1.2). Water reabsorption along the proximal tubule occurs largely, possibly exclusively, via aquaporin-1 (AQP-1) channels located on the apical and basolateral membranes.

Most of the filtered glucose, amino acid and phosphate reabsorption occurs in the S1 segment of the proximal tubule, via a sodium-dependent transcellular route. Both the S1 segment and the initial portion of the S2 segment are involved in bicarbonate reabsorption, which is predominantly dependent on the apical Na^+/H^+ exchanger and, to a lesser extent, H^+ATPase secreting H^+ into the lumen. The secreted H^+ ions combine with filtered HCO_3^- to form H_2CO_3, a substrate for brush-border carbonic anhydrase (type IV), and is rapidly converted to CO_2 and H_2O, which can readily diffuse across the apical cell membrane. Once in the cytoplasm, intracellular carbonic anhydrase (type II) reassociates the molecules to form H^+ and HCO_3^-; the HCO_3^- is transported across the basolateral membrane (via the $Na^+HCO_3^-$ cotransporter).

Activity of the Na^+/H^+ exchanger can be modulated by increased angiotensin II levels (stimulated by extracellular volume depletion and/or acidosis) which acts to directly

stimulate the activity of this exchanger, to ultimately increase H^+ secretion (and therefore bicarbonate reabsorption) and Na^+ reabsorption in the proximal tubule.

The initial portion of the S2 segment has a primary role in chloride reabsorption, but is also involved in the reabsorption of sodium and any remaining glucose or amino acids. Reabsorption of potassium occurs in the S2 segment, although the mechanism is unclear; it is thought that it may occur via a passive paracellular route, the primary driving force being the lumen-positive potential difference (~2 mV) created from the passive paracellular reabsorption of Cl^- ions in this segment.

Finally, the pars recta (i.e., the remaining portion of the S2 segment and the S3 segment) is involved in the secretion of organic acids and bases via a transcellular route. It is also believed that potassium secretion occurs here. In addition to these secretory processes, solute and water reabsorption also occurs in the pars recta (albeit at a lower rate than that of the S1 or S2 segments of the proximal convoluted tubule).

1.4 Loop of Henle

Anatomically, the pars recta is regarded as the first section of the loop of Henle. The pars recta leads into a thinner region of the nephron known as the thin descending limb (tDL) and the thin ascending limb (tAL). Cells in these segments are thin and flat, with short microvilli and few mitochondria and demonstrate little or no Na^+ K^+-ATPase activity. The tDL has a relatively low permeability to sodium but a high permeability to water owing to the expression of AQP-1 channels on the apical and basolateral membranes, enabling water to move passively from the tubule into the hypertonic medullary interstitium. The loss of water from the tDL results in a rise luminal NaCl concentration. This provides a driving force for these ions to move out passively from the tubule into the interstitium in the tAL, which lacks AQP-1 channels but demonstrates high solute permeability.

1.4.1 Thick ascending limb (TAL)

The tAL leads into the TAL. Compared to the thin limbs, cells in this region are thicker, have more microvilli and a much greater number of mitochondria; they also

display high levels of basolateral Na^+-K^+ATPase activity. This region of the nephron is responsible for most of the solute reabsorption that occurs in the loop of Henle. Reabsorption of sodium occurs both transcellularly and paracellularly. Transcellular NaCl transport occurs via the Na^+-K^+-$2Cl^-$ cotransporter located on the apical membrane. Both the Na^+ and Cl^- ultimately exit the basolateral membrane, the Na^+ via the basolateral Na^+-K^+ATPase and the Cl^- via Cl^- channels and a K^+-Cl^- cotransporter. However, the K^+ that enters across the apical membrane is recycled back into the lumen (through channels), so that it can sustain the apical Na^+-K^+-$2Cl^-$ cotransporter (see Fig. 1.2). In addition, although the Na^+-K^+-$2Cl^-$ cotransporter is intrinsically electroneutral, the release of K^+ into the lumen, together with the Cl^- conductance in the basolateral membrane, establishes a transepithelial potential difference that is lumen positive, providing a driving force for the paracellular movement of cations such as Na^+, K^+, Ca^{2+} and Mg^{2+}. The transepithelial potential difference would also, in theory, cause anion secretion to occur; however, the paracellular tight junction is selective for cations. Overall, the TAL has a considerable reserve for reabsorbing more Na^+, so that if the proximal tubule fails to reabsorb the usual two-thirds of filtered Na^+, the TAL is able to compensate partially by reabsorbing more. Like the tAL, the TAL displays no aquaporin channels and is water impermeable. A unique feature of the TAL is its production of Tamm-Horsfall protein; this glycoprotein is thought to have a protective role in preventing bacteria adhering to tubular cells.

Overall, the loop of Henle (including the pars recta) is responsible for the reabsorption of ~25% filtered water; ~40% Na^+, ~45% Cl^- and K^+ and a significant fraction of Ca^{2+} and Mg^{2+}.

1.5 Distal tubule

The distal tubule of the nephron may be defined as the nephron segment interposed between the macula densa region (located in the distal part of the TAL) and the first confluence with another nephron to form the cortical collecting duct. On this basis, the distal tubule comprises four anatomically discrete subsegments: a short region of the TAL (also known as the distal straight tubule), the distal convoluted tubule

(DCT), the connecting tubule (CNT) and the initial portion of the cortical collecting tubule (CCT).

1.5.1 Distal convoluted tubule (DCT)

The DCT is made up of two segments: the initial segment, DCT_1 (made up solely of DCT_1 cells), and the latter portion, DCT_2 (made up of DCT_2 cells and intercalated cells [see below]). The DCT demonstrates the highest Na^+-K^+ ATPase activity of the nephron. Sodium transport in this region occurs transcellularly predominantly via the thiazide-sensitive apical Na^+-Cl^- cotransporter. Both DCT_1 and DCT_2 cells express this cotransporter; DCT_2 cells in addition have an apical Na^+ channel.

1.5.2 Connecting tubule (CNT)

The CNT comprises connecting tubule cells and intercalated cells (25 to 45%). Sodium transport across the apical membrane mainly occurs via the amiloride-sensitive Na^+ channel (ENaC). The apical membrane also expresses a K^+ channel, through which some K^+ secretion occurs. As well as expressing apical AQP-2 channels, this segment also displays basolateral vasopressin V_2 receptors, suggesting that vasopressin-sensitive water reabsorption occurs (see below).

Overall, the distal tubule of the mammalian kidney reabsorbs ~5% of the filtered sodium and chloride under normal conditions and participates in net K^+ secretion, the latter using the same mechanism as in the cortical collecting duct (see below). Although the majority of Ca^{2+} reabsorption occurs along the proximal tubule and the thick ascending limb through a paracellular route, the remaining Ca^{2+} reabsorption occurs in the DCT and CNT, transcellularly. Ca^{2+} entry into the cell occurs via a channel located on the apical membrane; once inside the cytosol, Ca^{2+} binds onto a calcium-binding protein, Calbindin-D, which transports it to the basolateral side for exit via a Ca^{2+} ATPase or Na^+/Ca^{2+} exchanger.

1.6 Collecting duct

The collecting duct may be divided into the cortical collecting tubule and the outer and inner medullary collecting ducts. The collecting duct normally reabsorbs approximately 3-4% of the filtered sodium chloride. Reabsorption of chloride most likely occurs through the paracellular pathway, driven by the lumen-negative transepithelial voltage (up to 40mV) created by ENaC-mediated Na^+ reabsorption. Another possible route is via β-intercalated cells (see below).

1.6.1 Cortical collecting tubule (CCT)

The cortical collecting tubule is made up mainly of principal cells, interspersed with intercalated cells (30 to 40 %). The principal cell is primarily concerned with Na^+ and H_2O reabsorption and K^+ secretion. K^+ enters the cell via the Na^+-K^+ ATPase pump located on the basolateral membrane; it is then released into the lumen via channels located on the apical membrane. Secretion of K^+ is mainly attributed to the reabsorption of Na^+ (occurring via ENaC-channels expressed on the apical membrane), whereby the entrance of Na^+ into the cell electrogenically favours K^+ secretion. Na^+ reabsorption and K^+ secretion by principal cells depend on the activity of the Na^+-K^+-ATPase pump in the basolateral membrane. Its activity provides a chemically favourable environment for the movement of both ions across the apical membrane.

The reabsorption of these ions in principal cells is influenced by aldosterone, which acts to increase the permeability of the luminal membrane to Na^+ (and possibly to K^+) and increase the activity of Na^+ K^+-ATPase in the basolateral membrane, achieved by increasing the synthesis of these channels and transporters and ATP production; the net result being increased Na^+ reabsorption and K^+ secretion.

Water reabsorption in principal cells is mediated via AQP-2 channels expressed on the apical membrane and sub-apical regions. The expression of AQP-2 on the apical membrane is influenced by vasopressin, where, upon binding to vasopressin receptors on the basolateral membrane, vesicles containing AQP-2 are translocated to the apical

membrane. Movement of water through the basolateral membrane is mediated via AQP-3 and AQP-4, which, unlike AQP-2, are constitutively expressed.

Intercalated cells

Intercalated cells represent the minority cell type within DCT_2, CNT, CCT and medullary collecting duct. Based on the polarity for the expression of H^+-ATPase, these cells may be sub-classified into either α- or β-intercalated cells.

Alpha

Alpha-intercalated cells have an apical H^+-ATPase and an apical H^+/K^+-ATPase which function in series with the basolateral HCO_3^-/Cl^- exchanger to secrete H^+ into the lumen. In addition to its effects on principal cells, aldosterone may also stimulate H^+-ATPase activity in these cells, thereby stimulating H^+ secretion.

Beta

Beta-intercalated cells have an apical HCO_3^-/Cl^- exchanger and a basolateral H^+-ATPase. They secrete HCO_3^- into the intraluminal environment, particularly during metabolic alkalosis.

1.6.2 Outer medullary collecting duct

The outer medullary collecting duct has a similar structure to that of the CCD, composed of modified principal and intercalated (mainly α-intercalated) cells. As the collecting duct progresses towards the inner medulla, the proportion of intercalated cells gradually declines.

1.6.3 Inner medullary collecting duct

The initial section of the inner medullary collecting duct is similar to the outer medullary collecting duct, containing modified principal cells expressing ENaC channels on the apical membrane (but no apical K^+ channels) and α-intercalated cells. The number of α-intercalated cells gradually diminishes, becoming absent as the duct progresses towards the papilla. The terminal regions of the inner medullary

collecting duct consists of a single cell type known as the inner medullary collecting duct cells.

Vasopressin-sensitive water reabsorption continues throughout the medullary collecting duct, with a small amount of NaCl reabsorption. K^+ secretion is not thought to occur.

Fig 1.2 summarizes the major transport mechanisms occurring along the nephron.

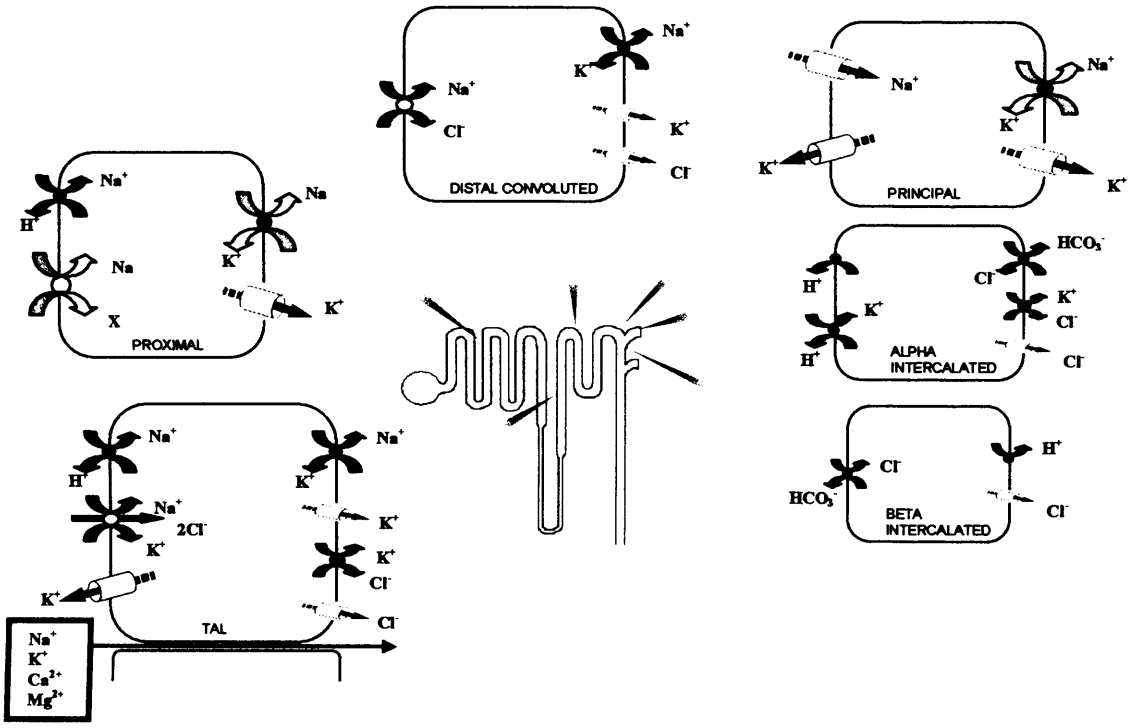

Fig. 1.2: Schematic diagram showing major transport pathways along the nephron.

CHAPTER 2

PURINOCEPTORS AND RENAL PHYSIOLOGY

2.1 Introduction

Extracellular nucleotides such as ATP, ADP, UTP and UDP, as well as the nucleoside adenosine (see Fig 2.1), are now widely accepted as autocrine or paracrine signalling agents in most tissues including the kidney. Their actions were first recognised in the nervous system where nucleotides and nucleosides act on a group of receptors commonly known as 'purinergic receptors'. However, receptors sensitive to nucleotides and nucleosides were subsequently identified in many non-neuronal tissues, and so the term 'purinoceptors' was adopted (Gordon, 1986; Burnstock and Knight, 2004). Purinoceptors sensitive to nucleotides are known as P2 receptors and consist of ligand-gated P2X receptors (which are non-selective cation channels) and G-protein-coupled P2Y receptors. Purinoceptors sensitive to the nucleoside adenosine are known as P1 (adenosine) receptors. Each family comprises a number of subtypes. Activation of these receptors has been found to modulate ion and water transport in many epithelia including those in the kidney (Leipziger, 2003).

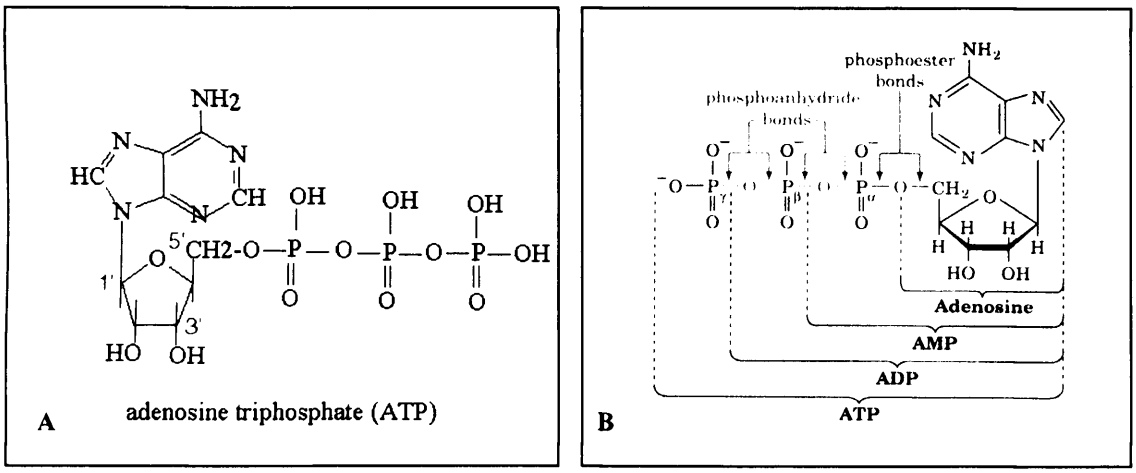

Fig. 2.1: (A) Structure of ATP molecule (note that, at physiological pH, most ATP is present in the anionic form). (B) Structure of ATP, showing potential cleavage sites at phosphodiester and phosphoanhydride bonds for the formation of ADP, AMP and adenosine.

2.2 Structure and signalling cascade of purinoceptors

2.2.1 The P2X family

Like all other ligand-gated ion channels, functional P2X receptors are formed by the assembly of a number of subunits. To date, seven P2X sub-units ($P2X_{1-7}$) have been cloned that form into either homomeric or heteromeric assemblies. A functional P2X receptor (either homomeric or heteromeric) may consist of three or six subunits. Each P2X subunit is between 379 and 595 amino acids in length, with $P2X_6$ being the shortest and $P2X_7$ the longest (North, 2002).

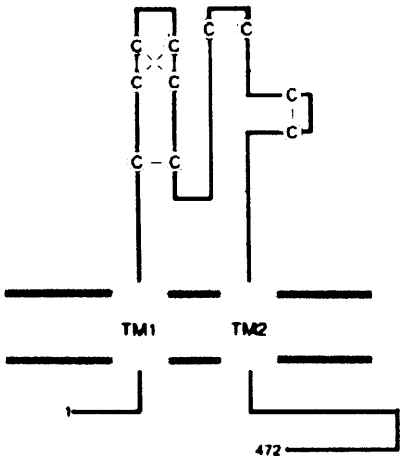

Fig. 2.2: Structure of the $P2X_2$ receptor subunit. Both the N and C termini of each P2X subunit are intracellular, and there are two transmembrane spanning regions (TM1 and TM2) concerned with channel gating and formation of the ion pore, respectively. The extracellular loop has 10 conserved cysteine residues (©) which contribute to the formation of disulphide bridges (from North 2002).

(i) Homomers of P2X receptors

Homomeric receptors are composed of multiples of a single receptor subunit. Torres and colleagues (Torres et al, 1999) examined the possibility of each of the seven P2X subunits forming physiological homomers, by transfecting cells with a single subunit P2X receptor subtype cDNA. The homomeric assembly formed was functionally tested for its ability to generate cation currents. The results showed that all, with the

exception of the $P2X_6$ receptor, were able to generate cation currents and thus were able to form homomeric channels.

All members of the P2X family share a common feature in that they are receptive to ATP. However, some homomeric P2X receptors, namely $P2X_{1, 3, 4 \& 5}$, have variable preferences for other nucleoside triphosphates such as UTP, CTP, GTP and ITP (as shown in Table 2.5). Neither ADP nor AMP activates P2X receptors, except for $P2X_7$ which will respond to ADP and AMP following prior activation by ATP. The assembly of each of the homomers (with the exception of $P2X_6$) is believed to exist as a trimer of identical subunits (Aschrafi et al, 2004). The duration of activation and inactivation of P2X receptor subtypes varies between the homomers and can take place over a few seconds, as seen with $P2X_{1, 3 \& 5}$, or over tens of seconds, as seen with $P2X_{2 \text{ and } 4}$. Activation of the $P2X_7$ receptor is irreversible (King and Townsend-Nicholson, 2003).

Following activation, these ligand-gated ion channels depolarise cell membranes through the influx of extracellular Na^+ ions and/or activate internal enzymes through the influx of extracellular Ca^{2+} ions. The sensitivity to ATP as well as the permeability properties can vary significantly amongst the P2X assemblies. Exogenous ATP acts on $P2X_1$ homomers to elicit cation currents with an EC_{50} (the concentration required to induce 50% of the maximal effect) close to 0.1μM. Once activated, this receptor has high permeability to Ca^{2+} as well as to Na^+ and K^+. The $P2X_2$ receptor homomer has a higher EC_{50} value (5μM) and is less permeable to Ca^{2+}. Further studies indicated that a point mutation increased the sensitivity of this receptor, reducing the EC_{50} value from 5μM to 1μM. Even less permeable to Ca^{2+} is the $P2X_3$ receptor homomer, which has an EC_{50} value of 1.2μM. The $P2X_4$ homomeric receptor displays a permeability to Ca^{2+} that is higher than that of $P2X_2$ but lower than that of $P2X_1$, and has an EC_{50} of 4μM to ATP. Little is known concerning the $P2X_5$ homomer; however, activation of $P2X_5$ (EC_{50} = 0.4μM) elicits smaller currents than $P2X_{1, 2, 3 \text{ or } 4}$. $P2X_6$ does not form a functional homomer. $P2X_7$, which will *only* function as a homomer, has the highest EC_{50} value of 0.4mM (North, 2002). Once activated, the $P2X_7$ receptor displays high permeability to Ca^{2+}, Na^{2+}, K^+ and even Cl^- (Burnstock and Knight, 2004). Table 2.5 lists the EC_{50} values (for ATP)

of the various homomers of the P2X receptors and their affinities for other naturally occurring nucleotides.

(ii) Heteromers of P2X receptors

The potential of the P2X subunits to oligomerize with other P2X subunits was examined using coimmunoprecipitation studies on subunits that were tagged using oligonucleotide primers 'FLAG' or 'haemagglutinin' epitopes at the C-termini of all P2X receptor subunits. These flags were then probed with antibodies using western blot procedures and potential heteromeric complexes identified as shown below (Table 2.1).

	$P2X_1$	$P2X_2$	$P2X_3$	$P2X_4$	$P2X_5$	$P2X_6$	$P2X_7$
$P2X_1$	+	+	+	–	+	+	–
$P2X_2$		+	+	–	+	+	–
$P2X_3$			+	–	+	–	–
$P2X_4$				+	+	+	–
$P2X_5$					+	+	–
$P2X_6$						–	–
$P2X_7$							+

Table 2.1: Summary table showing which P2X receptor subunits are able to coassemble to form a potentially functional multimeric receptor. $P2X_1$ and $P2X_2$ will coassemble with each other as well as with $P2X_3$, $P2X_5$ and $P2X_6$. $P2X_3$ will assemble with $P2X_1$, $P2X_2$ and $P2X_5$. $P2X_4$ will assemble with $P2X_5$ and $P2X_6$. $P2X_5$ will form coassemblies with $P2X_{1-6}$, whereas $P2X_6$ will assemble with $P2X_1$, $P2X_2$, $P2X_4$ and $P2X_5$. $P2X_7$ receptors will only form homomers. (Table taken from Torres et al, 1999).

To date, several functional heteromultimers have been described, and include $P2X_{2/3}$ (Radford et al, 1997), $P2X_{4/6}$, (Le et al, 1998), $P2X_{1/5}$ (Haines et al, 1999), $P2X_{2/6}$ (King et al, 2000) and $P2X_{1/2}$ (King and Townsend-Nicholson, 2003). These heteromultimer complexes were largely identified by western blot procedures performed on cells transfected with different P2X subunits, whereby heteromultimer

complexes were confirmed by the observation of consistent positive staining when antibodies specific for either subunit were used. Evidence was also obtained from pharmacological characterization, observing changes in sensitivity (measured by changes in current activity) upon exposure to various agonists and antagonists in whole tissue and transfected cell lines. So far, the heteromeric combinations listed above have been found naturally in the vasculature and central nervous system (CNS).

Little is known concerning the functional role and responses of the heteromers, as most of the P2X subunits also function as homomers. Some heteromeric complexes have been identified that share some properties/characteristics of their homomeric counterparts. Thus, the $P2X_{1/4}$ heteromer has a similar pharmacological profile to the $P2X_1$ homomer. Conversely, the $P2X_{2/6}$ heteromer displays a lower sensitivity to ATP than does the $P2X_2$ monomer. The heteromeric $P2X_{1/5}$ receptor is more sensitive than either the $P2X_1$ or $P2X_5$ homomer, eliciting currents with ATP concentrations as low as 3-10nM. Although this heteromer displays high sensitivity to ATP, the receptor is much less permeable to Ca^{2+} than is the $P2X_1$ homomer (the permeability of $P2X_5$ to Ca^{2+} has not been quantified). The $P2X_{2/3}$ heteromer displays similar permeation characteristics to the $P2X_3$ homomer (North, 2002). The duration of activation may also vary amongst the P2X heteromeric receptors and can occur either over a few seconds, as seen with $P2X_{1/2}$ and $P2X_{1/5}$, or over tens of seconds, as seen with $P2X_{2/3}$ and $P2X_{2/6}$ receptor assemblies (King and Townsend-Nicholson, 2003).

2.2.2 The P2Y family

The P2Y family consists of G protein-coupled, metabotropic receptors, the activation of which may then either activate phospholipase C to release intracellular calcium stores, or alternatively influence adenylate cyclase to alter cAMP levels (Burnstock and Knight, 2004). In mammals, there are currently known to be eight P2Y receptors ($P2Y_{1, 2, 4, 6, 11-14}$), each of which exists in the cell membrane as a single monomer. Evidence for the existence of homodimeric or heterodimeric assemblies remains controversial; co-expression of $P2Y_1$ with a member of the adenosine receptors (A_1) has been demonstrated in coimmunoprecipitation and immunocytochemistry studies, but so far has only been identified in rat brain (Yoshioka et al, 2002; King and Townsend-Nicholson, 2003).

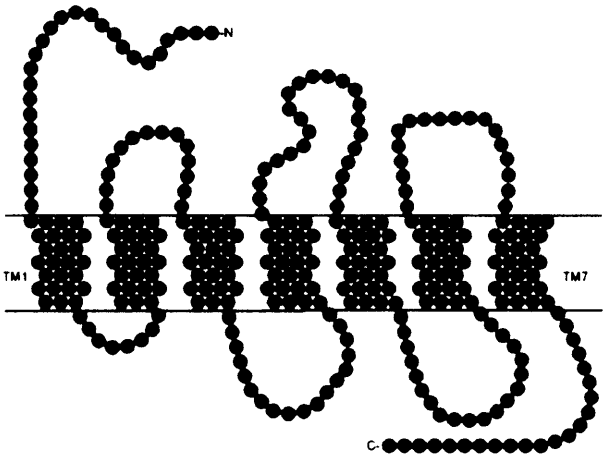

Fig. 2.3: Structure of a P2Y receptor, consisting of seven transmembrane regions (TM 1-7) which help to form the ligand docking pocket. The N-terminus is extracellular and does not have critical importance in agonist binding, whereas the intracellular C-terminus, (which varies in length amongst the different subtypes of the P2Y receptors) is believed to have a significant role in coupling to $G_{q/11}$, G_s and/or G_i proteins. The majority of P2Y receptors couple to $G_{q/11}$ proteins, activating phospholipase C and promoting inositol lipid-dependent signalling. However, $P2Y_{11}$ can couple to both $G_{q/11}$ and G_s protein to stimulate adenylate cyclase activity, and $P2Y_{12}$, $P2Y_{13}$ and $P2Y_{14}$ couple to G_i or $G_{i/o}$ to inhibit adenylate cyclase activity (Burnstock and Knight, 2004; Wolff et al, 2004).

P2Y receptors may be activated by both purine- and pyrimidine-based nucleoside tri- and diphosphates. $P2Y_{11}$ is only activated by ATP, with an EC_{50} value of approximately 28μM, whereas ADP is the prime agonist for $P2Y_1$, $P2Y_{12}$ and $P2Y_{13}$, with EC_{50} values of 50nM, 0.1μM and 10nM respectively. Both $P2Y_2$ and $P2Y_4$ are sensitive to UTP, with EC_{50} values of 0.1μM and 0.3μM respectively. $P2Y_6$ is primarily activated by UDP (EC_{50} of 0.2μM); $P2Y_{14}$ is activated by UDP-glucose (EC_{50} of 79nM). With the exception of $P2Y_6$ and $P2Y_{14}$, all P2Y receptors may be activated by ATP as well as by the nucleotides listed, and some receptors display sensitivity to several other nucleoside tri- and diphosphates such as GTP, ITP and IDP, albeit with lower affinities. Table 2.5 shows the EC_{50} values (for adenine- and uridine-based nucleotides) of the various homomers of the P2Y receptors and their affinities for other naturally occurring nucleotides. It should be noted that naturally

occurring agonists are susceptible to degradation by surface enzymes, and the hydrolysis products may also activate receptors and interfere with potency measurements (King and Townsend-Nicholson, 2003).

(i) G proteins and intracellular signalling cascade of P2Y receptor activation

There are at least three different G-protein groups involved in P2Y receptor signalling, namely G_s, G_i and $G_{q/11}$, which are associated classically with three transductional pathways: (i) stimulation of adenylate cyclase (an intracellular membrane-bound enzyme that converts ATP to 3',5'-adenosine monophosphate (cAMP)) by G_s; (ii) inhibition of adenylate cyclase by G_i; and (iii) activation of phospholipase C by $G_{q/11}$. The cascade of events following activation of each G-protein subtype is outlined below. G proteins are made up of α, β and γ subunits, each of which has several closely related isoforms. Of the α subunit, four major classes are known to exist, each class consisting of several members, as shown in the table below.

Classes of Gα subunits		
Class	**Members**	**Primary function**
α_s	α_s, α_{olf}	Stimulation of adenylate cyclase
α_i	α_{i-1}, α_{i-2}, α_{i-3}, α_o α_{t-1}, α_{t-2}, α_{gust}, α_z	Inhibition of adenylate cyclase
α_q	α_q, α_{11}, α_{14}, α_{15}, α_{16}	Activation of phospholipase C

Table 2.2: Classes of Gα subunits (Information taken from Neer, 1995)

(ii) G_i and G_s proteins in modulation of adenylate cyclase activity

Activation of $P2Y_{11}$ and, possibly, $P2Y_6$ receptor subtypes triggers an increase in the activity of adenylate cyclase, whereas activation of $P2Y_{2,\ 12\ and\ 13}$, and possibly $P2Y_4$, results in the inhibition of this enzyme. The activation (or inhibition) of adenylate cyclase is mediated via the G-protein trimer (composed of α, β and γ subunits) (Fig.

2.4A) which interacts directly with the nucleotide-bound P2Y receptor to promote the exchange of the guanine nucleotide on the α subunit, whereby GTP is substituted for GDP. The activated G-protein α subunit (carrying GTP) then dissociates from the βγ dimer and subsequently stimulates (or inhibits) adenylate cyclase. Production of cAMP by adenylate cyclase activates protein kinase A which subsequently phosphorylates intracellular substrate proteins, which may act on the cell's ion channels, or may activate or inhibit enzymes.

(iii) $G_{q/11}$ proteins and calcium/phosphatidylinositol system

Activation of $P2Y_{1,\ 2,\ 4,\ 6\ \&\ 11}$ receptor subtypes activates a membrane-bound phosphodiesterase called phospholipase C via G-protein ($G_{q/11}$). Activation of phospholipase C subsequently cleaves membrane-bound phosphatidylinositol 1,4,5-triphosphate, releasing two fragments: inositol 1,4,5- triphosphate (IP3) and diacylglycerol (DAG). IP3 and DAG work synergistically as second messenger molecules. IP3 binds to receptors on the endoplasmic reticulum to induce the release of intracellular Ca^{2+} stores to increase cytosolic Ca^{2+}. DAG activates a membrane-bound protein kinase C, an enzyme that, when activated, phosphorylates intracellular proteins. Protein kinase C requires Ca^{2+} for maximum activity; thus the rise of intracellular calcium (by IP3) favours this reaction (Fig. 2.4B).

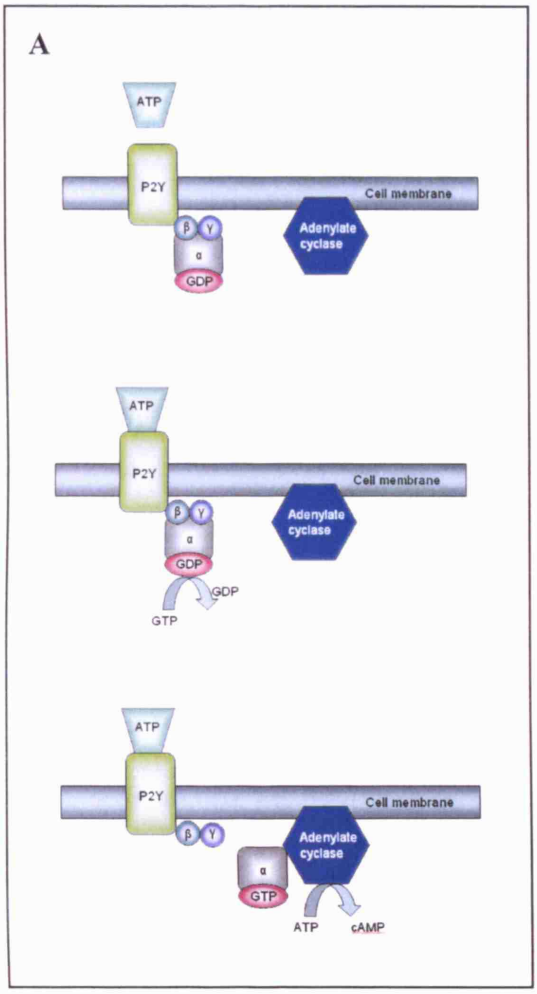

Fig. 2.4: (A) Modulation of adenylate cyclase activity by G_i or G_s composed of α, β and γ subunits. Activation of G-protein involves substitution of GTP for GDP. Activation of adenylate cyclase results in increased intracellular cAMP

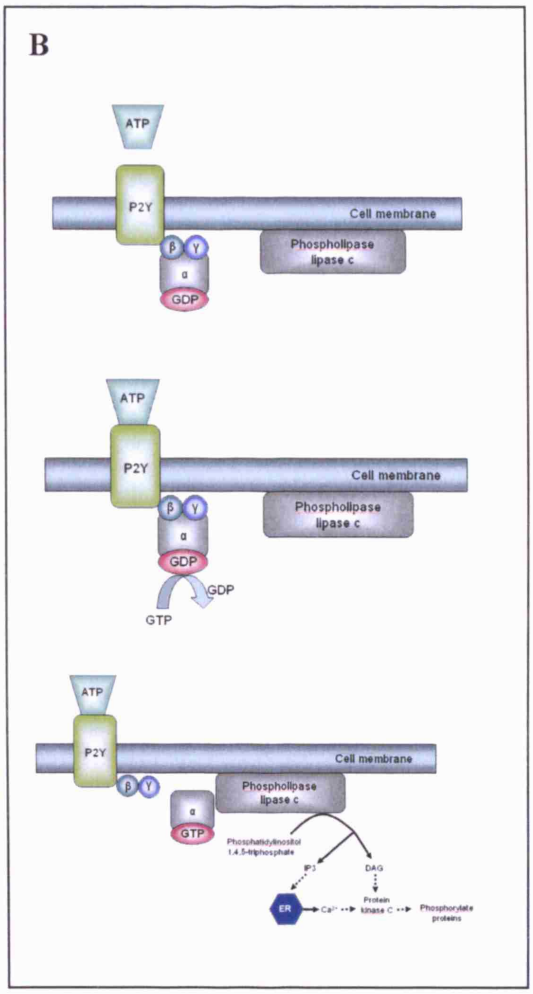

Fig. 2.4: (B) Activation of phospholipase C by G-protein ($G_{q/11}$) composed of α, β and γ subunits. Activation of G-protein involves substitution of GTP for GDP. Activation of phospholipase C results in the release of Ca^{2+} from endoplasmic reticulum

2.2.3 P1 (adenosine) receptors

To date, four adenosine receptor subtypes (A_1, A_{2A}, A_{2B} and A_3) have been identified and cloned. The A_3 subtype is the shortest in length, consisting of 318 amino acids, and A_{2A} (having 412 residues) is the longest. The potency of adenosine at these receptors varies between different subtypes, and all members of the adenosine receptors are either positively or negatively linked to adenylate cyclase via G proteins. The A_1 receptor is coupled to the G_i protein and has an EC_{50} value of 0.31μM for adenosine; both the A_{2A} and A_{2B} receptors are coupled to the G_s protein and have EC_{50}

values of 0.7μM and 24μM respectively; and the A_3 receptor is coupled to both/either the G_i and/or the $G_{q/11}$ protein and has an EC_{50} value of 0.29μM (King and Townsend-Nicholson, 2003; Burnstock, 2001). In common with P2Y receptors, all adenosine receptors have seven transmembrane-spanning regions, with an extracellular N-terminus and intracellular C-terminus

2.3 Expression of purinoceptors in the kidney

P2 receptor expression in the kidney has been examined at the protein level by immunological studies and at the mRNA level by the use of reverse transcriptase polymerase chain reaction (RT-PCR). These studies have used tubular cell lines or intact tissue tubular segments. Although mRNA studies suggest the presence of a number of receptors, not all of them have been confirmed at the protein level. One possible explanation for this apparent discrepancy is that receptor expression may be very low and undetectable using conventional immunohistological studies. Alternatively, cells expressing only the mRNA may express the receptor at the protein level in response to certain stimuli such as cytokines or pathophysiological conditions; the mRNA studies should therefore be viewed as an 'indication' for 'potential' expression of the receptor subtype.

2.3.1 Expression of P2X receptors in the kidney

Several P2X subtypes are known to be present along the renal tubule. Using RT-PCR, mRNA for the $P2X_1$ receptor subtype has been found in LLC-PK1 cells (a renal epithelial cell line originally derived from porcine kidneys and thought to be characteristic/representative of proximal tubular cells) (Filipovic et al, 1998). Unfortunately, its expression in native proximal tubule has not been verified by RT-PCR or immunohistochemical techniques. RT-PCR studies performed on mouse S1 proximal convoluted tubule cell lines and outer medullary collecting duct cells revealed the presence of mRNA transcripts for the $P2X_4$ receptor subtype (Takeda et al, 1998) and transcripts of mRNA for $P2X_5$ were identified in primary cell cultures of the proximal tubule (Unwin et al, 2003). Expression of P2X receptor subtypes at the

protein level along the nephron has been investigated by immunohistochemical studies using native tissue in the rat (Wildman et al, 2006; Chapman et al, 2006; Turner et al, 2003). $P2X_4$ and $P2X_6$ subtypes were expressed throughout the nephron, including the proximal convoluted tubule (but excluding the pars recta), the loop of Henle, the distal tubule and the collecting duct; $P2X_5$ was expressed in the pars recta of the proximal tubule and in principal cells in the collecting duct; and $P2X_2$ was expressed in the apical membrane of principal cells in the collecting duct.

Outside the nephron, mRNA for $P2X_2$, $P2X_3$, $P2X_4$, $P2X_5$ and $P2X_7$ has been identified in cultured rat mesangial cells (Solini et al, 2005), although immunohistochemical data confirmed protein expression of only $P2X_4$, $P2X_5$ and $P2X_7$ (Turner et al, 2003). In the renal vasculature, $P2X_1$ expression was found on most smooth muscle cells including the renal artery, arcuate and cortical radial arteries and the afferent arteriole, but not the efferent arteriole. $P2X_2$ was also expressed on vascular smooth muscle; in this case, however, expression was confined to the larger intrarenal arteries and veins. A summary of P2X receptor expression in the kidney and nephron is given in Table 2.3 and Fig. 2.5.

2.3.2 Expression of P2Y receptors in the kidney

Messenger RNA for $P2Y_{1,2,4\ \&\ 6}$ receptor subtypes has been found in the proximal tubule of the rat (Bailey et al, 2000; Bailey et al, 2001). Immunohistochemistry studies have localised protein expression of $P2Y_4$ to the basolateral membrane of the proximal convoluted tubule, whilst $P2Y_1$ was only found in the apical membrane of the pars recta (Turner et al, 2003). However, functional studies (involving the perfusion of $P2Y_1$ receptor-specific agonist) have suggested that $P2Y_1$ receptors are also expressed on the apical membranes of the proximal convoluted tubule, and western blots performed on brush-border membrane preparations of the same segment are in agreement with this (J. Marks, unpublished observation).

RT-PCR studies also identified mRNA transcripts of $P2Y_{1,2,4\ \&\ 6}$ in various segments of the loop of Henle of the rat: $P2Y_1$, $P2Y_2$ and $P2Y_6$ in the descending thin limb, $P2Y_2$ and $P2Y_4$ in the thin ascending limb and $P2Y_6$ in the thick ascending limb (Unwin et al, 2003; Bailey et al, 2000; Bailey et al, 2001). Protein expression of

$P2Y_2$, but not $P2Y_4$, in the thin and thick ascending limbs of Henle has been shown through immunohistochemical studies in the same species (Turner et al, 2003).

In the distal nephron, mRNA for $P2Y_{1, 2, 4 \& 6}$ was identified in the outer medullary collecting duct (Bailey et al, 2000; Bailey et al, 2001) and for $P2Y_2$ in the inner medullary collecting duct of the rat (Kishore et al, 2000). According to immunohistochemical data, $P2Y_2$ was expressed in the (inner medullary) collecting duct of the same species, where it was found on the apical and basolateral membrane of principal cells (Kishore et al, 2000). In contrast, in the immunohistochemistry study of Turner et al (2003), $P2Y_2$ expression in the collecting duct was restricted to intercalated cells. Very recently, a further immunohistochemical study identified $P2Y_2$ receptors in the basolateral membrane of both cell types in the inner medullary collecting duct (Wildman et al, 2006). The same study also found evidence for $P2Y_{4, 6, 11 \text{ and } 12}$ subtypes in the apical membrane of principal cells throughout the rat collecting duct

In the rat, mRNA for $P2Y_{1, 2, 4 \& 6}$ has been found in the glomerulus (Bailey et al, 2000). However, only the expression of $P2Y_{1 \& 2}$ could be confirmed through immunohistochemical studies; these receptors were found in mesangial and podocyte cells, respectively.

In the renal vasculature, the expression of $P2Y_1$ was confirmed immunologically in vascular smooth muscle cells of the afferent and efferent arteriole and the large intrarenal arteries and veins. Although functional studies using pyrimidine-based nucleotides suggest the expression of other P2Y receptors, namely $P2Y_2$ and/or $P2Y_4$, their protein expression in the renal vasulature has not been confirmed. A summary of P2Y receptor expression in the kidney and nephron is given in Table 2.4 and Fig. 2.5.

Receptor	Distribution in the normal rat kidney	Principal agonist	Transduction mechanism
$P2X_1$	Vascular smooth muscle cells	**ATP**	Intrinsic cation channel: (influx of Ca^{2+} and Na^+, efflux of K^+).
$P2X_2$	Vascular smooth muscle cells (larger intrarenal vessels); apical membrane of the collecting duct	**ATP**	Intrinsic cation channel: (influx of Ca^{2+} and Na^+, efflux of K^+).
$P2X_3$	Not detected	**ATP**	Intrinsic cation channel: (influx of Ca^{2+} and Na^+, efflux of K^+).
$P2X_4$	Low-level expression in mesangial cells and throughout the nephron	**ATP**	Intrinsic cation channel: (influx of Ca^{2+} and Na^+, efflux of K^+).
$P2X_5$	Mesangial cells; S3 segment of proximal tubule (apical); cortical and medullary collecting duct (principal cells)	**ATP**	Intrinsic cation channel: (influx of Ca^{2+} and Na^+, efflux of Cl^- and K^+).
$P2X_6$	Low-level expression throughout the nephron	**Does not function alone**	Intrinsic cation channel: (influx of Ca^{2+} and Na^+, efflux of K^+).
$P2X_7$	Low-level expression in some glomeruli	**ATP**	Intrinsic cation channel: (influx of Ca^{2+} and Na^+, efflux of Cl^- and K^+).

Table 2.3: P2X receptor subtypes/subunits, their distribution in the kidney at the protein level, principal nucleoside di- or triphosphate agonists for their homomeric forms and cell effector mechanisms following activation (data from Burnstock and Knight, 2004; Turner et al, 2003; Wildman et al, 2006; Chapman et al, 2006).

Receptor	Distribution in the normal rat kidney	Principal agonist	Transduction mechanism
$P2Y_1$	Vascular smooth muscle cells; proximal convoluted tubule; S3 segment of proximal tubule (apical); glomerulus (mesangial cells); peritubular fibroblasts	**ADP > ATP**	G_q/G_{11}: PLC activation
$P2Y_2$	Glomerulus (podocytes); thin and thick ascending limbs of Henle; medullary collecting duct (intercalated cells), and principal cells of the IMCD	**UTP = ATP**	G_q/G_{11} and G_i: PLC activation
$P2Y_4$	Basolateral membrane of proximal convoluted tubule; apical membrane of the collecting duct	**UTP > ATP**	G_q/G_{11} and possibly G_i: PLC activation
$P2Y_6$	Apical membrane of the collecting duct	**UDP >UTP >>ATP**	G_q/G_{11} and possibly G_s: activation of PLC and adenylate cyclase
$P2Y_{11}$	Apical membrane of the collecting duct	**ATP**	G_q/G_{11} and G_s: activation of PLC and adenylate cyclase
$P2Y_{12}$	Apical membrane of the collecting duct	**ADP**	G_i: inhibition of adenylate cyclase.
$P2Y_{13}$	No information available	**ADP >ATP**	G_i: inhibition of adenylate cyclase
$P2Y_{14}$	No information available	**UDP-glucose**	$G_{i/o}$: modulation of adenylate cyclase and PLC activity

Table 2.4: P2Y receptor subtypes, their distribution in the kidney at the protein level, principal nucleoside di- or triphosphate agonists and cell effector mechanisms following activation (data from Burnstock and Knight, 2004; Turner et al, 2003; Kishore et al, 2000; J. Marks, UCL, unpublished observations; Wildman et al, 2006; Chapman et al, 2006).

2.3.3 Expression of adenosine receptors in the kidney

Using northern blot analysis in the rat, Yamaguchi et al (1995) identified transcripts of A_1 receptor mRNA in the glomeruli, medullary and cortical thick ascending limb of Henle and medullary collecting duct; whilst weak levels were detected in the proximal convoluted and straight tubules.

Expression of this receptor at the protein level was confirmed at most of these sites using immunohistochemistry (in the same species) by Smith et al (2001) who identified the A_1 receptor on the mesangial cells of the glomerulus, the proximal convoluted tubule and the inner medullary collecting ducts. Outside the nephron, A_1 receptors were localised to the afferent arteriole. Their expression in the thick ascending limb was not examined in the above study.

Messenger RNA in the rat studies have suggested that renal A_{2A} receptors are primarily located in the glomeruli (Vitzthum et al, 2004), and A_{2B} receptor mRNA has been found in the cortical thick ascending limb and the distal convoluted tubule (Vitzthum et al, 2004). At the protein level, Pawelczyk et al (2005) reported that the expression of A_{2A} receptor was barely detectable using immunohistochemistry in the normal rat, but that its expression in the glomerulus, distal convoluted tubules and collecting ducts was up-regulated in the diabetic kidney. No immunohistological findings have been reported for the A_{2B} receptor. Finally, most studies have failed to identify A_3 receptors in renal tubular structures. However, a functional study using an A_3 receptor-specific agonist led to the conclusion that this receptor is expressed on glomerular mesangial cells (Zhao et al, 2002). A summary of P1 receptor expression in the nephron is included in Fig. 2.5.

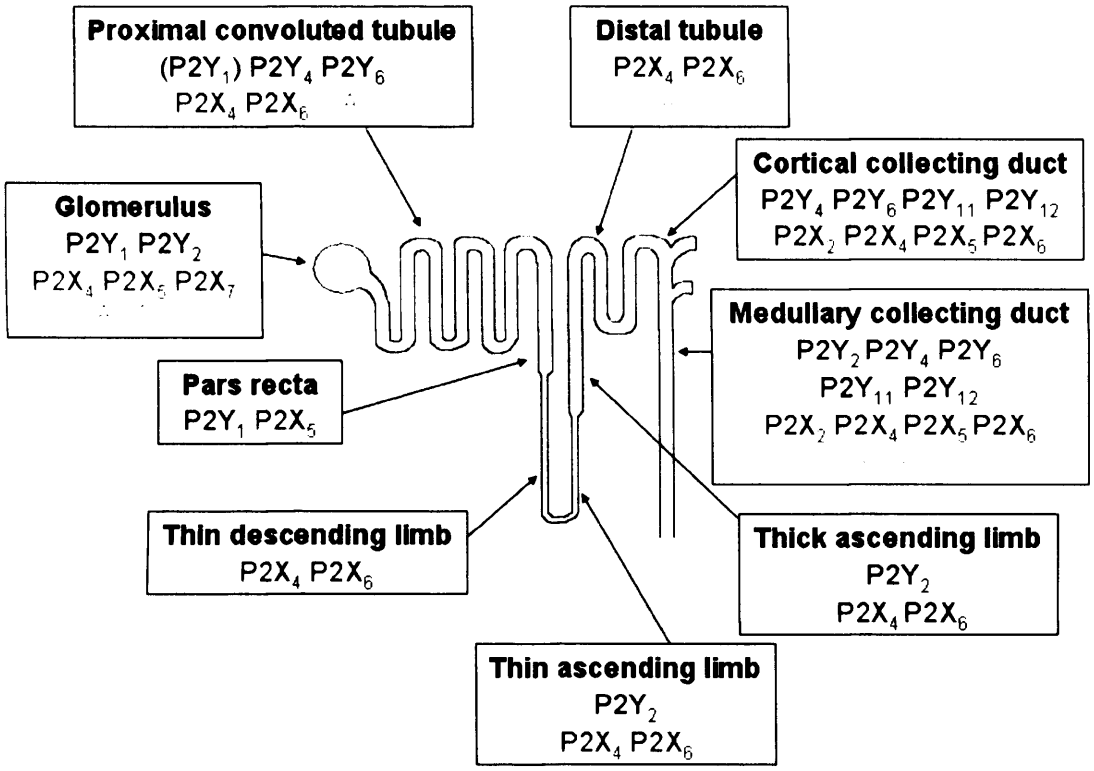

Fig 2.5. Schematic diagram showing the expression of purinoceptors at the protein level along the nephron. (data from Burnstock and Knight, 2004; Turner et al, 2003; Kishore et al, 2000; J. Marks, UCL, unpublished observations; Wildman et al, 2006; Chapman et al, 2006)

2.4 Functional role of purinoceptors in the kidney

The precise functional role of individual P2Y receptor subtypes in the kidney has been difficult to establish for several reasons. These include (i) the lack of selective agonists or antagonists (as shown in Table 2.5) or specific antibodies to the extracellular domains of the receptor; (ii) the co-expression of several receptor subtypes on the same cell membrane in native tissue; and (iii) the endogenous release of nucleotides from tissues/cells, which could activate different receptors from the one being examined using exogenous agonist (Lazarowski, 2003). The co-expression of various P2X receptor subtypes in native tissue poses further problems when examining the functional role of these receptors, as functional responses may be

attributed to either homomeric or heteromeric P2X assemblies of a particular receptor, both forms possibly sharing the same pharmacological profiles. Nevertheless, functional studies have been able to distinguish broadly between P2X and P2Y responses through the use of uridine-based nucleotides, which in low concentrations do not activate P2X receptors. Further analysis of the receptor subtype involved has been made through dose-response measurements using relatively selective synthetic agonists and antagonists or by using cell lines specifically transfected with the purinoceptor in question.

Receptor subtype	Naturally occurring agonists	Synthetic agonists	Synthetic antagonists
$P2X_1$	ATP (0.1μM) > CTP	2-MeSATP > α,β-meATP	Suramin = RB-2
$P2X_2$	ATP (5μM)	2-MeSATP = ATPγS > α,β-meATP	RB-2 > Suramin
$P2X_3$	ATP (1.2μM) > UTP (100μM)	2-MeSATP > ATPγS > α,β-meATP	Suramin > RB-2
$P2X_4$	ATP (4μM) > CTP	α,β-meATP > 2-MeSATP	
$P2X_5$	ATP (0.4μM) > GTP > CTP	2-MeSATP > α,β-meATP	Suramin > RB-2
$P2X_6$	ATP (0.4μM)	-	-
$P2X_7$	ATP (0.4mM) > ADP (2mM)	2-MeSATP	-
$P2Y_1$	ADP (50nM) > ATP (1.8μM)	2-MeSADP 2-MeSATP	MRS 2279 > Suramin
$P2Y_2$	UTP (0.1μM) = ATP (0.1 μM) > GTP	ATPγS	Suramin
$P2Y_4$	UTP (0.3μM) > ATP (12μM) > GTP > ITP	-	RB-2
$P2Y_6$	UDP (0.2μM) > ATP (1μM) > UTP (7.9μM) > ITP > ADP (45μM)	-	RB-2
$P2Y_{11}$	ATP (28μM)	2-MeSATP	Suramin
$P2Y_{12}$	ADP (0.1μM) > ATP (0.9μM)	2-MeSATP 2-MeSADP	RB-2 > Suramin
$P2Y_{13}$	ADP (0.1μM)> ATP (0.3μM)> IDP	2-MeSADP 2-MeSATP	-
$P2Y_{14}$	UDP-glucose (79nM)	-	-
A_1	Adenosine (0.3μM)	CPA > CGS	-
A_{2A}	Adenosine (0.6μM)	CGS > CPA	-
A_{2B}	Adenosine (25μM)	CPA > CGS	-
A_3	Adenosine (0.3μM)	CPA > CGS	-

Table 2.5: Naturally occurring agonists and synthetic agonists and antagonists (in order of potency) for P2 and P1 receptors used in the studies described below. EC_{50} values for adenine- and uridine-based nucleotides and nucleosides are also shown (in parentheses). (From King and Townsend-Nicholson, 2003; Filipov et al, 1999).

Early studies assessed purinoceptor activation in the kidney by measuring changes in intracellular Ca^{2+} concentration. According to this criterion, practically every segment responded to ATP. In the following, only studies where *functional* responses (such as changes in solute and water transport) were observed following purinoceptor activation will be discussed. Notably, not all functional responses are related to changes in intracellular Ca^{2+}concentration.

2.4.1 Proximal tubule

Stimulation of apical P2 receptors *in vivo* (using 2meSADP, a $P2Y_1$ agonist) in the proximal convoluted tubule caused inhibition of bicarbonate reabsorption in the rat by inhibiting the apical Na^+/H^+ exchanger (in this case NHE3) activity (Bailey, 2004). This effect was blocked by MRS2279, a highly selective $P2Y_1$ antagonist. Indeed the antagonist alone (i.e., in the absence of exogenous nucleotide), *stimulated* bicarbonate reabsorption, suggesting an inhibitory effect of endogenous nucleotide. Conversely, basolateral stimulation by perfusion of peritubular capillaries with ATP (10μM) *increased* transepithelial bicarbonate reabsorption in the rat *in vivo*. Increased bicarbonate reabsorption was also observed when basolateral fluid viscosity was increased by 30%; an effect abolished by the introduction of P2 antagonists (suramin and reactive blue 2 [RB-2]) into the peritubular perfusate (Diaz-Sylvester et al, 2001).

In a study performed on a rat proximal tubule cell line, inhibition of basolateral Na^+/K^+-ATPase (the prime driving force for the movement of ions and other solutes across the tubular epithelium) was observed following the introduction of extracellular ATP applied to the apical membrane. The effect of ATP was dose dependent; the EC_{50} was ~0.32mM. Pharmacological classification (through the use of relatively selective antagonists) of purinoceptors suggested that this response was mediated through the stimulation of $P2Y_1$ receptors on the apical membrane of the proximal tubule (Jin and Hopfer, 1997).

Recently, Lee et al (2005) reported that ATP inhibited phosphate uptake in a dose-dependent (>1μM) manner in primary cultures of rabbit proximal tubular cells; a

mechanism that was inhibited by the P2 antagonists suramin and RB-2. The inhibition of phosphate uptake by ATP was correlated with reduced levels of mRNA for type II Na^+/P_i cotransporter (although the particular subtype was not mentioned in the study).

With respect to adenosine receptors, inactivation of A_1 receptors *in vivo,* using a relatively selective antagonist, was reported to have a natriuretic and diuretic effect in the rat (Wilcox et al, 1999). *In vitro* studies have demonstrated direct stimulation of the basolateral $Na^+HCO_3^-$ cotransporter in microperfused rabbit proximal tubule following basolateral stimulation of A_1 receptors (Takeda et al, 1993).

In addition to effects on tubular transport, nucleotides have also been shown to affect gluconeogenesis activity in the proximal tubule. *In vitro* studies in rat proximal tubule suspensions showed increased gluconeogenesis following exposure to solutions of adenine-based nucleotides such as ATP and ADP, and of adenosine. In particular, exogenous adenosine was more potent in stimulating gluconeogenesis than either ATP or ADP (the latter being equipotent) (Edgecombe et al, 1997). In a further study by the same group, UTP also stimulated gluconeogenesis and was more potent than ATP, suggesting that the response is mediated via $P2Y_2$ or $P2Y_4$ receptors. No significant change in gluconeogenesis activity was observed with UDP, suggesting that $P2Y_6$ is not involved in this response (Mo and Fisher, 2002).

2.4.2 Loop of Henle

To date, functional activation of P2 receptors and the possible effect on electrolyte transport in the loop of Henle has not been reported. However, *in vitro* studies have demonstrated that stimulation of A_1 receptors (using 10nM adenosine) in the TAL inhibits NaCl reabsorption (Beach and Good, 1992).

2.4.3 Distal tubule

As with the loop of Henle, no *in vivo* studies have been performed to assess the role of purinoceptors in the distal tubule. However, *in vitro* studies have been performed using immortalized distal-like cell lines. Activation of basolateral $P2Y_1$ receptors on A6 cells (immortalized *Xenopus* distal-like cell lines) was shown to increase

intracellular calcium followed by a rise in chloride efflux (Guerra et al, 2004). An increase in chloride efflux following P2 receptor activation has also been demonstrated consistently in other distal tubule-like cell lines including Madin-Darby canine kidney (MDCK) cells (Simmons, 1981) and rabbit immortalised distal convoluted tubule cells (Rubera et al, 2000); in the latter study the increase in chloride secretion was pharmacologically attributed to stimulation of apical $P2Y_2$ receptors. This variation in response may be the result of using cell lines (which share, but also lose, many characteristics of native tissue).

Using a mouse distal convoluted tubule (DCT) cell line, Dai et al (2001) have shown transient increases in intracellular calcium levels coupled with decreased vasopressin- and parathyroid hormone (PTH)-stimulated Mg^{2+} uptake following exposure to 100μM ATP. Furthermore, because both UTP and ADP were without effect in inhibiting hormone-stimulated Mg^{2+} uptake, it was suggested that this response was most likely to be mediated via P2X receptors.

The same group also examined the effects of adenosine on Mg^{2+} transport in the same cell line and concluded that application of adenosine increased intracellular Ca^{2+} and PTH-mediated Mg^{2+} uptake. Furthermore, using the relatively selective A_1 receptor agonist N6-cyclopentyladenosine (CPA), the same study also reported how activation of this receptor *inhibited* PTH-mediated Mg^{2+} uptake. In contrast, activation of A_2 receptors in the same cells, using the relatively selective A_2 agonist 2-[p-(2-carbonyl-ethyl)-phenylethylamino]-5'-N-ethylcarboxamidoadenosine (CGS), *stimulated* hormone-mediated Mg^{2+} uptake (Kang et al, 2001). Neither the A_2 receptor subtype nor the polarity of the purinoceptors in these DCT cells (apical vs. basolateral) was determined. Nevertheless, the fact that the distal convoluted tubule is involved in the reabsorption of approximately 15% of filtered Mg^{2+} highlights the potential influence of nucleotides and the nucleoside on the excretion of this cation.

With respect to adenosine, Lang et al, 1985 reported that this nucleoside stimulated sodium reabsorption in an A6 cell line. Similar observations were made by Ma and Ling (1996), using the same cell line; the effect was attributed to the activation of A_1 receptors on the apical membrane. Whilst activation of A_1 receptors stimulated sodium reabsorption, activation of A_2 receptors on the same membrane were found to

inhibit sodium uptake; an effect observed when higher adenosine concentrations (1-10 μM) were used. Conversely, Casavola et al (1996) reported an increase in sodium transport following the interaction of an adenosine analogue with basolateral A_2 receptors on the same cell line.

2.4.4 Collecting duct

Using patch-clamp techniques on split open murine CCD, Giebisch's group reported that the application of nucleotides such as ATP and UTP inhibited the activity of small-conductance potassium channels on the apical membrane of principal cells (involved in K^+ secretion). Because UTP and ATP-γ-S induced the same inhibitory responses, while α, β-MeATP and 2-MeSATP were without effect, the response was believed to be mediated via $P2Y_2$ receptors expressed on the apical membrane (Lu et al, 2000).

In vitro studies in which nucleotides such as ATP, ADP and UTP have been applied to the basolateral membrane of rabbit CCD, at concentrations of 100nM, have demonstrated decreased vasopressin-sensitive water permeability (Rouse et al, 1994). Similar studies performed on the inner medullary collecting ducts of the rat, but using ATP at concentrations of 10μM, showed the same effect. However, no effect was observed with ADP, suggesting either a species difference in receptor expression or that different P2 receptors may be involved in the cortical and medullary regions of the collecting duct (Kishore et al, 1995). The lack of sensitivity to ADP makes it possible that the effect is mediated via $P2Y_2$ receptors, and this is further supported by a recent study that showed increased levels of $P2Y_2$ mRNA in inner medullary collecting duct tissue derived from hydrated rats (Kishore et al, 2005). An even more recent study has shown that activation of the $P2X_2$ receptor subtype as well as $P2Y_4$ and $P2Y_2$, when co-expressed with AQP-2 in *Xenopus* oocytes, inhibits AQP-2-mediated osmotic water effluxes (Wildman et al, 2006); and the former two subtypes are colocalised to the *apical* membrane of the rat collecting duct (Wildman et al, 2006). Finally, adenosine and its analogues in submicromolar concentrations inhibited water reabsorption in this region of the nephron, an effect mediated via A_1 receptors (Edwards and Spielman, 1994). Overall, these studies strongly suggest that

nucleotides and adenosine play important roles in modulating water reabsorption in the collecting duct.

In vitro studies showed that apical or basolateral administration of 100μM ATP or UTP inhibited short circuit current, taken to be an index of sodium transport, in mouse CCD, an effect believed to be mediated via $P2Y_2$ receptors present in the apical membrane (Lehrmann et al, 2002). Recently, the effect of nucleotides on collecting duct sodium reabsorption *in vivo* has been investigated in our laboratory, using microperfusion of late distal tubules in rats (Shirley et al, 2005). Addition of ATPγS to the luminal perfusate was found to inhibit ^{22}Na reabsorption (i.e., urinary ^{22}Na recovery was increased), but only when baseline ENaC activity was upregulated by feeding the animals a low sodium diet. Intriguingly, despite firm evidence from *in vitro* studies for $P2Y_2$ mediation, 'selective' $P2Y_2/P2Y_4$ and $P2Y_1$ agonists were ineffective *in vivo*, and a P2X heteromer-mediated effect was suggested (Shirley et al, 2005). In this connection, another recent study, using the *Xenopus* oocyte expression system, has shown that expression and subsequent activation of a number of P2X receptors ($P2X_2$, $P2X_{2/6}$, $P2X_4$ or $P2X_{4/6}$) leads to downregulation of co-expressed ENaC (Wildman et al, 2005).

Stimulation of basolateral A_1 receptors in primary cultures of the IMCD was found to reduce apical reabsorption of sodium (Yagil et al, 1994). Overall, renal A_1 receptor inhibition is natriuretic and diuretic, as the effect on proximal tubular reabsorption predominates (Wilcox et al, 1999).

2.4 Pathophysiological role in the kidney

In addition to the effects observed on water and electrolyte transport, purinoceptor activation has been implicated in a number of renal pathophysiological conditions, notably polycystic kidney disease and glomerular inflammation.

2.5.1 Polycystic kidney disease

Polycystic kidney disease (PKD) is a genetic disorder in which the tubules become dilated (due to uncontrolled cell proliferation), ultimately leading to the characteristic formation of fluid-filled cysts contained by a monolayer of renal epithelium. It has been shown that fluid derived from the cysts contains ATP in high nanomolar to micromolar concentrations (Wilson et al, 1999). As indicated earlier, in many epithelia and cell lines, *in vitro* studies have frequently shown that nucleotides such as ATP inhibit Na^+ absorption and stimulate Cl^- secretion (Leipziger, 2003). The high concentration of ATP in cyst fluid is believed to augment cyst development by stimulating Cl^- and (consequently) water secretion into the lumen of the cyst, thereby promoting cyst expansion (Wilson et al, 1999). Furthermore, transcripts of mRNA for multiple P2X receptor subtypes have been identified in PKD models, and P2Y receptor-mediated Cl^- secretion has been reported in the same models (Schwiebert et al, 2002). Alternatively or additionally, 'trapped' nucleotides in PKD cysts may augment cell proliferation required for cyst development; *in vitro* studies have demonstrated increased cell proliferation following activation of $P2Y_2$, $P2Y_4$ and/or P2X receptors in various renal (and non-renal) cell lines (Harada et al, 2000; Paller et al, 1998; Weisman et al, 2005).

Further studies have shown increased $P2X_7$ receptor expression at the protein level in polycystic kidney epithelia derived from the mouse collecting duct, compared with normal mouse collecting ducts. Activation of $P2X_7$ receptors using BzATP, a relatively selective agonist, was found to reduce cyst number in a dose-dependent manner (Hillman et al, 2004). Activation of $P2X_7$ receptors can lead to the formation of non-selective pores which allow leakage of solutes up to 900 Da, inducing a necrotic effect on the cell (Auger et al, 2005). Indeed, several studies have reported apoptotic effects following $P2X_7$ receptor activation in a number of cell types including renal cells (Schulze-Lohoff et al, 1998; Harada et al, 2000; Wang et al, 2004; Bulanova et al, 2005). Thus, $P2X_7$ receptor-dependent activation of apoptosis/necrosis in PKD may have a protective effect in reducing cyst development. In addition to cell death, $P2X_7$ receptor activation has been implicated in other responses in various cell lines, including cytokine (IL-1β) release from activated macrophages and microglial cells (Verhoef et al, 2003; Ferrari et al, 1997), cell

proliferation in human leucocytes (Baricordi et al, 1999) and membrane blebbing in renal cells (Verhoef et al, 2003). These alternative effects may contribute to the advancement/augmentation of the disease. However, overall, the functional significance of $P2X_7$ receptors to the pathophysiology of PKD is undefined and remains speculative.

Recent studies, performed on a rat model (Han-SPRD) of autosomal dominant PKD, provided evidence for increased renal mRNA levels for the $P2X_7$ receptor and $P2Y_2$ and $P2Y_6$ receptor subtypes. The increase in mRNA levels for $P2Y_2$ may explain the overriding proliferating effects in cyst development over the cyst-reducing apoptotic effects of $P2X_7$ (Turner et al, 2004).

2.5.2 Glomerulonephritis

Glomerulonephritis is a disorder caused by inflammation of the glomeruli, subsequently resulting in impaired filtration and proteinuria. An *in vivo* perfusion study demonstrated increased platelet aggregation in the glomeruli of nephritic rats treated with the poorly-hydrolysable adenine derivative, ADP-β-S (Poelstra et al, 1992). The same study also showed increased superoxide (O_2^-) production *in vitro* following application of ATP-γ-S to granulocytes of nephritic glomeruli, highlighting the significance of nucleotides in the advancement of the disease. In contrast to the above findings, the application of 2chloro-adenosine in the early phase of the same nephritic kidneys inhibited intraglomerular superoxide production, which was coupled with reduced proteinuria (Poelstra et al, 1992).

Tumour necrosis factor (TNF) has been shown to be essential for the development of glomerulonephritis, and this cytokine has been reported to stimulate a rise in the levels of mRNA for the $P2X_7$ receptor in mesangial cells; this potentially may lead to increased $P2X_7$ receptor expression, the activation of which has been shown to induce apoptosis/necrosis as indicated above (Harada et al, 2000; Vielhauer et al, 2005).

2.6 Physiological concentrations of nucleotides in the kidney

As indicated in earlier sections, several studies have demonstrated physiological effects of nucleotides and nucleosides on renal tissues; and further studies have revealed that the response is in some cases reversed when higher concentrations of the same nucleotide/nucleoside or analogue are used. In the kidney, this may sometimes occur to counteract and reduce the severity of an induced effect. An example of this is given by adenosine, where the activation of A_1 receptors by nanomolar concentrations of the nucleoside promoted vasoconstriction in the afferent arteriole, whereas micromolar concentrations of adenosine activated A_2 (A_{2A} or A_{2B}) receptors and induced vasorelaxation in the same tissue (Maddox and Brenner, 2000). As described in Section 2.4.3, electrolyte transport may also be stimulated or inhibited, depending on the extracellular adenosine concentration. The same may also be true with nucleotides, where an array of purinoceptor subtypes with differing EC_{50} values may co-exist on the same membrane of native tissues.

Moreover, although ATP is a suitable agonist for both major families of P2 receptors, the effects elicted by activation of the different receptor subtypes may vary. For instance, stimulation of P2X receptors on the afferent arteriole induces vasoconstriction whereas stimulation of P2Y receptors induces vasodilatation. In this case the variation in response is largely attributed to the specific distribution of the P2 receptors on the afferent arteriole. P2Y receptors (inducing vasodilatory responses) are primarily activated by intrarenal infusion of ATP, suggestive of apical expression of these receptors, whereas the P2X receptors (inducing vasoconstrictive responses) are stimulated when ATP is introduced interstitially, suggesting that their expression is largely confined to the exterior of the same tissue. Thus, the response that the nucleotide or nucleoside elicits is not only dependent on the extracellular concentrations of the agonist but also on the site of its release (Chan et al, 1998).

2.6.1 Release of ATP

Several studies have reported basal release of ATP *in vitro* both in primary cultures of renal epithelial cells such as human proximal convoluted tubule and cortical epithelial

cells (Wilson et al, 1999) and in renal epithelial cell lines including MDCK-D_1 and HEK-293 cells (Ostrom et al, 2000).

In vitro quantification of ATP in bulk solutions from various tissues varies significantly from picomolar to low micromolar concentrations (Lazarowski et al, 2003a). *In vitro* studies using cell cultures are limited/complicated by techniques that may mechanically perturb cells during tissue isolation, cell centrifugation and other routine cell culture procedures, all of which may induce the release of ATP either by mechanical stimulation or through cell lysis/damage. The fact that the intracellular concentration of ATP in most tissues is ~5mM (Gordon, 1986) favours the movement of ATP out of the cell down a chemical gradient.

2.6.2 Measurement of nucleotide release

Several methods for the quantification of nucleotides in biological fluids have been adopted in past studies. The most favoured is the firefly luciferin:luciferase assay for quantification of ATP. In this reaction, ATP molecules that are present in biological/cell media fluid samples react with the substrate luciferin and the enzyme luciferase to ultimately produce oxyluciferin and photons of light (as given in the equation below).

$$\text{ATP} + \text{D-luciferin} + O_2 \xrightarrow{\text{luciferase}} \text{AMP} + \text{inorganic pyrophosphate} + \text{oxyluciferin} + \text{light}$$

The intensity of light yielded is measured using a luminometer (represented in arbitrary units) and is proportional to the amount of ATP present in the fluid. This assay is applied widely and is highly sensitive for quantification of ATP.

Other methods of nucleotide detection include high performance liquid chromatography (HPLC), which allows the detection of a variety of nucleotides and their respective products of hydrolysis, such as di- and mononucleotide as well nucleoside formations. However, this assay is often limited to measurement of nucleotides in bulk solutions and in many cases detection/quantification is

misrepresented by other purine- or pyrimidine-based tri- or dinucleotides migrating and being detected at the same time as the nucleotide of interest.

2.6.3 Quantification of ATP release at the cell surface

Measurement of nucleotides in bulk solutions surrounding cells is unlikely to represent physiological levels present near the cell surface, i.e., in the vicinity of P2 receptors. This is predominantly attributable to local hydrolysis by membrane-bound or soluble nucleotidases located on or released by the same or adjacent cell. Therefore, in recent years, novel methods have been developed to determine ATP concentrations near the cell surface. One method involves anchoring the luciferase molecule indirectly to the plasma membrane of the cell via a protein, IgG, and a plasma membrane complex (as shown in Fig. 2.6). The advantage of this is that the conjugated luciferase molecule will favourably compete against cell-surface ectonucleotidases for an ATP molecule released from the same or neighbouring cell, thereby indicating the concentration of ATP release in 'real time' at the cell surface (Schwiebert, 2001).

This method, as well as other methods incorporating the concept of membrane-bound luciferase, has so far been limited to *in vitro* studies using cells or cell lines grown in culture, including human embryonic kidney (HEK-293) cells (Pellegatti et al, 2005) and platelets (Beigi et al, 1999), where basal/quiescent ATP concentration at the cell surface was reported to be widely different in the two tissues: 80 $\pm$ 20 nM and 15-20 μM, respectively. Notably, in a recent study comparing ATP concentrations at the cell surface and in the bulk medium of a single cell type, cell-surface ATP concentration in airway epithelial Calu-3 cells under basal conditions was reported as 7.3 $\pm$ 0.6 nM, similar to that measured in the bulk medium 2.6 mm from the cell surface in media (7.6 $\pm$ 0.7 nM) taken from the same cell line (Okada et al, 2005). However, when ATP secretion was stimulated, there was a major difference between the measurements made at the two sites (645 $\pm$ 63.5nM and 34.1 $\pm$ 5.6nM, respectively).

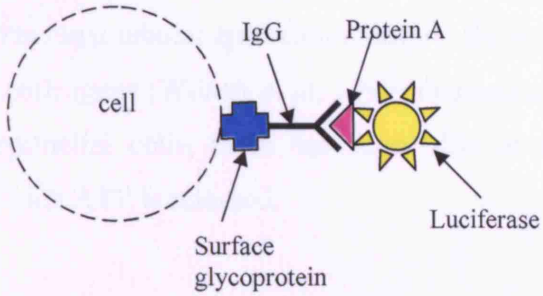

Fig. 2.6: Schematic diagram showing the conjugation of luciferase enzyme to the plasma membrane.

2.7 Mechanism of ATP release

Until recently, it was generally assumed that the only source of extracellular ATP was from cells that were either damaged or undergoing apoptosis. However, the physiological release of ATP from healthy and intact cells is now increasingly being recognised.

Using transfected and non-transfected cell lines or selective inhibitors, various transporters and channels have been proposed to be involved in ATP transport across the cell membrane. These include transporters of the ATP binding cassette (ABC) proteins, such as cystic fibrosis transmembrane regulator (CFTR) and multi-drug resistant (MDR-1) gene product, P-glycoprotein, and channels, such as large anion channels and connexin hemichannels (Reisin et al, 1994; Cantiello, 2001; Roman et al, 2001; Sabirov et al, 2001; Cotrina et al, 1998; Bahima et al, 2005). However, other studies using similar experimental procedures believe that these transporters or channels either do not directly mediate, or, in some cases, do not have any role in the release of ATP from cells (Reddy et al, 1996, Sabirov et al, 2001; Dutta et al, 2004, Roman et al, 2001; Hazama et al 1999; Hazama et al 2000). In addition to release via transporters or channels, various other workers have shown ATP release to occur via exocytosis in many cells (including non-neuronal cells) (Bodin and Burnstock, 2001; Suzuki et al, 1997; Mitchell et al, 1998; Sorensen and Novak, 2001). A full account of all these release mechanisms will be dealt with in Chapter 4.

With respect to the renal tubular epithelium, despite the *in vitro* observations made by Schwiebert and colleagues (Wilson et al, 1999) demonstrating the release of ATP in cultured renal epithelial cells, there has been little or no attempt to explore the mechanism by which ATP is released.

2.8 UTP as a signalling molecule

From Table 2.4, it can be seen that, in addition to adenine nucleotides, uridine tri- and dinucleotides are suitable agonists for several P2Y receptors including $P2Y_2$, $P2Y_4$ and $P2Y_6$. The concentration of extracellular UTP released under basal conditions from a variety of cell types, including platelets, leucocytes, astrocytes and primary cultures of airway epithelial cells, has been reported to range between 1 and 10nM (Lazarowski and Harden, 1999). Although these concentrations are insufficient to activate P2 receptors, it should be noted that these measurements were taken from the bulk media of cell cultures and therefore may not represent the concentration of UTP at the cell surface, in the vicinity of the P2 receptors. In a further study by the same group, stimulation of platelets with thrombin was reported to increase the extracellular UTP concentration 10-fold, to concentrations that *are* capable of stimulating $P2Y_2$ or $P2Y_4$ receptors (Lazarowski and Boucher, 2001; Lazarowski and Harden, 1999). The intracellular concentration of UTP is considerably lower than that of ATP, but greater than or equal to the levels of other nucleotides (Anderson and Parkinson, 1997). The mechanism by which uracil-based nucleotides are released is unknown, but it has been reported that both UTP and UDP, together with ATP, are stored in granules in chromaffin cells and platelets. Whether the same is true for synaptic vesicles is not known (Anderson and Parkinson, 1997).

2.8.1 UDP-glucose

The release of UDP-glucose has been demonstrated *in vitro* in response to mechanical stimulation in a variety of cell lines, including human bronchial primary epithelial

cells, human astrocytoma; Calu-3 (airway epithelial cells), CHO-K1 cells and COS-7 cells (Lazarowski et al, 2003b). Although the release UDP-glucose into the extracellular milieu was found to be 2-3 fold less than that of ATP, UDP-glucose had a longer half life. Thus, the mean UDP-glucose levels in the extracellular fluid over a 2 hour period were as high, or significantly higher, than ATP levels. In addition, the released UDP-glucose was sufficient to activate transfected $P2Y_{14}$ receptors (indicated by G protein-dependent inositol phosphate accumulation), which was reversed following the removal of UDP-glucose from the media by enzymatic degradation (Lazarowski et al, 2003b). Using fluorescent granular/vesicle probes (acridine orange and FM 1-43) that label granular compartments and sub-apical vesicles, and ionomycin to induce nucleotide release, the same group has recently suggested that UDP-glucose, in addition to other nucleotides such as ATP, UTP and UDP, is released via exocytosis from various epithelial cells such as Calu-3, A459, SPOC1 (airway epithelial cells) and HT-29 (human colonic carcinoma cells) (Lazarowski et al, 2005).

However, despite the above findings, to date, neither the release of UDP-glucose nor the expression of $P2Y_{14}$ receptors (receptive to UDP-glucose) has been reported in the kidney.

2.9 Degradation of ATP

As described above, the expression of many P2 receptor subtypes along the nephron has been established by immunohistochemical, functional and mRNA studies. If ATP is released into the tubular lumen, the nucleotide would be expected to act on P2 receptors on adjacent or neighbouring cells to elicit various responses. Alternatively, nucleotides that are released at one nephron site may potentially travel downstream to activate purinoceptors and induce responses (that may not necessarily be desired) in more distal segments of the same nephron. In this context, the expression of a group of enzymes, collectively known as ectonucleotidases, that specialise in the hydrolysis of nucleotides and are located on the surface membranes of epithelial and endothelial cells, influences the activation of purinoceptors. Through their hydrolytic activity, these enzymes provide a mechanism whereby the physiological effects of

extracellular nucleotides may be terminated. At the same time, degradation of ATP and ADP also serves as a source of adenosine, which might then activate adenosine receptors.

To date, four families of these ectonucleotidases are known to exist: ectonucleotide pyrophosphatase phosphodiesterases 1-3 (NPP 1-3), ectonucleoside triphosphate diphosphohydrolases 1-8 (NTPDases1-8), ecto-5'-nucleotidase and alkaline phosphatase. These families of enzymes differ in their hydrolysis pathways and/or in their affinities for nucleotides, and their specific expression along various segments of the nephron may serve to either terminate or augment purinoceptor-mediated responses. As will be discussed in detail in Chapter 5, information on ectonucleotidase distribution along the nephron is limited. Whilst the expression of ecto-5'-nucleotidase and alkaline phosphatase are reasonably well documented, relatively little is known about the NPP and NTPDase families.

2.10 Ectokinases

Ectokinases are enzymes that catalyze the transphosphorylation of nucleoside diphosphates to nucleoside triphosphates and include membrane-bound or secreted enzymes such as adenylate kinase or nucleoside monophospho- and diphosphokinases (Schwiebert, 2003). Transphosphorylation of nucleoside diphosphates occurs using other nucleoside-based triphosphates as the γ-phosphate donor. For example, UDP may be converted to UTP in the presence of ATP (which, being the phosphate donor, would then be converted into its diphosphate form, ADP). The activity and influence of these ectokinases on purinoceptor signalling has been partially examined *in vitro*, using astrocytoma cells stably expressing the $P2Y_4$ (sensitive to UTP) receptor. The report concluded that co-addition of UDP and ATP resulted in a marked increase in intracellular Ca^{2+} concentration, suggesting $P2Y_4$ activation following interconversion of UDP to UTP. Generation of other nucleoside triphosphates such as ATP, GTP and CTP was also observed from the corresponding radiolabelled diphosphate nucleotides, with nucleoside diphosphokinase (NDPK) showing substrate preference for ADP or GDP over UDP. Similarly, ATP and GTP were favoured as γ-phosphate donors over UTP and CTP, with CTP being the least favoured substrate for this enzyme.

Moreover, activity of NDPK was reported to be approximately 20-fold higher than that of an ectonucleotidase (Lazarowski et al, 1997). (Unfortunately, the study did not specify the particular ectonucleotidase tested.)

Northern blot analysis has identified the mRNA of NDPK in the rat kidney (Kimura et al, 1990), and the activity of this enzyme was found to be high in the proximal convoluted tubule, thick ascending limb and distal convoluted tubule of the rat (Cole et al, 1982). The latter study also reported the activity of other relevant enzymes: (i) adenylate kinase, involved in the conversion of AMP to ADP, was found to have highest activity in glomeruli, proximal segments, thick ascending limb of Henle and distal convoluted tubule; (ii) phosphodiesterases, which convert cAMP and cGMP into 5'-AMP and 5'-GMP respectively, had high activity in the glomeruli and distal tubular segments and low activity in the proximal segments; and (iii) guanylate kinase, which is involved in the conversion of GMP to GDP, had consistent activity throughout all segments of the nephron.

Overall, the presence of extracellular nucleoside diphosphates may provide suitable substrates for ectokinases in the presence of secreted nucleoside triphosphates to influence and, more importantly, complicate our ability to understand purinoceptor activation.

2.11 The present investigation

In order to answer a number of the questions raised concerning the purinoceptor system and renal function, three approaches were adopted in the present investigation. Firstly, because the intraluminal concentrations of ATP within the nephron are unknown *in vivo*, it is not clear whether apical P2 receptors (known to be present along the nephron) are activated during normal physiological conditions. Therefore, using micropuncture in anaesthetised rats, I attempted to detect and quantify the levels of ATP present in tubular fluid from superficial nephrons *in vivo*, both under control conditions and during pathophysiological manoeuvres. Furthermore, by directly comparing ATP levels in fluid collected from the Bowman's capsule and from proximal tubular fluid, I also assessed whether the ATP that was found in tubular fluid is filtered from the blood at the glomerulus or released from proximal tubular cells.

Secondly, since ATP was found to be released/secreted by proximal tubular cells, I investigated the mechanism of its release, using a proximal tubular epithelial cell line. Intracellular stores of ATP were visualised using an intracellular ATP marker, and the fate of these stores was monitored following stimulation of ATP release.

Finally, because current knowledge of the distribution of ectonucleotidases along the nephron is fragmentary and incomplete, I used immunohistochemistry to examine the expression of five major ectonucleotidases along the nephron. The enzymes studied were NTPDase1, NTPDase2, NTPDase3, NPP3 and ecto-5'-nucleotidase. Using antibodies specific to well-defined segments of the nephron, the distribution of these enzymes was examined in the proximal tubule, the TAL, the distal tubule and the collecting duct.

CHAPTER 3

MICROPUNCTURE ASSESSMENT OF TUBULAR FLUID ATP CONCENTRATIONS

3.0 INTRODUCTION

As described in the preceding chapter (see Section 2.3), an array of P2 receptors is expressed along the renal epithelium; and activation of intraluminal purinoceptors either *in vivo* or *in vitro* using stable nucleotide-based analogues has been shown to have modulatory effects on solute and water transport across various segments of the nephron. These findings clearly support the proposal that intraluminal nucleotides, acting on apical P2 receptors, can function as autocrine/paracrine regulators of tubular transport.

Before making such inferences concerning a functional role of intraluminal nucleotides, however, it is necessary to ascertain whether their normal endogenous concentrations are sufficient to activate P2 receptors, and whether they can be influenced by physiological/pathophysiological manoeuvres known to affect tubular transport.

ATP secretion by renal epithelial cultures and by cell lines derived from specific nephron segments has previously been reported by Schwiebert's group (Schwiebert et al, 2003; Wilson et al, 1999). It was shown that cultured cells released measurable amounts of ATP into both apical and basolateral media, with apical release predominating. However, although *in vitro* studies are useful pointers, determinations of ATP concentrations in cell culture media clearly cannot provide information on ATP concentrations in the tubular lumen *in vivo*. To date, no such measurements in native, intact tubules have been reported. The purpose of the present study, therefore, was to assess endogenous ATP concentrations within the lumen of proximal and distal tubules of the rat nephron, and to determine whether the ATP was filtered or secreted. Tubular fluid samples were obtained using *in vivo* micropuncture techniques, and the samples were assayed for ATP using the luciferin/luciferase reaction.

3.1 SECTION 1: The effects of anaesthesia and micropuncture surgery on renal function

3.1.1 Introduction

First developed in 1924 by J.T. Wearn and A.N. Richards, micropuncture was one of the greatest advances in renal physiology during the 20th century. The technical skills required to puncture a glomerular capsule or tubule with a micropipette and measure the composition of its fluid are challenging; but the novel scientific findings that have resulted from using this technique are of fundamental importance in helping us to understand renal function (Sands, 2004). Although a large number of studies have employed micropuncture techniques in order to determine directly the changes that occur in specific sites of the nephron, relatively little research has been made into the influence of anaesthesia and surgical preparation for micropuncture on overall renal function. Nevertheless, because of its importance, this section will briefly focus on the possible effects of anaesthesia and surgery on GFR and tubular function.

3.1.2 GFR

In the rat, a reduction in GFR was reported following anaesthesia with thiobutabarbitone (Atherton et al, 1983; Walker et al, 1983; Atherton and Jammaz, 1986) or pentobarbitone (Walker et al, 1983; Mercer and Kline, 1984). Thomsen and Olesen (1981) found that amylobarbital anaesthesia plus surgery reduced GFR in Wistar rats but not in Sprague-Dawley rats. In agreement with the latter observation, Shirley et al (1990) found that GFRs in Long-Evans rats anaesthetised with thiobutabarbitone and surgically prepared for micropuncture were comparable to those in the same rats when conscious; and Chamberlain (1996) reported similar findings following anaesthesia with thiopentabarbitone and surgery in the Sprague-Dawley rat. In contrast, a study by Holstein-Rathlou et al (1982) reported that GFR was reduced in Wistar or Sprague-Dawley rats following halothane-nitrous oxide or thiobutabarbitone anaesthesia and micropuncture surgery, when compared with that in separate groups of acutely catheterised conscious animals. One possible explanation

for this discrepancy is that in the studies by Shirley et al (1990) and Chamberlain (1996) a flank incision was used to expose the left kidney, whereas Holstein-Rathlou et al (1982) employed a mid-line approach, which, being more invasive, has been shown to result in a greater depression of renal haemodynamics (McVicar, 1988). Table 3.1.1 shows a summary of the findings.

Anaesthetic	Strain	Surgery	Effect on GFR	Reference
Thiobutabarbitone	Sprague-Dawley	-	Decreased	Atherton & Jammaz (1986)
Pentobarbitone/Thiobutabarbitone	Long-Evans	-		Walker et al (1983)
Thiobutabarbitone	Wistar	-		Atherton et al (1983)
Pentobarbitone	Wistar	-		Mercer & Kline (1984)
Amylobarbital	Wistar	+	Decreased	Thomsen & Olesen (1981)
Thiobutabarbitone	Sprague-Dawley	+		
Thiobutabarbitone	Sprague-Dawley	+	No change	Knight et al (1978)
Amylobarbital	Sprague-Dawley	+	No change	Thomsen & Olesen (1981)
Thiobutabarbitone	Long-Evans	++	No change	Shirley et al (1990)
Thiopentabarbitone	Sprague-Dawley	++		Chamberlain (1996)
Halothane-nitrous oxide	Wistar and Sprague-Dawley	++	Decreased	Holstein-Rathlou et al (1982)
Thiobutabarbitone				

Table 3.1.1: The effect of anaesthesia with or without (+/-) surgery on GFR in the rat (- anaesthesia alone; + clearance surgery; ++ micropuncture surgery).

3.1.3 Excretion rates of sodium and water

It is generally accepted that anaesthesia and surgery can reduce excretion rates of sodium and water. In the rat, reductions in the urinary excretion of sodium and water have been reported following thiobutabarbitone (Atherton et al, 1983; Atherton and Jammaz, 1986) or pentobarbitone (Walker et al, 1983) anaesthesia alone, and after thiobutabarbitone (Maddox et al, 1977; Knight et al, 1978; Shirley et al, 1990),

amylobarbitol (Thomsen and Olesen, 1981) or thiopentabarbitone (Chamberlain, 1996) anaesthesia plus surgery. However, in the study by Walker et al (1983), the reductions in sodium and water excretion during pentobarbitone anaesthesia, after surgery, in the Long-Evans rat were variable and only transient. Furthermore, Thomsen and Olesen (1981) reported that sodium clearance in Sprague-Dawley rats during amylobarbital anaesthesia (without surgery) was no different from that in conscious unoperated animals. Similarly, Walter et al (1989) reported that sodium and water excretion rates in rats after thiobutabarbitone anaesthesia and preparation for clearance surgery were no different from those found in the same rats during their inactive period (i.e., during daylight hours). Table 3.1.2 shows a summary of the findings.

Anaesthetic	Strain	Surgery	Effect on urinary excretion of sodium & water	Reference
Pentobarbitone	Wistar	-	Decreased	Atherton et al (1983)
Thiobutabarbitone	Sprague-Dawley			Atherton & Jammaz (1986)
Pentobarbitone	Long-Evans			Walker et al (1983)
Pentobarbitone	Wistar			Mercer and Kline (1984)
Amylobarbital	Sprague-Dawley	-	No change	Thomsen & Olesen (1981)
Thiobutabarbitone	Sprague-Dawley	+	Decreased	Knight et al (1978)
Pentobarbitone	Long-Evans	+	Variable	Walker et al (1983)
Thiobutabarbitone	Long-Evans	+	No change	Walter et al (1989)
Thiobutabarbitone	Wistar	++	Decreased	Maddox et al (1977)
Amylobarbital	Wistar			Thomsen & Olesen (1981)
Pentobarbitone	Wistar/ Sprague-Dawley			Thomsen & Olesen (1981)
Thiobutabarbitone	Long-Evans			Shirley et al (1990)
Thiopentabarbitone	Sprague-Dawley			Chamberlain (1996)

Table 3.1.2: The effect of anaesthesia with or without (+/-) surgery on urinary excretion rates of sodium and water in the rat (- anaesthesia alone; + clearance surgery; ++ micropuncture surgery).

3.1.4 Potassium excretion

Information concerning changes in the urinary excretion of potassium after anaesthesia and surgery is even more variable. A reduction in potassium excretion was found in rats anaesthetised with thiobutabarbitone or pentobarbitone alone (Walker et al, 1983), and after thiobutabarbitone (Maddox et al, 1977) or thiopentabarbitone (Chamberlain, 1996) anaesthesia plus surgery. However, Walker et al (1983) reported that, as with sodium, this reduction in potassium excretion was variable and transient. Furthermore, other studies have reported that potassium excretion was *increased* in the Long-Evans rat following thiobutabarbitone anaesthesia and surgical preparation for clearance (Walter et al, 1989) or micropuncture (Shirley et al, 1990). Thomsen and Olesen (1981) also found that potassium excretion tended to increase after amylobarbital anaesthesia plus surgery, but in this case the increase was not statistically significant. Table 3.13 shows a summary of the findings.

Anaesthetic	Strain	Surgery	Effect on K^+ excretion	Reference
Thiobutabarbitone Pentobarbitone	Long-Evans	-	Decreased	Walker et al (1983)
Amylobarbital	Wistar Sprague-Dawley	+	No change	Thomsen and Olesen (1981)
Thiobutabarbitone	Long-Evans	+	Increased	Walter et al (1989)
Thiobutabarbitone	Long-Evans	++	Increased	Shirley et al (1990)
Thiobutabarbitone Thiopentabarbitone	Wistar Sprague-Dawley	++	Decreased	Maddox et al (1977) Chamberlain (1996)

Table 3.1.3: The effect of anaesthesia with or without (+/-) surgery on urinary K^+ output in the rat (- anaesthesia alone; + clearance surgery; ++ micropuncture surgery).

3.1.5 Tubular reabsorption

The reductions in urinary excretion rates of water and electrolytes usually observed following anaesthesia and surgery may, in some cases, be explained by a reduced GFR and therefore filtered load. However, some studies that found reductions in GFR following anaesthesia plus surgery reported that the reductions in sodium and water excretion were greater than that in GFR (Thomsen and Olesen, 1981). Others found that excretion rates were reduced even in the absence of a change in GFR (Knight et al, 1978; Shirley et al, 1990). These findings therefore suggest that the reduction in urinary excretion rates of sodium and water is partly due to increased fractional sodium and water reabsorption in the tubule. In contrast, the study by Walker et al (1983) found that, although GFR was reduced, urine flow rate was unchanged after thiobutabarbitone anaesthesia in the Long-Evans rat, suggesting that anaesthesia and surgery was associated with a *decrease* in the fractional reabsorption of sodium and water. Using lithium clearance as an index of fluid delivery to the end of the proximal tubule (Thomsen and Shirley, 1997), Thomsen and Olesen (1981) reported that proximal fractional fluid reabsorption in the Long-Evans rat was unchanged after amylobarbital anaesthesia and clearance surgery in the Sprague-Dawley rat, when compared with that in conscious animals. Shirley and colleagues also found no change in lithium clearance after clearance or micropuncture surgery (compared with conscious, uncatheterized rats in their active period) (Walter et al, 1989; Shirley et al, 1990).

Beyond the proximal tubule, Atherton and Jammaz (1986), also using lithium clearance as an index of end-proximal fluid delivery, found that fractional fluid reabsorption in distal nephron segments was increased during thiobutabarbitone anaesthesia. Other studies using lithium clearance also reported that the fractional reabsorption of distally delivered sodium and water was increased after thiobutabarbitone anaesthesia and surgical preparation for either clearance (Walter et al, 1989) or micropuncture (Shirley et al, 1990). In contrast, Chamberlain (1996) found increased fractional reabsorption in the proximal *and* distal segments of the nephron following anaesthesia with thiopentabarbitone and surgery in the Sprague-Dawley rat. Table 3.1.4 shows a summary of the findings.

Anaesthetic	Strain	Surgery	Effect on tubular function	Reference
Amylobarbital	Sprague-Dawley	-	Proximal fractional fluid reabsorption unchanged	Thomsen and Olesen (1981)
Thiobutabarbitone Amylobarbital	Sprague-Dawley Wistar	-	Proximal fractional fluid reabsorption decreased	Atherton & Jammaz (1986) Thomsen and Olesen (1981)
Thiobutabarbitone	Sprague-Dawley	-	Fractional reabsorption in distal nephron increased	Atherton & Jammaz (1986)
Thiobutabarbitone	Long-Evans	+	Proximal fractional fluid reabsorption unchanged and fractional reabsorption in distal nephron increased	Walter et al (1989)
Thiobutabarbitone	Long-Evans	++	Proximal fractional fluid reabsorption unchanged	Shirley et al (1990)
Thiopentabarbitone	Sprague-Dawley	++	Fractional reabsorption in proximal and distal nephron increased	Chamberlain (1996)

Table 3.1.4: The effect of anaesthesia with or without (+/-) surgery on tubular reabsorption in the rat (- anaesthesia alone; + clearance surgery; ++ micropuncture surgery).

3.1.6 Possible causes of the effects of anaesthesia and surgery on renal function

Rogenes and Gottschalk (1982) reported that in rats that had been subjected to unilateral renal denervation, pentobarbitone anaesthesia caused greater reductions in the urinary excretion of sodium, potassium and water in the innervated kidney than in the denervated kidney, suggesting that the renal nerves were important in mediating the responses.

An increase in circulating levels of catecholamines could, in theory, reduce sodium and water excretion, by decreasing GFR and/or stimulating reabsorptive rates in the proximal tubule (Insel and Snavely, 1981). However, information on plasma catecholamine levels after anaesthesia and surgery is incomplete and conflicting. Joyce et al (1982) observed a significant rise in plasma noradrenaline concentration in patients anaesthetised with halothane, whereas a *reduction* in plasma levels of adrenaline and noradrenaline was reported in dogs anaesthetised with thiopentone (Gagnon et al, 1982) or pentobarbitone (Baum et al, 1985).

An increase in the plasma level of aldosterone has been reported in humans and in rats during anaesthesia alone (Pettinger et al, 1975; Oyama et al, 1979) or in combination with surgery (Hume et al, 1962; Cochrane, 1978; Fromm et al, 1983). The renin-angiotensin system plays a major role in mediating the secretion of aldosterone. Various studies have reported that anaesthesia, using cyclopropane, diethyl ether, halothane, ketamine, methoxyflurane, morphine, pentobarbitone or urethane is associated with an increase in serum renin activity (Pettinger et al, 1971; Tananka and Pettinger, 1974; Pettinger et al, 1975). More direct evidence to suggest that the renin-angiotensin system is important in mediating the renal response to anaesthesia and surgery was provided by Walker et al (1986), who reported that the reduction in GFR observed following pentobarbitone anaesthesia was prevented when rats were pretreated with captopril, an inhibitor of the angiotensin converting enzyme.

A possible role for vasopressin in mediating the decrease in urine flow rate during anaesthesia and surgery was suggested by a study demonstrating that the antidiuretic response to anaesthesia and surgery in humans was blunted by infusion of ethanol, which inhibits vasopressin secretion (Deutsch et al, 1967). However, whilst an increase in the plasma level of vasopressin after anaesthesia with diethyl ether, methoxyflurane or halothane has been reported (Oyama, 1973), others have found no significant effect of these or other anaesthetic agents on plasma vasopressin levels (Moran et al, 1964; Simpson and Forsling, 1976; Philbin and Coggins, 1978; Cochrane et al, 1981).

3.1.7 Conclusion

The above studies illustrate that, whilst the findings from *in vivo* micropuncture studies may represent observations close to the physiological state, they by no means absolutely represent it. Nevertheless, as with *in vitro* experiments, findings from *in vivo* studies provide a stepping stone to our understanding of physiological systems.

The above studies also show that the effects of anaesthetics and micropuncture surgery on renal function are variable, depending on the type of anaesthetic employed as well as the procedure adopted for surgery, and indeed on the strain of animal. In the present investigation, thiopentone was used to anaesthetise Sprague-Dawley rats and a flank incision was adopted to expose the left kidney; the latter has been found to cause less disruption to renal function than the mid-line incision. There has been little attempt to explain the vastly different findings between studies, but it seems likely that a major factor is the skill of the worker in performing the surgery.

3.2 SECTION 2: Assessment of the micropuncture preparation

3.2.1 Introduction

In the first part of this study, renal function was assessed after micropuncture surgery in rats. Radiolabelled inulin (infused intravenously) was used to determine GFR. With a molecular weight of 5500, inulin is the ideal substance to use as it is small enough to pass freely through the glomerular filtration barrier and is neither reabsorbed, secreted nor metabolized by the kidney. Thus, the volume of plasma that is cleared of inulin per unit time is equal to the total GFR.

In order to assess the preparation and micromanipulative skills required in micropuncture experiments, both GFR and individual superficial nephron filtration rates (SNGFR) were determined, and the values were compared with those reported in the literature.

3.2.2 Methods

3.2.2.1 Surgical preparation of animal

Male Sprague-Dawley rats that had been allowed free access to water and a standard rat diet (140mmol of Na^+ and 180mmol K^+ kg^{-1} dry weight) were anaesthetized with an intraperitoneal injection of sodium thiopentone (100mg kg^{-1} body weight; Link Pharmaceuticals Limited, Horsham, UK), and prepared surgically for micropuncture. Rectal temperature was maintained at 37°C using a homeothermic heating blanket. The right jugular vein was cannulated to allow the administration of 0.9% saline (at a rate of 4ml/hr), supplementary doses of anaesthetic and radiolabelled inulin. A tracheotomy was performed and the bladder was cannulated for urine collections and to prevent reflex effects from bladder distension. The right femoral artery was cannulated with polyethylene tubing containing heparinised saline for the collection of blood samples.

A lateral section of the body wall was then cauterized and the left kidney exposed and placed in a Perspex kidney cup, with a gap to allow entry/exit of renal vessels and the ureter; the cup was clamped to the operating table to restrict movement of the kidney. Mineral oil was used consistently throughout the procedure to prevent internal tissues from drying out. The kidney was further immobilized by gently placing absorbent cotton wool around it in the empty spaces inside the kidney cup. The ureter of the left kidney was cannulated for the collection of urine samples. The rats were then left to equilibrate for two hours before the clearance study (and before any tubular fluid collections were made).

3.2.2.2 Clearance measurements

After 1 hour of equilibration, a bolus injection of [^{3}H] inulin (30μCi; Amersham Biosciences, Chalfont St Giles, Bucks, UK), followed by the immediate infusion of [^{3}H] inulin (30μCi/hr) prepared in isotonic saline, was administered via the jugular cannula. One hour later, when the [^{3}H] inulin had equilibrated, clearance determinations were begun. Urine from each kidney was collected into previously weighed pots. Before the first urine collection, a small (~100 μl) blood sample was taken from the cannulated femoral artery. Using micropuncture, proximal tubular fluid samples were also collected (as described below) throughout the course of the experiment. Urine collections were made at approximately 1 hour intervals; small blood samples (~100μl) were taken at the start and end of each urine collection period. An outline of the experimental protocol is shown in Fig. 3.2.1

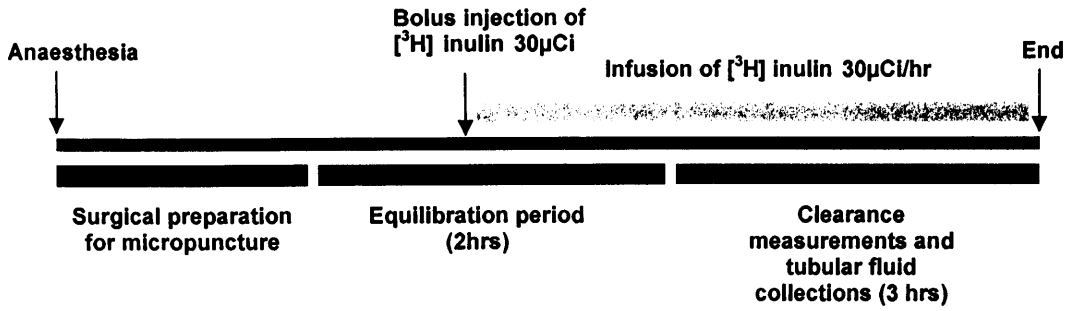

Fig. 3.2.1: Outline of experimental protocol for clearance study

3.2.2.3 Tubular fluid collections - SNGFR measurements

Sharpened glass micropipettes (10 μm tip diameter), filled with Sudan black-stained oil, were carefully inserted into superficial proximal tubules, using a micromanipulator (Leitz, Wetzlar, Germany). Once the tip was inside the lumen, identification of the proximal tubule was confirmed by injecting small droplets of the Sudan black-stained oil. The number of reappearances of the droplet flowing along the proximal convolutions gave an indication of the number of loops remaining before the end of the proximal convoluted tubule, thereby indicating the position of the micropipette (see Fig. 3.2.2). Once the position of the micropipette was confirmed, a column of the oil (4-5 tubule diameters in length) was injected downstream into the proximal tubule, to occlude the tubule and ensure complete collection. The tubular fluid arriving upstream of the oil column was then collected into the same micropipette for 8-10 minutes. During this collection, the oil column needed to remain stable *in situ*, as this would indicate that the rate of fluid collection was the same as the tubular fluid flow rate. Tubular fluid samples were taken throughout the course of the experiment (and measured for [^{3}H] inulin activity) for SNGFR measurements, as described below.

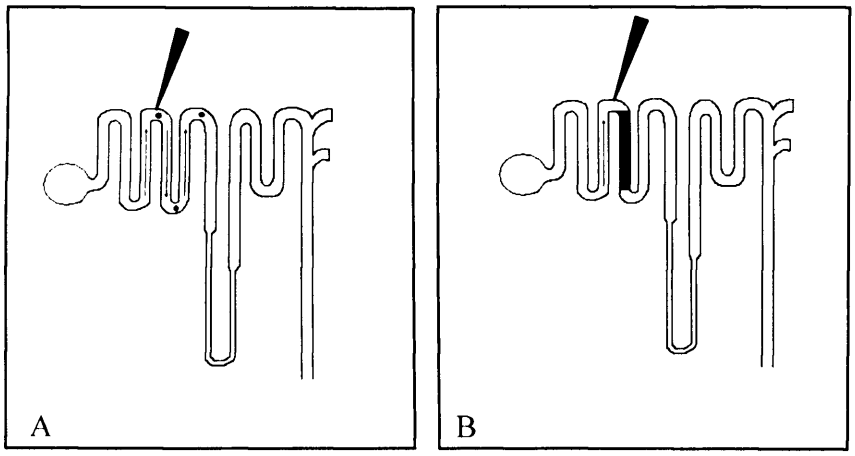

Fig. 3.2.2: (A) Schematic diagram of the nephron and site of puncture (proximal convoluted tubule) with an oil-filled micropipette. Droplets of oil are deposited into the tubule which travel along the nephron, reappearing in the adjoining superficial convolutions. (B): Once the position of the pipette is confirmed, a column of oil is deposited immediately downstream of the site of puncture; tubular fluid filtered upstream of the site of puncture is then collected into the same pipette.

3.2.2.4 Analyses

(i) Measurement of tubular fluid

With the aid of a microscope, all micropuncture collections were initially deposited onto a watch-glass under mineral oil and their volumes measured using calibrated constriction pipettes.

(ii) Calibration of constriction pipettes

Previously prepared constriction glass pipettes were calibrated using [^{3}H] inulin. For this, a droplet of the [^{3}H] inulin infusate was deposited under oil and aliquots were subsequently taken up by the pipette to the constriction site. The [^{3}H] inulin was then deposited into scintillation vials containing 8ml Aquasol 2 (Perkin Elmer Life Sciences, Cambridge, UK) and later measured for activity. This procedure was repeated at least three times for each pipette. The volume taken up by the constriction pipette was calibrated against 10µl of the same [^{3}H] inulin standard.

(iii) Assessment of tubular fluid absorption by mineral oil

Because the volumes of tubular fluid were small (~200nl), any absorption of fluid/water by the mineral oil (however trivial) would cause significant inaccuracies in the measurement SNGFR. Therefore, known volumes (either 38 or 82nl) of tubular fluid were deposited under oil and measured subsequently using the same constriction pipette. In these experiments no differences in tubular fluid volumes were found when measured immediately, 30 min, 2 hrs or 48 hrs after deposition; confirming that mineral oil does not absorb tubular fluid.

(iv) Analyses of [^{3}H] inulin activity in plasma, urine and tubular fluid samples

Blood samples taken from the cannulated femoral artery were deposited into a heparinized tube and immediately spun (at 1300 rpm for 3 minutes) to separate the blood plasma from the erythrocytes. Using a microcap, 10µl of plasma was accurately measured and dispensed into a vial containing 8ml Aquasol 2 for liquid

scintillation counting. Tubular fluid volumes were measured as described above using calibrated constriction pipettes. Duplicate samples (38nl) of fluid from the same collection were accurately measured and deposited into separate vials containing 8ml Aquasol 2. Using a microcap, 10µl samples of urine (from each kidney; diluted 1 in 10) were deposited into separate scintillation vials containing 8ml Aquasol 2. All samples deposited in Aquasol 2 were then measured for [^{3}H] inulin activity using β-emission spectroscopy (model 2900 TR, Packard, Pangbourne, UK).

(v) Calculation of GFR

The clearance of [^{3}H] inulin was used to calculate GFR. The following formula was applied:

$$C_{IN} = (U_{IN} / P_{IN}).V,$$

where C_{IN} is the clearance of [^{3}H] inulin, U_{IN} is the [^{3}H] inulin activity in urine, P_{IN} is [^{3}H] inulin activity in the plasma and V is the urine flow rate.

(vi) Calculation of SNGFR

SNGFR was calculated using the equation below:

$$SNGFR = (TF_{IN} / P_{IN}).V_{TF,}$$

where TF_{IN} is the [^{3}H] inulin activity in tubular fluid, P_{IN} is the [^{3}H] inulin activity in plasma and V_{TF} is the tubular fluid flow rate.

(vii) Analysis of Na^+ and K^+ in urine

Urinary sodium and potassium concentrations were measured by flame photometry (Model 543, Instrumentation Laboratory, Warrington, UK).

(viii) Transit time measurements

Proximal and distal tubular transit times were measured using Lissamine green (Steinhausen, 1963), where 30µl of a 5% (w/w) solution of Lissamine green dye was injected into the jugular cannula. The proximal transit time was taken as the delay

between the initial "blush" of dye on the kidney surface and the convergence of columns of dye in late proximal tubules before their descent beneath the surface to the pars recta. The distal transit time was taken as the delay between the initial blush of dye on the kidney surface to the earliest appearance of dye in distal tubules.

(ix) Statistics

Results are expressed as means ± standard error of the means (SEM). Mean values were compared using Student's paired *t* test. The difference between two mean values was considered statistically significant when $P < 0.05$.

3.2.3 Results

3.2.3.1 Urinary flow rate and Na^+ and K^+ output

Table 3.2.1 shows urinary flow rate and Na^+ and K^+ outputs from both micropunctured and contralateral kidneys. There were no significant differences between the micropunctured and contralateral (non-micropunctured) kidneys with respect to any of these variables ($P = 0.731$, $P = 0.961$, $P = 0.089$ for urine flow rate, Na^+ excretion and K^+ excretion, respectively).

3.2.3.2 GFR and SNGFR

Values for GFR were calculated for both micropunctured and contralateral kidneys and are given in Table 3.2.2. Corresponding SNGFR values for the same rats are also shown. Each GFR value shown is an average of 2-3 measurements, whereas each SNGFR value is an average of 2-4 measurements per rat. In any given animal, these measurements showed little change over the course of the experiment. The mean GFR values obtained for both the micropunctured and contralateral kidneys are well within the normal range for rats of this size (220 – 280g). The same is true for the SNGFR values. The small difference in GFR between the two kidneys was not significant statistically ($P = 0.4$).

Urinary flow rate (µl/min)	Micropunctured kidney	18.3 ± 6.2
	Contralateral kidney	16.4 ± 6.3
Na^+ output (µmol/min)	Micropunctured kidney	3.3 ± 0.6
	Contralateral kidney	3.3 ± 0.5
K^+ output (µmol/min)	Micropunctured kidney	2.0 ± 0.4
	Contralateral kidney	1.6 ± 0.3

Table 3.2.1: Urinary flow rate and Na^+ and K^+ output in the micropunctured and contralateral kidney during the experimental period (means ± SEM; n = 7).

	GFR (ml/min)		**Proximal tubule SNGFR (nl/min)**
	Micropunctured kidney	**Contralateral kidney**	
	0.94	1.16	38.0
	0.88	0.76	30.8
	0.82	0.88	39.9
	1.15	1.21	23.8
	0.98	1.24	29.5
	1.04	0.91	44.3
	1.24	1.25	39.9
Mean ± SEM	**1.01 ± 0.06**	**1.06 ± 0.08**	**35.2 ± 2.7**

Table 3.2.2: GFR and SNGFR values (means ± SEM; n = 7).

3.2.3.3 Transit times

Proximal and distal transit times were 8.9 ± 0.4 seconds and 28.6 ± 0.9 seconds (n = 7), respectively. The value in each individual animal was derived from four measurements.

3.2.4 Discussion

During micropuncture experiments not only is the surgical setup of the animal of vital importance but also the micromanipulative skills required for the puncturing and collection of fluid from tubules; during these collections, the hydrostatic intratubular pressure should remain constant. Falls in pressure in the tubule resulting from the application of excessive negative pressure at the pipette may be transmitted to the Bowman's capsule and may lead to inaccurate SNGFR results. Movements in the oil column are indicative of unwanted pressure changes. The application of insufficient negative pressure at the pipette would result in the oil column drifting away from the site of collection; alternatively, excessive collection would lead to the distal oil column moving back up into the pipette. Thus, when the oil column remains stable *in situ*, the rate of tubular fluid collection should be the same as the tubular flow rate, with little or no change in intraluminal pressure.

The GFR values found in this study were within the normal range and relatively constant in both kidneys over the course of the experiment. The consistency in results suggests that the rat was in a stable condition following surgery and indicates competence in the surgical setup. This is supported by the corresponding SNGFR values obtained, which were also within the normal range. Furthermore, no significant differences in urinary flow rates or urinary Na^+ and K^+ outputs were observed between the micropunctured and contralateral kidneys. Finally, both proximal and distal tubular transit times were consistent with normal renal function, and showed no significant variation over the course of the experiment in any given rat. All these results indicate that the exposure and extra manipulation of the micropunctured kidney had not adversely affected its overall function.

Limitations of SNGFR measurements Although the GFRs were well within the normal range, on the assumption that there are 35,000 nephrons in a rat kidney (Kaufman et al, 1976) the mean SNGFR value (35.2nl/min) is marginally high, compared with the corresponding whole-kidney GFR (1.01 ml/min). This small discrepancy was no different from, and certainly no worse than, that seen in most published studies. Although a widely accepted procedure for assessment of SNGFR, micropuncture is not without limitations. Previous reports have documented that SNGFR measured from proximal tubular collections is usually higher than that measured from distal tubular collections, in both rats and dogs (Navar et al, 1974). This difference has been attributed to the tubular blockade during proximal tubular micropuncture collections. The reduced flow rate to the macula densa triggers the TGF response mechanism to cause vasodilatation of the afferent arteriole (see Introduction). In this way SNGFR is increased in attempt to restore tubular flow rate. In contrast, SNGFR measured from distal tubular collections is not subject to this artefact.

3.3 SECTION 3: Measurement of ATP in the renal tubule

3.3.1 Introduction

In an initial pilot study, to ascertain whether intraluminal ATP concentrations were measurable, tubular fluid from the proximal tubule was collected using micropuncture and was assayed for ATP concentration using the luciferin-luciferase assay. In the second part of the investigation, ATP levels in tubular fluid derived from accessible early, mid and late portions of the S2 segment of the superficial proximal tubule were compared. Finally, ATP levels in tubular fluid from superficial distal tubules were compared with those in the proximal tubule.

3.3.2 Methods

3.3.2.1 Proximal tubular collections for ATP measurements

Six male Sprague-Dawley rats were anaesthetised and prepared surgically for micropuncture in accordance with the protocol described above (see Section 3.2.2.1). Following equilibration, tubular fluid collections were made from superficial proximal tubules using a micropipette (as described above Section 3.2.2.3). If the number of convolutions (as indicated from the number of oil droplet reappearances) were greater than three, the site of puncture was assumed to be the proximal convoluted tubule rather than the distal tubule (which usually has no more than two convolutions). Following the tubular fluid collection (each collection lasting 4 mins), the sample in the pipette was immediately deposited onto a watch-glass, under mineral oil, and the volume measured using a previously calibrated constriction pipette. For measurement of ATP, the tubular fluid sample was then deposited into a vial containing 50µl of ice-cold water and immediately frozen to halt the degradation of ATP. A total of 6-10 collections (600 - 1000nl) of proximal tubular fluid were pooled to allow the measurement of ATP using the luciferin-luciferase enzyme reaction, the vial being kept frozen between additions of fresh collections. This

procedure was adopted for quantification of ATP concentration in all tubular fluid collections.

3.3.2.2 ATP measurements

The amount of ATP in the samples was quantified by luminometry using the luciferin-luciferase assay. In this technique, luciferin-luciferase reagent (ATP reagent SL, Bio Thema, Sweden) was reconstituted with 15ml of deionised 18.2mΩ grade water in a clean vial and mixed thoroughly. Once reconstituted, the reagent was protected from light using aluminium foil and left to stand for 20-30 minutes at room temperature. ATP standards, as well as water (used for blank/background reading), were subsequently pipetted (50µl) into a white (nonphosphorescent) 96-well microplate. The plate was placed in a luminometer machine (Lucy 1, Anthos Labtech, Salzberg, Austria) and 100µl of the luciferin-luciferase reagent was then automatically loaded into each well and the light emitted from the reaction given in the equation below was measured and quantified.
Firefly luciferase catalyses the following reaction:

$$\text{ATP} + \text{D-luciferin} + O_2 \xrightarrow{\text{luciferase}} \text{AMP} + \text{inorganic pyrophosphate} + \text{oxyluciferin} + \text{light}$$

The reagent contains D-luciferin as substrate, inorganic pyrophosphate, which stabilizes the light emission, and bovine serum albumin, which stabilizes the reagents, avoiding the inactivaton of luciferase.

After the establishment of a standard curve, frozen vials containing tubular fluid samples from the micropuncture experiments were quickly thawed and immediately loaded into empty wells of the same plate and measured using the same procedure described above. Following this, ATP standards were then loaded again into empty wells of the same plate and read again, using the procedure described above. This was to test whether any significant change in the values for ATP standards had occurred over the course of the measurements. In no case was this seen. The ATP concentrations in the tubular fluid were then calculated from the calibration curve

constructed from the ATP standards (see Fig. 3.3.1 for typical calibration curve). The detection limit was calculated using the mean baseline noise plus 3 standard deviations of the baseline noise in a sample of deionized water.

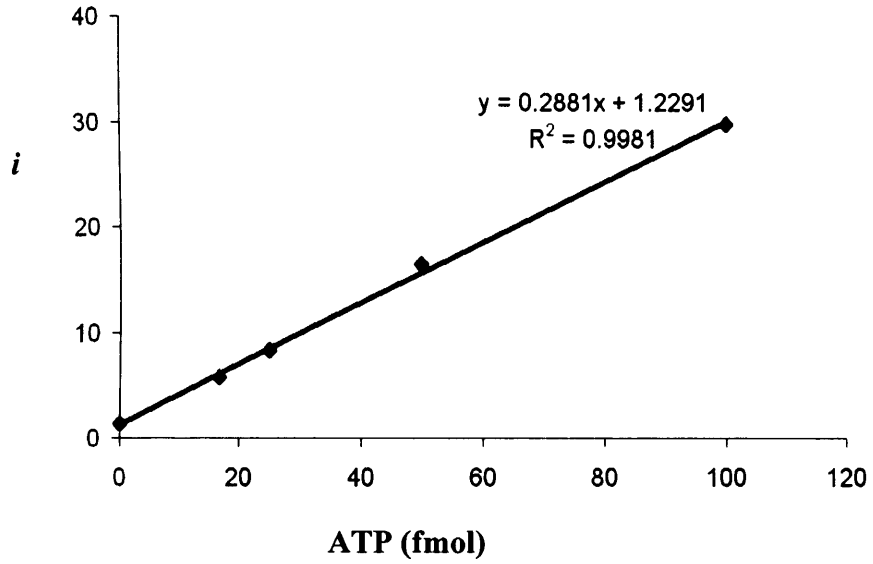

Fig. 3.3.1: A typical ATP calibration curve, where i is a measure of the light intensity emitted from the luciferin-luciferase reaction. This standard curve varied little between experiments.

In these initial pilot studies the ATP concentration found in random superficial S2 proximal tubular segments was 267 ± 24 nmol/l (mean ± SEM). These levels of ATP would be high enough to stimulate some P2 receptor subtypes (Schwiebert et al, 2003; King and Townsend-Nicholson, 2003). Therefore, in further investigations, direct comparisons were made between the luminal ATP concentrations of different (early, mid and late) regions of the S2 segment and between proximal and distal tubular fluid.

3.3.2.3 Collection of fluid from early, mid and late S2 proximal tubular segments

Nine male Sprague-Dawley rats were anaesthetised and prepared surgically for micropuncture in accordance with the protocol described above (see Section 3.2.2.1).

Identification of the location of the collecting pipette was achieved by injecting small droplets of Sudan black-stained oil into the tubule; the number of reappearances of the droplet flowing along the proximal convolutions gave an indication of the number of loops remaining before the end of the proximal convoluted tubule. If 6-7 convolutions remained, the site was defined as being 'early'; if 3-4 convolutions remained, it was defined as 'mid'; and if 0-1 convolutions remained, it was defined as 'late'. Late segments of the proximal tubule were confirmed through intratubular injections of Microfil silicone rubber compound (Flow Tech, Carver, MA, USA) which was subsequently microdissected (as described below). Tubular fluid collections (n = 7-10; each collection lasting 4 min) from each of the three puncture sites were pooled in three separate vials; thus a single pooled value for each site was obtained per rat. The samples were later assayed for ATP as described above.

Urine from the micropunctured and contralateral kidneys was collected at 1-2hr intervals from the end of the equilibration period throughout the tubular fluid collections. The samples were then assayed for Na^+ and K^+ content using the protocol described above in Section 3.2.2.4.

3.3.2.4 Comparison of ATP concentrations in proximal and distal tubular segments

Nine male Sprague-Dawley rats were anaesthetised and prepared surgically for micropuncture in accordance with the protocol described above (see Section 3.2.2.1), and collections were made from mid-proximal convoluted tubules and from early distal tubules, as far as possible, alternately. Early distal tubular segments were initially identified by administering a bolus injection (30µl of a 5% solution) of Lissamine green dye into the jugular catheter (Steinhausen, 1963). Following a brief delay, the dye appears over the kidney surface, highlighting superficial proximal tubules, then disappears (as it travels down the loop of Henle) and then reappears in the superficial distal tubular segments. The micropipette was targeted to an early segment of the distal tubule for the collection of tubular fluid, following the same procedure as the collection of proximal tubular fluid described above, except that the tip diameter of the micropipette used in this study was slightly smaller (8-9µm). Due to the lower flow rate and the lack of abundance of surface distal tubules, distal

tubular fluid collections were made for 8 minutes rather than 4 minutes, and up to 16 collections were pooled for a single reading (compared to a maximum of 10 for the proximal tubule). For consistency, proximal tubular collections also lasted 8 min. On two occasions, distal tubular fluid had to be pooled from two rats to obtain sufficient volume (900-1500nl); in these cases, the ATP concentrations of the pooled proximal tubule collections from the corresponding two rats were averaged for comparison with the early distal ATP concentration. Confirmation of the distal tubular site was achieved through intratubular Microfil injections, introduced after tubular collections and later microdissected (as described below).

Urine from the micropunctured and contralateral kidney was collected at 1-2 hr intervals from the end of the equilibration period throughout the tubular fluid collections. The samples were then assayed for Na^+ and K^+ content using the protocol described above in Section 3.2.2.4.

3.3.2.5 Microdissection of the kidney

The possibility of a proximal tubule being mistaken for an early distal tubule cannot be ruled out using the micropuncture technique, as both regions have 0-1 further surface convolutions. As indicated above, Microfil was therefore injected into the same late proximal tubules and early distal tubules from which collections were made. The Microfil, introduced into the tubule as a liquid, then solidified, taking the shape of a significant portion of the region of tubule into which it was injected. At the end of the experiment, the micropunctured kidney was then removed, cut in half and decapsulated. The kidney was then stored in distilled water for a few days, after which it was placed in 20 % NaOH (5M) for 10 minutes. The tubules that had been previously filled with Microfil were then dissected out and the structure of the late proximal or early distal tubule segment was visually confirmed (Cortell, 1969). Distal tubules were identified by the presence of the ascending limb of Henle upstream and the convergence of the distal tubule into a single collecting duct. Late proximal tubules were confirmed by the presence of several convolutions upstream and the pars recta downstream.

3.3.2.6 Statistics

Results are expressed as means ± standard error of the mean (SEM). Changes in ATP concentration and tubular flow rates between the different sites were assessed using Student's Newman Keules paired *t* test. The difference between two mean values was considered statistically significant when $P < 0.05$.

3.3.3 Results

3.3.3.1 Early *vs.* mid *vs.* late proximal tubule

(i) Urinary flow rate and Na^+ and K^+ output

Table 3.3.1 shows urinary flow rate and Na^+ and K^+ outputs from both micropunctured and contralateral kidneys. Neither urine flow rate nor K^+ excretion differed significantly between the micropunctured and contralateral kidneys ($P = 0.09$ and 0.81 respectively), whereas Na^+ output was significantly lower in the micropunctured kidney than in the contralateral kidney ($P = 0.002$).

Urine flow rate (µl/min)	Micropuncture kidney	22.2 ± 4.1
	Contralateral kidney	30.2 ± 4.3
Na^+ output (µmol/min)	Micropuncture kidney	2.8 ± 0.4
	Contralateral kidney	3.5 ± 0.4
K^+ output (µmol/min)	Micropuncture kidney	1.2 ± 0.1
	Contralateral kidney	1.2 ± 0.1

Table 3.3.1: Urine flow rate and Na^+ and K^+ outputs in the micropunctured and contralateral kidney during the experimental period (mean ± SEM; n = 8).

(ii) Tubular flow rates

Significant differences in tubular flow rates were observed between the different sites ($P = 0.004$). The tubular flow rate in the early region of the proximal tubule was 35 $\pm$ 3 nl/min (mean $\pm$ SEM; $n = 9$). The corresponding value in the mid region of the proximal tubule was 29 $\pm$ 3 nl/min ($P = 0.02$, paired t test). The tubular flow rate in the late region of the proximal tubule was 26 $\pm$ 2 nl/min, which was significantly lower ($P = 0.04$) than that of the mid region. *N.B.* Each mean $\pm$ SEM is calculated from the average tubular flow rates from 9 rats; and each average value per rat is calculated from 6-10 collections.

(iii) Intraluminal ATP concentration in the early, mid and late regions of the proximal tubule S2 segment

As shown in Fig. 3.3.2, ATP concentration in tubular fluid derived from the early region of the S2 segment of the proximal convoluted tubule was 126 $\pm$ 16 nmol/l (mean $\pm$ SEM; $n = 9$), that in the mid region was 146 $\pm$ 20 nmol/l, and that in the late region was 112 $\pm$ 8 nmol/l. No significant differences in ATP concentration were found between the early and mid regions ($P = 0.24$) or between the mid and late regions of the proximal convoluted tubule ($P = 0.12$).

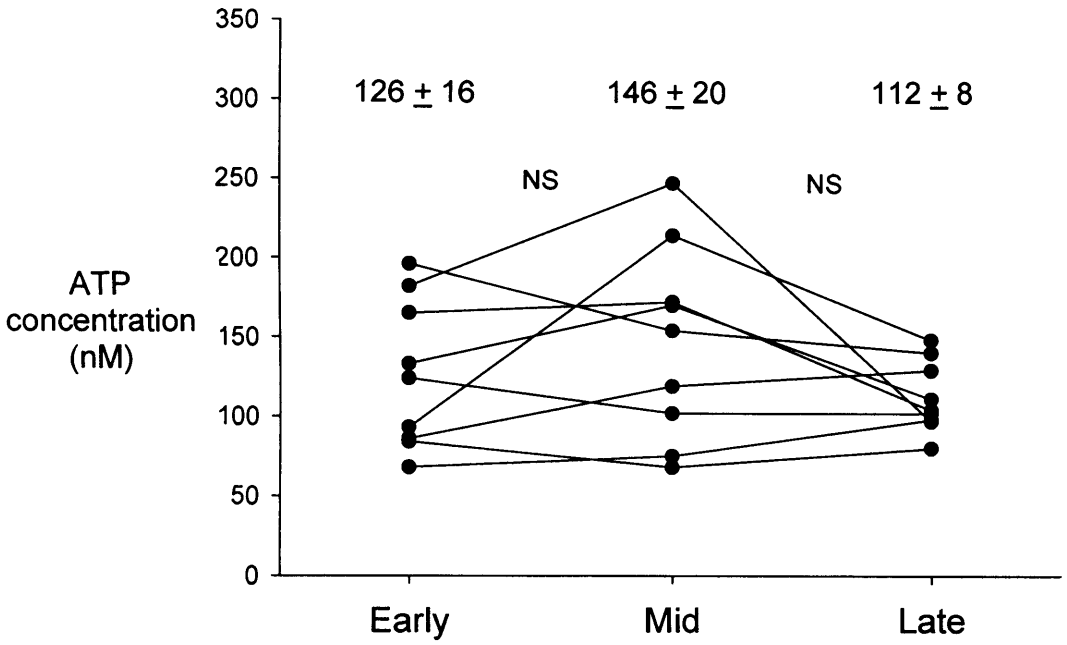

Fig. 3.3.2: Intraluminal ATP concentrations in early, mid and late regions of the proximal convoluted tubule. Each point represents a single pooled collection, made up of 7-10 samples. Values in each rat are linked by solid lines. Means ± SEM are indicated.

3.3.3.2 Proximal tubule *vs.* distal tubule

(i) Tubular flow rates

The tubular flow rate in the mid region of the proximal convoluted tubule was 26 ± 1 nl/min (mean ± SEM; $n = 9$), whilst that in the early distal convoluted tubule was 11 ± 1 nl/min ($P < 0.0001$).

(ii) Intraluminal ATP concentration in proximal and distal convoluted tubules

The concentration ATP in tubular fluid derived from early distal tubules was 33 ± 14 nmol/l, compared with 116 ± 33 nmol/l in mid-proximal tubules (Fig. 3.3.3). In every comparison ($n = 7$), the ATP concentration in distal tubules was lower than in

proximal tubules. A paired t test showed the difference in these concentrations to be statistically significant ($P < 0.01$).

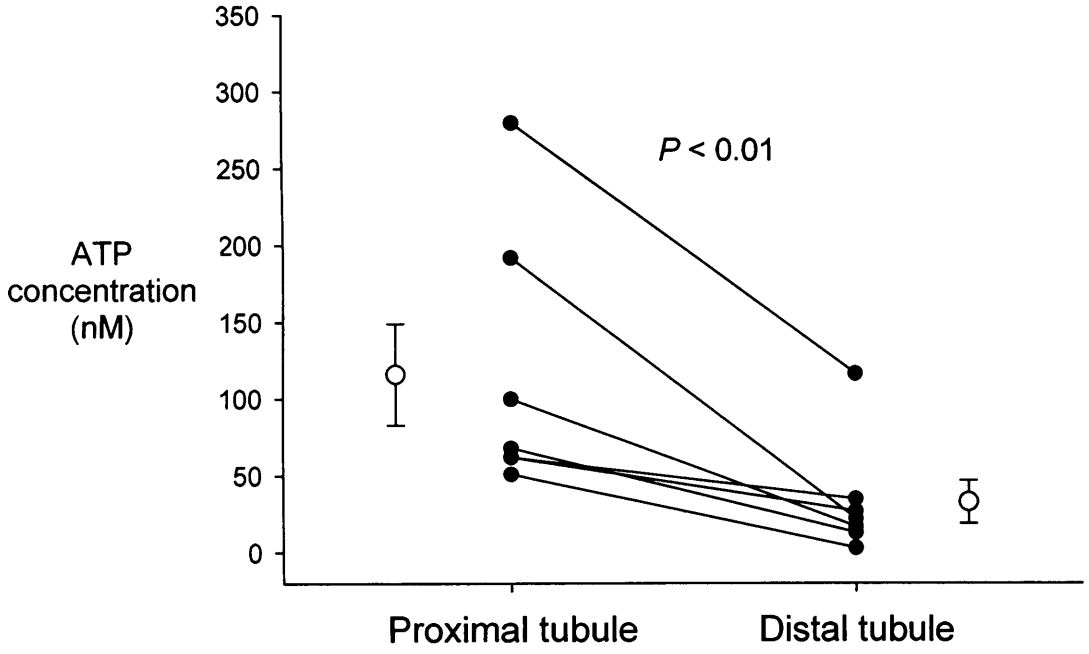

Fig 3.3.3: Intraluminal ATP concentrations in mid-proximal convoluted tubule and early distal tubule. Each point represents a single pooled collection, made up of 7-10 proximal samples or 10-16 distal samples. Values in each rat (or pair of rats) are linked by solid lines. Means ± SEM are also shown.

3.3.4 Discussion

Tubular flow rates in the early, mid and late regions of the proximal convoluted S2 segment, as well as in the early distal convoluted tubule, were well within the expected range.

Using the luciferin-luciferase assay, the readings for the ATP standards taken before and after the tubular fluid measurements were consistent. In addition, the standard calibration curves that were generated for each experiment did not vary significantly;

and all readings for ATP in tubular fluid were well above the detection limit (~20 fmoles per vial; < 1 nmol/l).

In this investigation, the levels of ATP present in the proximal tubular fluid were lower than those predicted on the basis of *in vitro* experiments with tubular cultures (Schwiebert et al, 2003) but were nevertheless high enough to stimulate a number of P2 receptor subtypes (Schwiebert et al, 2003; King and Townsend-Nicholson, 2003). The ATP concentrations in fluid derived from the early, mid and late regions of the S2 segment of the proximal tubule were not significantly different from one another. The overall average ATP level found in these regions was approximately 130nmol/l. This luminal ATP may have originated from one of two possible sources: filtration from plasma at the glomeruli and/or release of ATP from tubular epithelial cells. If the latter were true, a variety of mechanisms exist by which ATP could be released from the tubular cells, including (i) ATP release from cells damaged by the introduction of the pipette into the tubule (in which case the ATP measured would be an artifact of the technique), (ii) physiological release of ATP from tubular epithelial cells, and/or (iii) release of ATP from epithelial tubular cells that had physiologically undergone apoptosis. Where feasible, these possibilities have been assessed and will be discussed in the ensuing sections.

The ATP concentration in tubular fluid from the distal tubule averaged 33 nmol/l, significantly lower than that of the proximal tubule. There are several possible reasons for this. One obvious explanation is that ATP secretion by distal epithelial cells may be significantly lower than that of proximal epithelial cells; in this context, the proximal tubule, with its brush-border apical membrane having a greater luminal surface area, might be able to secrete more ATP than a distal tubular segment of the same length. Another possibility may be variability in the expression of membrane-bound ectonucleotidases. The specific expression of the different members of these enzymes (varying in their catalytic activity) in different regions of the same nephron may influence the overall intraluminal ATP concentration at these sites. Alternatively, distal tubular epithelial cells may not themselves release ATP; thus the ATP found in the lumen of the distal convoluted tubule may simply be proximal tubular ATP that has flowed downstream.

Whatever the reason may be, the finding that ATP concentrations in the distal tubule *in vivo* are markedly lower than those in the proximal tubule echoes the *in vitro* findings of Schwiebert's group in cultured cells (Schwiebert et al, 2003) and suggests that an effect of P2 receptor stimulation in the distal tubule under physiological conditions is less likely. However, in view of the longer collection times employed and the presence of some ectonucleotidases in this nephron segment (as will be discussed in Chapter 5), such an effect cannot be ruled out.

3.4 SECTION 4: Examination of potential artifacts in the micropuncture technique for quantifying ATP *in vivo*

3.4.1 Introduction

In any study of this nature, care must be taken to exclude possible artifacts and potential sources of contamination. Although precaution was taken in using ultra-fine sharpened micropipettes, the procedure of micropuncture inevitably involves puncturing the tubular wall. Because the intracellular concentration of ATP (~5mmol/l) is several orders of magnitude greater than that measured in the lumen, this could potentially pose problems when trying to quantify the normal physiological levels of ATP in tubular fluid, as damage to the tubular cells caused by insertion of the collection pipette might itself lead to release of intracellular ATP into the lumen, or the pipette tip might become contaminated with ATP as it traverses the tubular cells ultimately leading to artifactual intraluminal ATP concentrations. In addition, disturbances of intraluminal pressure caused by the oil column distal to the point of collection might induce mechanical stress and stimulate ATP release by the proximal tubular cells. To assess these possibilities, experiments were conducted in which the method of tubular fluid collection was modified, and the intraluminal ATP levels directly compared with those from collections using the conventional oil column method in the same rats.

3.4.2 Methods & Results

3.4.2.1 Normal *vs.* delayed collection

In these experiments (n = 3), a period of 4 minutes was allowed to elapse after the pipette was introduced into the tubule before the oil column was injected. The rationale for this was that mechanical damage induced by the introduction of the pipette into the tubule would be expected to cause a bolus release of ATP from damaged tubular cells, and that the immediate introduction of an oil column might

effectively 'trap' this bolus release of ATP. Although 10 – 20 seconds were always allowed to elapse before injection of the oil column in the conventional experiments, these additional experiments were performed to assess whether there was a significant change in intratubular ATP concentration if more time was allowed to elapse. The results showed that there was no significant difference (P = 0.59; paired t test) in measured ATP concentrations between normal (125 ± 15 nmol/l) and delayed (166 ± 57 nmol/l) pooled collections, indicating that if there is a bolus release of ATP from damaged tubular cells during the insertion of the pipette, it occurs almost instantaneously and is washed away downstream rapidly.

3.4.2.2 Use of an oil column

The presence of the oil column distal to the point of collection might cause the intraluminal pressure within the tubule (at the point of fluid collection) to increase, thereby inducing the release the ATP from adjacent tubular epithelial cells. In order to assess this possibility, experiments were conducted to make a direct comparison between ATP concentrations in (pooled) collections made using the conventional method (i.e. depositing the oil column and making a complete collection) and those in (pooled) collections made where tubular fluid was merely sampled (i.e. no oil column was deposited). These experiments (n = 3) found no significant difference (P = 0.59) in ATP concentration between collections made using the conventional oil column (104 ± 52 nmol/l) and collections made without the presence of an oil column (147 ± 18 nmol/l), suggesting that the ATP concentrations previously documented were not due to ATP released as a result of the presence of an oil column.

3.4.2.3 Possible contamination from puncturing the tubule

In a further experiment, tubules were punctured repeatedly using a clean micropipette, but no tubular fluid was collected. The aim was to assess whether any ATP from the intracellular fluid of tubular cells was adhering to the tip of the pipette, resulting in artifactually high ATP values measured in tubular fluid. Following each puncture of the tubule, the pipette tip was immediately submerged into a droplet of water (previously deposited under oil) to effectively 'rinse' the tip of possible intracellular fluid contamination. This procedure was repeated ten times, after which the complete

volume of the water droplet was deposited in ice-cold water and assayed for ATP (following the same procedure as that for tubular fluid). Proximal tubular fluid collections were also made in the same animal using the conventional method for comparative purposes. The results of this investigation revealed that the concentration of ATP in the droplet of water was undetectable and that the corresponding ATP concentration in pooled samples of tubular fluid was 289 nmol/l, leading to the conclusion that the levels of ATP detected in tubular fluid could not be attributed to intracellular ATP contamination.

3.4.3 Summary

No difference in luminal ATP concentrations were found whether or not an oil block was used, nor when a 4-min delay was interposed between insertion of the pipette and initiation of collection. Clearly, any pulse of ATP released on insertion of the pipette must have been washed away/metabolized within seconds, before tubular fluid collections began. In addition, experiments in which a pipette was repeatedly inserted into a number of tubules, but without tubular fluid collection, showed no trace of ATP. It can be concluded that the ATP measured in the proximal tubular lumen was not simply a consequence of the experimental manipulations employed.

3.5 SECTION 5: Degradation of ATP during micropuncture collection procedures

3.5.1 Introduction

From immunohistological studies (Kishore et al, 2005; Le Hir and Kaissling, 1993; and see Chapter 5), it is clear that many ectonucleotidases (that specialize in the hydrolysis of ATP) are expressed on the apical membrane along the tubule. As well as being membrane bound, some of these enzymes have the potential to be cleaved at the stalk close to the membrane to be released as soluble nucleotidases. In particular, all members of the NPP family, alkaline phosphatase and ecto-5'-nucleotidase have this potential (Zimmermann, 2001). Ecto-5'-nucleotidase, alkaline phosphatase and NPP3 are all expressed on the brush-border membrane of the proximal tubule, and the latter two enzymes can hydrolyse ATP. Their presence as soluble nucleotidases might mean that the true value of the intraluminal ATP concentration as found in Section 3.3 was underestimated, as the enzymes will remain active in the micropipette during the collections of tubular fluid.

The present study was therefore conducted to assess the activity of these soluble nucleotidases. This was done in two ways: firstly by incubating tubular fluid from proximal and distal tubules with exogenous ATP, and secondly by varying the duration of the collections made from proximal tubules. The half-life of ATP in tubular fluid could then be deduced. It should be stressed that these experiments were not conducted to determine the kinetics of soluble nucleotidases in the luminal environment but were designed to assess (i) if these enzymes were active and (ii) whether it was possible to apply a correction factor so that the concentration of ATP at time zero (i.e, before any degradation had occurred, when tubular fluid is still present in the lumen) could be determined.

(i) Degradation of exogenous ATP

3.5.2 Methods

In pilot experiments, the stability of ATP in mid-proximal and early distal tubular fluid was investigated by determining the degradation of exogenous ATP. In this study, male Sprague-Dawley rats were anaesthetised and prepared surgically for micropuncture in accordance with the protocol described above (see Section 3.2.2.1). Volumes of mid-proximal or early distal tubular fluid were collected, also as described above (see Section 3.3.2.1 and 3.3.2.4), and deposited under oil onto a watch-glass. Using a constriction pipette, paired aliquots of 82nl were accurately isolated from this pool and deposited onto a different area of the same watch-glass. Samples of standard ATP solution (12 nl of 100μM ATP) were then mixed with the aliquots of proximal or distal tubular fluid. The mixture was then allowed to incubate, at room temperature (23°C), for 5, 10, 20 or 40 min, at the end of which any degradation was halted by adding the whole solution to 50μl ice-cold de-ionized water and freezing it for subsequent assay. The same standard ATP solution was added (in triplicate) to de-ionized water as a control.

3.5.3 Results

When aliquots of proximal tubular fluid or distal tubular fluid were incubated with ATP standards, in each case the ATP content of the mixture decreased with time. Under these conditions, where substrate concentration was not a limiting factor, ATP was found to be degraded at a mean rate of 16 fmol/min in proximal tubular fluid (Fig. 3.4.1A) and 15 fmol/min in distal tubular fluid (Fig. 3.4.1B)

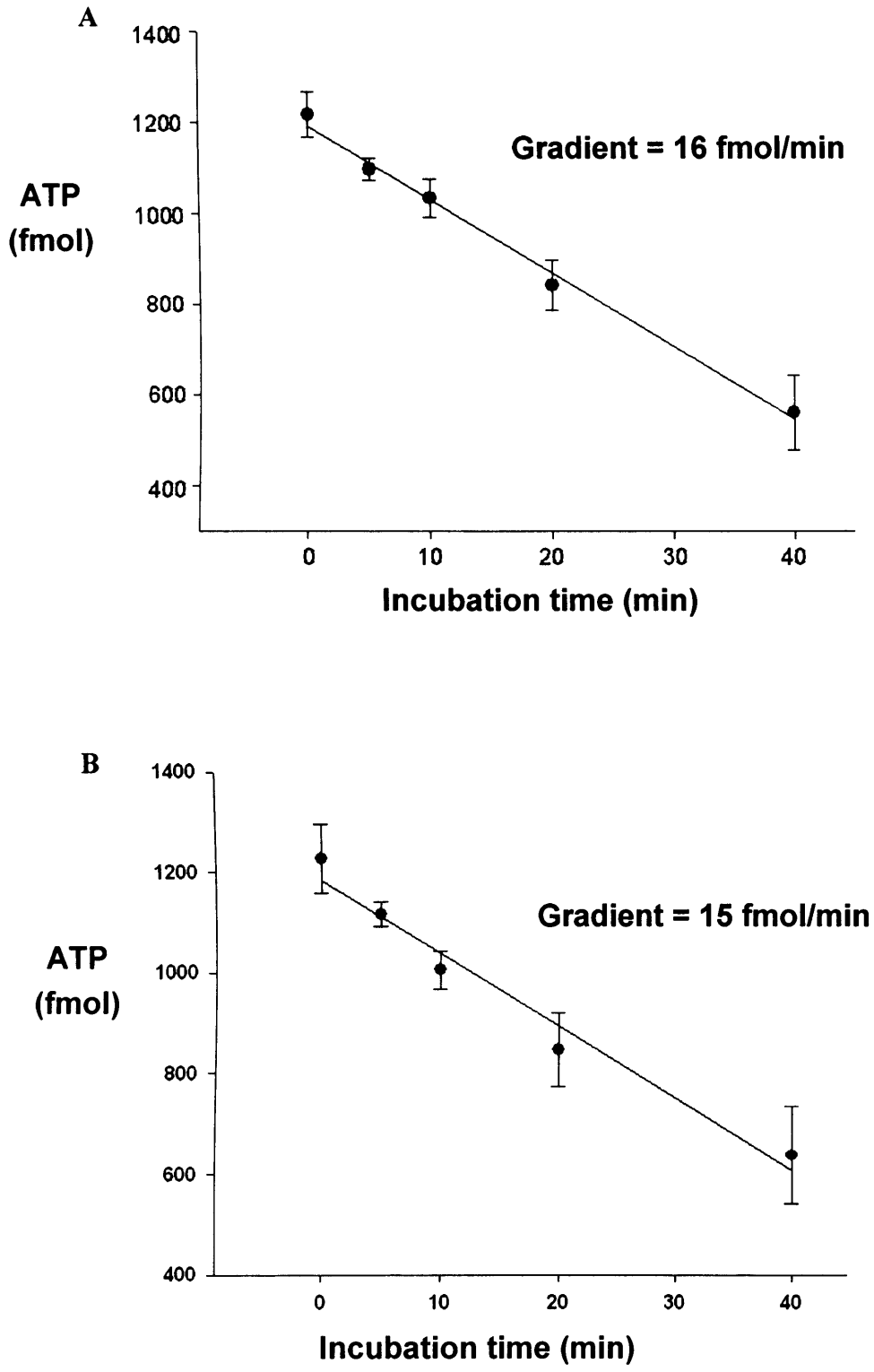

Fig. 3.4.1: (A) Degradation of exogenous ATP in samples of proximal tubular fluid. Each value shown is the mean (± SEM) of 9 pairs of incubated samples. (B) Degradation of exogenous ATP in samples of distal tubular fluid. Each value shown is the mean (± SEM) of 7 pairs of incubated samples.

(ii) Degradation of endogenous ATP

3.5.4 Methods

Because the pilot experiments indicated significant degradation of exogenous ATP by enzymes in tubular fluid, degradation of the (much lower levels of) endogenous ATP found in collected fluid was assessed. In these experiments, nine male Sprague-Dawley rats were anaesthetised and prepared surgically for micropuncture in accordance with the protocol described above (see Section 3.2.2.1). Mid-proximal tubular fluid collections of varying duration were made, also as described above (see Section 3.3.2.1). Tubular fluid collections lasted 4, 10 or 22 min, and the order in which these were made was randomized. To exceed detection limits for the luciferin-luciferase assay, samples of a given duration were pooled (n= 3-10 collections), so that a single (pooled) value for each time interval was obtained per rat.

3.5.5 Results

Endogenous ATP concentrations in mid-proximal tubular fluid collected for 4, 10 or 22 min were 117 $\pm$ 20 nmol/l, 59 $\pm$ 7 nmol/l and 17 $\pm$ 4 nmol/l, respectively (means $\pm$ SEM; n = 9). Fig. 3.4.2 shows these ATP concentrations plotted against "processing time" on a semi-log scale, where "processing time" was taken to be: half the total duration of collection (in order to obtain an average time for the existence of a droplet of tubular fluid in the pipette, assuming a constant collection rate) plus the 2 min taken for volume measurement. ATP concentration fell exponentially as "processing time" increased; its half-life was 3.4 min. Extrapolation back to zero time (i.e. before any degradation by soluble nucleotidases had occurred) gave a value of 275 nmol/l.

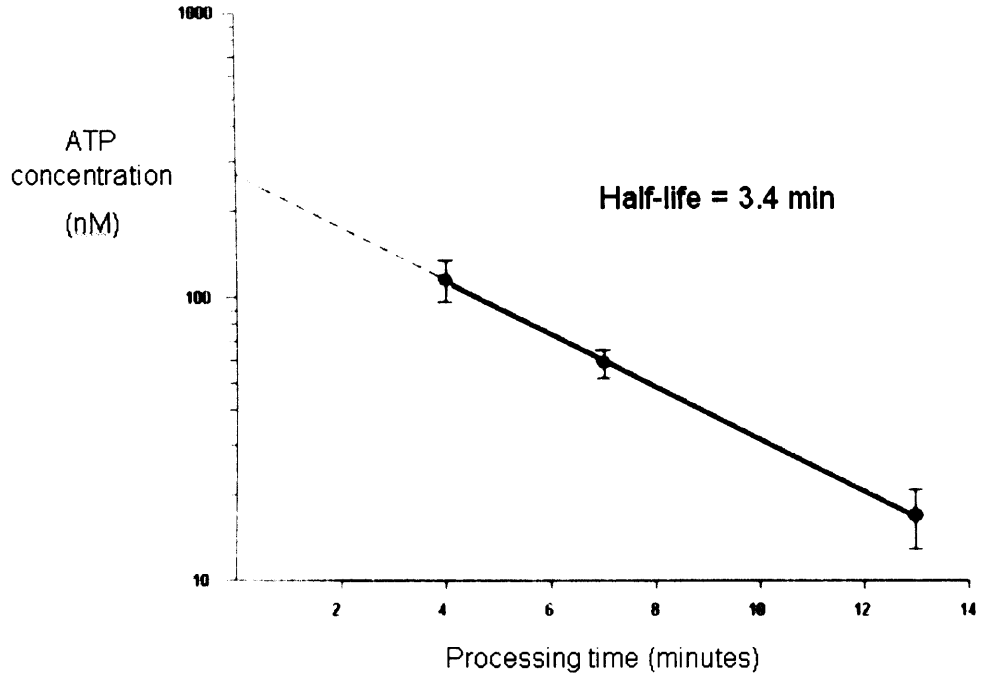

Fig. 3.4.2: Endogenous ATP concentrations in tubular fluid sampled from mid-proximal convoluted tubules of Sprague-Dawley rats, with varying duration of collection (4, 10 or 22 min). A single value for pooled collections for each time interval was determined in each rat, and the values shown are means ± SEM (n = 9 rats). "Processing time" was defined as half the total duration of collection plus 2 min (the time taken for volume measurement).

3.5.6 Discussion

Although the ATP concentrations in the proximal tubular fluid, as found in the previous chapter, are high enough to stimulate a number of P2 receptor subtypes (Schwiebert et al, 2003; King and Townsend-Nicholson, 2003), the concentrations measured are likely to underestimate significantly those in the tubular micro-environment owing to the presence of nucleotidases. In the initial studies, assessment of nucleotide catabolism by incubating an excess of exogenous ATP in proximal and distal tubular fluid indicated that tubular fluid contains enzymes capable of hydrolyzing ATP.

Because *endogenous* ATP concentrations were markedly lower (an influencing factor over the rate of nucleotide hydrolysis), a further investigation was made in which the duration of proximal tubular fluid collections was varied, thereby assessing the stability of endogenous ATP; the half life of endogenous ATP in collected proximal tubular fluid was found to be 3.4 minutes.

Reasoning behind timed collections ('processing time')

When assessing the half-life of endogenous ATP, proximal tubular fluid collections were made for 4, 10 and 22 minutes. Once tubular fluid is out of the nephron, the level of ATP in tubular fluid in the pipette will be consistently on the decline due to exposure to soluble nucleotidases. Thus, the final concentration of ATP in the initial part of the collection will be lower than that in fluid collected within the last part of the collection. Assuming that the rate of collection was constant, the average time that a given droplet of tubular fluid was out of the nephron for the 4, 10 and 22 minute collections would be 2, 5 and 11 minutes, respectively. In addition, the time taken to process the collected fluid (i.e. to measure and deposit it in ice-cold water) was on average 2 minutes, thereby increasing this time for each collection to 4, 7 and 13 minutes, respectively.

The linearity (on a semi-log plot) in the results from these experiments implies that the concentration of ATP at time zero (i.e. before any degradation by soluble nucleotidases) can be obtained by extrapolation; it was found to be in the region of 275nmol/l. It is worth noting that this value is indicative of the levels of ATP present in the tubular lumen and not necessarily at the vicinity of tubular cell membrane, where the concentration of newly released ATP from tubular cells may be significantly higher.

Rate of ATP hydrolysis by soluble nucleotidases

When assessing the stability of exogenous ATP, the concentration applied was significantly greater (almost 100 fold) than the endogenous ATP already present in the tubular fluid. Therefore the availability of substrate, being present at these high

concentrations, would not have been a limiting factor when assessing the rate of ATP hydrolysis. Under these conditions, the rate of hydrolysis in proximal tubular fluid was found to be approximately 16 fmol/min. However, these experiments were conducted at room temperature; because temperature is also rate limiting, the rate of hydrolysis by these soluble nucleotidases would be expected to be higher *in vivo* (where the temperature would be 37°C).

Due to the unfeasibility of collecting enough distal tubular fluid, an assessment of endogenous ATP degradation could not be conducted for the distal convoluted tubules; therefore, the intraluminal ATP concentration at time zero could not be extrapolated in the same way as for the proximal tubule. Nevertheless, degradation of exogenous ATP by soluble nucleotidases in the distal tubular fluid *was* examined. In these experiments the rate of ATP hydrolysis by soluble nucleotidases in distal tubular fluid was similar (~15 fmol/min) to that seen in proximal tubular fluid. On this basis it may be assumed that hydrolysis of endogenous ATP by soluble nucleotidases in the distal convoluted tubule occurs at a similar rate to that of the proximal tubule.

Finally, it is worth emphasizing that in addition to this degradation of endogenous ATP by soluble nucleotidases, an array of ectonucleotidases is known to line the proximal tubular apical membrane. These ectonucleotidases are poised to metabolize ATP close to its site of action, even before tubular fluid collections can proceed and may have a higher catalytic activity than their soluble forms. For this reason, it is possible that the concentration of ATP in the immediate vicinity of apical P2 receptors is higher than those measurable with the present methodology. Nevertheless, from the present investigation, the luminal ATP concentration (275nmol/l at time zero) represents a minimal value of ATP present in the proximal tubular microenvironment.

3.6 SECTION 6: Is ATP filtered or secreted?

3.6.1 Introduction

From the ATP assays performed on proximal and distal tubular fluid samples, it is clear that ATP is present in the tubular lumen. Moreover, it seems unlikely that this tubular ATP was a product of epithelial cellular damage while conducting the micropuncture experiments. So the next question to answer is: from where does tubular ATP originate?

One possible answer to this question would be that tubular ATP is secreted directly from the renal epithelial cells, as suggested by *in vitro* studies (Wilson et al, 1999). However, a second possibility is that ATP may have been filtered from the plasma at the glomerulus. No study has examined this possibility. Therefore, to distinguish between these two possibilities, a special strain of naturally mutated rats was used. These rats, namely Munich-Wistar rats, unlike other strains, have a number of glomeruli that lie close to the surface of the kidney, thereby allowing micropuncture access to Bowman's capsule. In this way a direct comparison could be made between the levels of ATP in Bowman's capsule fluid and in proximal tubular fluid in the same animals.

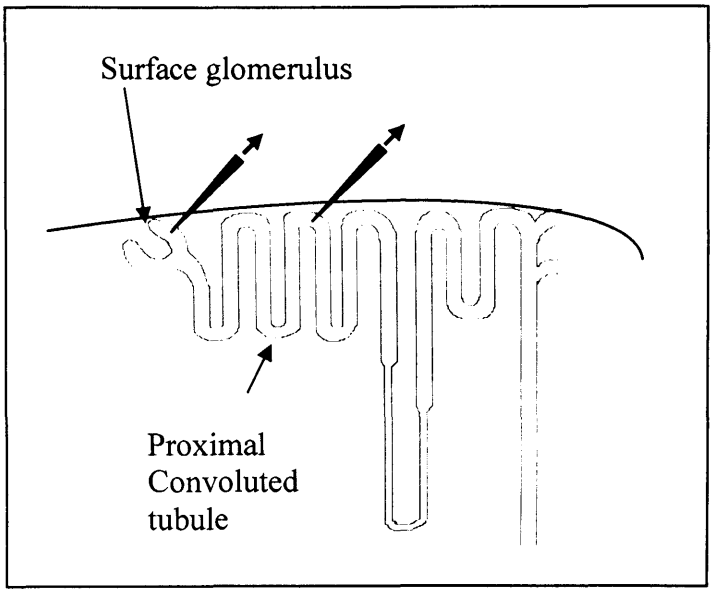

Fig. 3.6.1: A schematic diagram of a superficial nephron in a Munich-Wistar rat. Some glomeruli are found near the surface of the kidney, thereby allowing direct micropuncture access to Bowman's space.

3.6.2 Methods

3.6.2.1 Bowman's capsule and proximal tubular fluid collections

Twelve male Munich-Wistar rats were anaesthetised and prepared surgically for micropuncture in accordance with the protocol described above for Sprague-Dawley rats (see Section 3.2.2.1). In some Munich-Wistar rats (n = 4), [^{3}H]inulin (40μCi bolus, 40μCi/h) was infused intravenously from the end of the first hour of equilibration as described in Section 3.2.2.2. Fluid collections were made alternately from mid-proximal convoluted tubules (as described above in Section 3.2.2.3) and from Bowman's capsules (of different nephrons). Identification of Bowman's space was made initially on the basis of its proximity to the targeted glomerulus, the large number of proximal tubular segments seen to succeed it when a small oil droplet was allowed to move downstream, and its characteristic shape when partially filled with Sudan black-stained oil (Shirley et al, 2004). Where possible, further confirmation of the puncture site was achieved through the [^{3}H]inulin concentration of the collected fluid relative to that of plasma water.

Fluid collected from Bowman's space (n = 8-10 collections per rat; each collection lasting 4 minutes) was pooled (as described above in Section 3.3.2.1) and later assayed for ATP (as described above in Section 3.3.2.2). Mid-proximal tubular fluid collections (n = 8-10 collections per rat; each collection lasting 4 minutes) were pooled in a separate vial and later assayed for ATP using the same procedure.

In a sub-group of rats (n = 4), water reabsorption between the Bowman's capsule and the mid-proximal convoluted tubule was assessed using [^{3}H] inulin, to determine whether any differences in ATP concentration between the two sites could be attributed to water reabsorption. In these experiments, where rats were infused with [^{3}H] inulin, fluid samples from Bowman's space (using a 79nl constriction pipette) and from mid-proximal tubule (38nl) were deposited into Aquasol 2 for measurement of [^{3}H]inulin activity (as described above in Section 3.2.2.4).

3.6.2.2 GFR and SNGFR measurements

GFR and SNGFR measurements were made in accordance with the protocol described for Sprague-Dawley rats (Section 3.2.2.4)

3.6.2.3 Comparison of [^{3}H] inulin activity in total plasma and plasma water

In these experiments, a large (1ml) sample of blood was collected at the end of the micropuncture period. The plasma was divided into two equal portions. From one portion, 10µl samples were directly deposited into Aquasol 2, as described previously. The other portion was treated to precipitate out plasma proteins by diluting the sample 5:1 with 5% metaphosphoric acid (Briggs, 1940) The plasma, together with the protein precipitate, was centrifuged to separate the plasma water from the plasma protein precipitate. Ten microlitres of the supernatant (plasma water) was then deposited into a vial containing Aquasol 2 and counted as described previously.

3.6.3 Results

3.6.3.1 Urinary flow rate and Na^+ and K^+ output

Table 3.6.1 shows urinary flow rate and Na^+ and K^+ outputs from both micropunctured and contralateral kidneys. Urine flow rate in the micropunctured kidney was not significantly different from that of the contralateral kidney ($P = 0.07$); whereas in these experiments Na^+ ($P = 0.02$) and K^+ ($P = 0.02$) outputs were significantly lower in the micropunctured kidney compared with the contralateral kidney.

3.6.3.2 GFR and SNGFR

Mean values for GFR for both micropunctured and contralateral (non-micropunctured) kidneys are given in Table 3.6.2. Corresponding SNGFR results are

also shown. Each GFR value shown is an average of 2-3 measurements, whereas each SNGFR value is an average of 4 measurements taken per rat.

Urinary flow rate (µl/min)	Micropuncture kidney	4.2 ± 0.4
	Contralateral kidney	4.9 ± 0.3
Na^+ output (µmol/min)	Micropuncture kidney	0.4 ± 0.1
	Contralateral kidney	0.7 ± 0.1
K^+ output (µmol/min)	Micropuncture kidney	0.7 ± 0.1
	Contralateral kidney	1.3 ± 0.1

Table 3.6.1: Urinary flow rate and Na^+ and K^+ outputs in the micropunctured and contralateral kidney during the experimental period (means ± SEM; n = 11).

	GFR (ml/min)		**SNGFR (nl/min)**
	Micropunctured kidney	**Contralateral kidney**	**Proximal tubule**
	1.19	1.29	63.2
	1.18	1.43	63.9
	0.92	1.14	55.2
	1.62	1.68	66.3
Mean ± SEM	**1.23 ± 0.14**	**1.39 ± 0.11**	**62.1 ± 2.4**

Table 3.6.2: GFR values (for individual rats, as well as means ± SEM; n = 4) for both micropunctured and contralateral kidney; and corresponding SNGFR values.

3.6.3.3 ATP concentrations in Bowman's space *vs.* mid-proximal tubule

In all 12 Munich-Wistar rats, the ATP concentration was higher in the mid-proximal tubule than in Bowman's space (Fig. 3.6.2; $P<0.001$). The mean (± SEM) ATP concentration in mid-proximal convoluted tubule was 142 ± 23 nmol/l, compared with only 32 ± 7 nmol/l in Bowman's space. In some animals, the tubular fluid/plasma water [^{3}H]inulin concentration ratio (TF/P_{In}) was also measured at each site. TF/P_{In} at Bowman's space was 1.04 ± 0.02 (n = 14), and at the mid-proximal tubule it was 1.34 ± 0.06 (n = 14), indicating that ~25% of the filtered fluid had been reabsorbed between the two puncture sites.

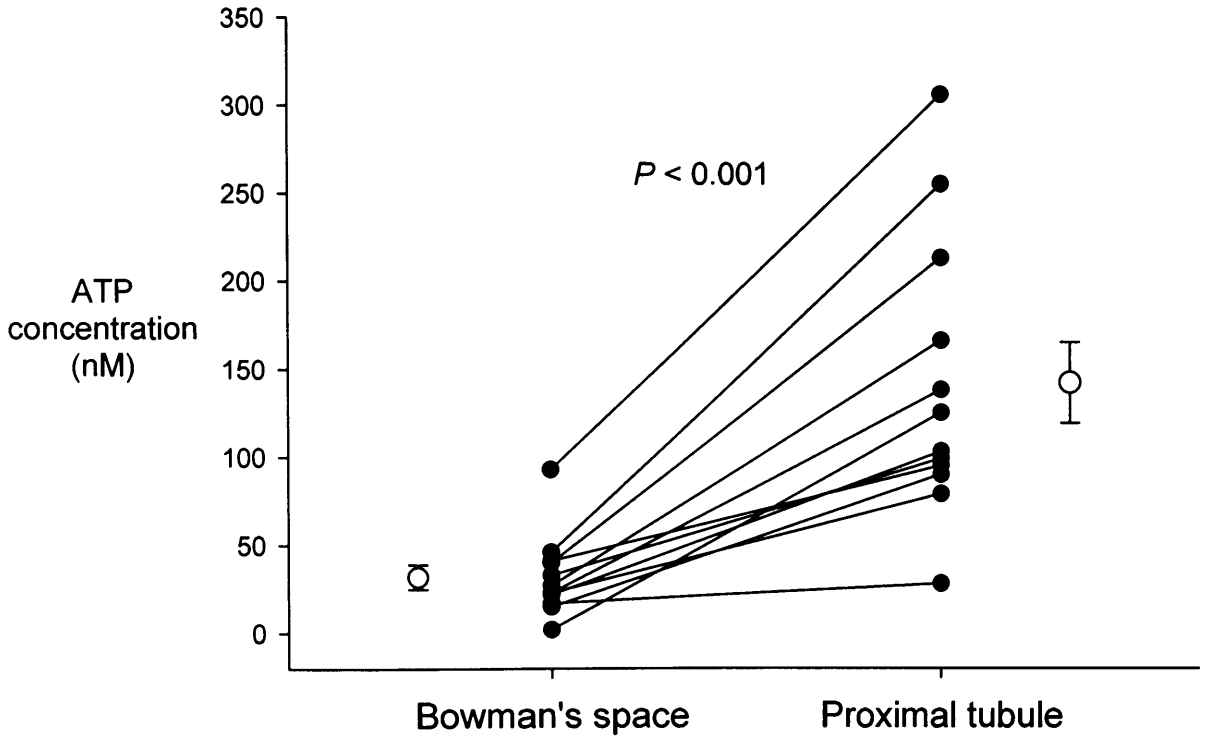

Fig. 3.6.2: ATP concentrations in Bowman's space and mid-proximal convoluted tubule of Munich-Wistar rats. Each point represents a single pooled collection, made up of 8 - 10 samples. Values in each rat are linked by solid lines. Means ± SEM are also shown.

3.6.4 Discussion

On initial consideration, it might be thought that the concentration of ATP in filtered fluid could be obtained simply by measuring its concentration in plasma. Previous studies have reported plasma ATP concentrations to be in the range 100-200nmol/l (Bodin and Burnstock, 1996; Born and Kratzer 1984). Such concentrations are consistent with those found in the proximal tubular fluid in the present study, raising the possibility that ATP found in proximal tubules was merely filtered from the plasma at the glomerulus. Because of this, I attempted to measure the plasma ATP concentrations of the Sprague-Dawley rats used in the present study. Although blood was taken from the cannulated femoral artery, thereby minimizing the risk of vascular damage, the results were extremely variable (ranging between 4 and 107 nM) and the possibility of release of intracellular ATP from red cells through necrotic or mechanically induced cell damage during centrifugation could not be ruled out. In addition, the activities of endothelial membrane-bound and soluble nucleotidases in the vasulature will also influence ATP measurements. In any case, even if the data could be relied upon, ATP concentrations in the blood derived from the femoral artery would not necessarily represent the concentration of ATP being filtered at the glomerulus, as ATP release and hydrolysis may be constantly shifting throughout the vascular system and ATP may also be degraded by enzymes in the glomerular membranes. For all these reasons, it was felt necessary to measure ATP directly in Bowman's space.

For this, Munich-Wistar rats were used instead of Sprague-Dawley rats (as used in every other study in this thesis), due to their unique natural anatomical feature of having some glomeruli close to the kidney surface, enabling access of the micropipette to Bowman's space. Although at first glance the GFRs in these rats were slightly higher than those reported in Sprague-Dawley rats, when account was taken of their greater weight (average weight ~ 310g) the GFRs of Munich-Wistar rats were normal. However, the SNGFR/GFR ratio was higher than seen in Sprague-Dawley rats. Given that the SNGFR measurements were in each case made from proximal collections, this might suggest that the TGF mechanism is more sensitive in Munich-Wistar rats. However, a similarly high SNGFR/GFR ratio was noted in a previous study in Munich-Wistar rats using distal tubular collections (Shirley et al,

2004). Alternative explanations are that Munich-Wistar rats may have fewer nephrons or that their superficial nephrons have abnormally high SNGFRs.

Although tubular flow rates as well as GFR were normal in Munich-Wistar rats, sodium and water outputs in both kidneys were lower than in Sprague-Dawley rats infused at the same rate. Because the surgical procedure and set-up for the Munich-Wistar rats was no different from that of the Sprague-Dawley rats, it is possible that these low sodium outputs were an effect of the different strain of rats responding differently to the anaesthesia and/or surgical procedure (see Section 3.1). However, no obvious explanation can be proposed for this phenomenon.

The major finding of the present study was that the concentration of ATP in the mid-proximal tubular lumen of Munich-Wistar rats was similar to that measured in Sprague-Dawley rats and was considerably greater (4-5 fold) than that in the glomerular filtrate. Comparison of the TF/P_{In} values at Bowman's space and mid-proximal convoluted tubule indicates that the fractional reabsorption of water between the two puncture sites was approximately 25%, which cannot account for the marked difference in ATP concentrations between the two sites. These data strongly suggest that the proximal tubule secretes ATP into its lumen.

3.7 SECTION 7: Effect of (patho)physiological manoeuvres on proximal tubular ATP concentrations *in vivo*

3.7.1 Introduction

In the following experiments, the pathophysiological manoeuvres of extracellular volume expansion (achieved through the infusion of isotonic saline at a high rate) and ischaemia (achieved by inducing haemorrhage via the femoral artery) were performed. These experiments were conducted to identify changes in the intraluminal concentration of ATP in the proximal tubule during these conditions. An important feature of this study was that comparisons of tubular ATP concentrations between control and pathophysiological states were made directly in the same rats, rather than in a separate group of animals. Therefore, time-control experiments were also conducted to assess any changes in ATP concentration in tubular fluid attributable to time *per se*. Urinary excretion rates of water, Na^+ and K^+, tubular fluid flow rates, and arterial blood pressure were also measured, to check that the expected physiological changes occurred in response to these stimuli.

3.7.2 TIME-CONTROL STUDY

Time-control experiments were conducted to assess whether any significant alterations to the intraluminal ATP concentrations occurred during the course of the experiments. This was in order to determine whether any changes (or lack of them) in ATP levels seen following pathophysiological stimuli were merely a variable of time.

3.7.2.1 Methods

Eight male Sprague-Dawley rats were anaesthetised and prepared surgically for micropuncture in accordance with the protocol described above (see Section 3.2.2.1).

Tubular fluid collections (n = 7-10; each collection lasting 4 min) were made from mid-proximal tubules (as described above, see Section 3.3.2.1) over a one-hour period and were pooled in 50 µl of ice-cold water and frozen immediately. Thirty minutes later, further tubular fluid collections (n = 7-10; each collection lasting 4 min) from the same region of (a different group of) proximal convoluted tubules were made over a one-hour period and were pooled in a separate vial of ice-cold water and frozen immediately. All tubular fluid pooled samples were later assayed for ATP (as described above, see Section 3.3.2.2). Fig. 3.7.1 shows an outline of the experimental protocol. Urine from the micropunctured and contralateral kidneys was collected throughout the tubular fluid collections. The urine samples were then assayed for Na^+ and K^+ content using the protocol described above in Section 3.2.2.4.

Mean arterial blood pressure (MABP) was also monitored throughout both control periods via the cannulated right femoral artery connected to an electronic transducer (Lectromed, Letchworth Garden City, UK). Arterial blood pressure was recorded on a Macintosh LCII (Rothwell Group, Farnborough, UK) using MacLab peripheral and Chart v3.3.5 software (AD Instruments, Hastings, Sussex, UK).

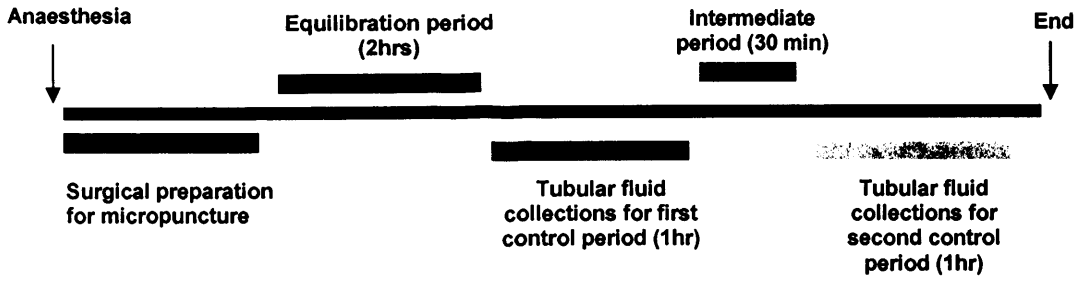

Fig. 3.7.1: Experimental protocol for time-control experiment

3.7.2.2 Results

(i) Urinary flow rate and Na^+ and K^+ output

Table 7.3.1 shows urinary flow rate and Na^+ and K^+ outputs from both micropunctured and contralateral kidneys during both control periods. No significant

change in urine flow rate or in Na^+ excretion was observed for either the micropunctured or contralateral kidney between the two control periods. However, a significant decrease in K^+ output was observed for both the micropunctured kidney and the contralateral kidney during the second control period. None of these variables differed between the micropunctured and contralateral kidneys, with the sole exception of urine flow rate during the first control period ($P = 0.024$).

		Control period 1	*P*	Control period 2
Urine flow rate (µl/min)	Micropuncture kidney	14.3 ± 4.3	0.160	9.2 ± 2.3
	Contralateral kidney	19.4 ± 6.1	0.270	16.2 ± 5.3
Na^+ output (µmol/min)	Micropuncture kidney	2.9 ± 0.5	0.462	2.8 ± 0.5
	Contralateral kidney	3.1 ± 0.6	0.756	3.2 ± 0.6
K^+ output (µmol/min)	Micropuncture kidney	1.3 ± 0.1	0.004	0.9 ± 0.1
	Contralateral kidney	1.2 ± 0.1	0.040	0.9 ± 0.1

Table 3.7.1: Urine flow rate and Na^+ and K^+ outputs in the micropunctured and contralateral kidney during both control periods (means ± SEM; n = 8).

(ii) Mean arterial blood pressure (MABP)

MABP was 110 ± 4 mmHg during the first control period and 108 ± 4 mmHg during the second control period (NS).

(iii) Tubular flow rates

Tubular flow rates in the mid-proximal tubule during the first and second control periods were 31 ± 4 nl/min and 32 ± 3 nl/min (mean ± SEM; $n = 7$), respectively ($P = 0.7$). These mean values were calculated from the average tubular flow rates per rat, which were themselves derived from 7-10 collections.

(iv) Intraluminal ATP concentrations

Although there was considerable variation in proximal tubular ATP concentration (in pooled samples) between animals, there was no systematic difference in ATP concentration between the two collection periods. Proximal tubular ATP concentration was 120 ± 15 nmol/l (mean ± SEM; n = 8) during the first control period, and 125 ± 17 nmol/l during the second control period (P = 0.63) (Fig. 3.7.2).

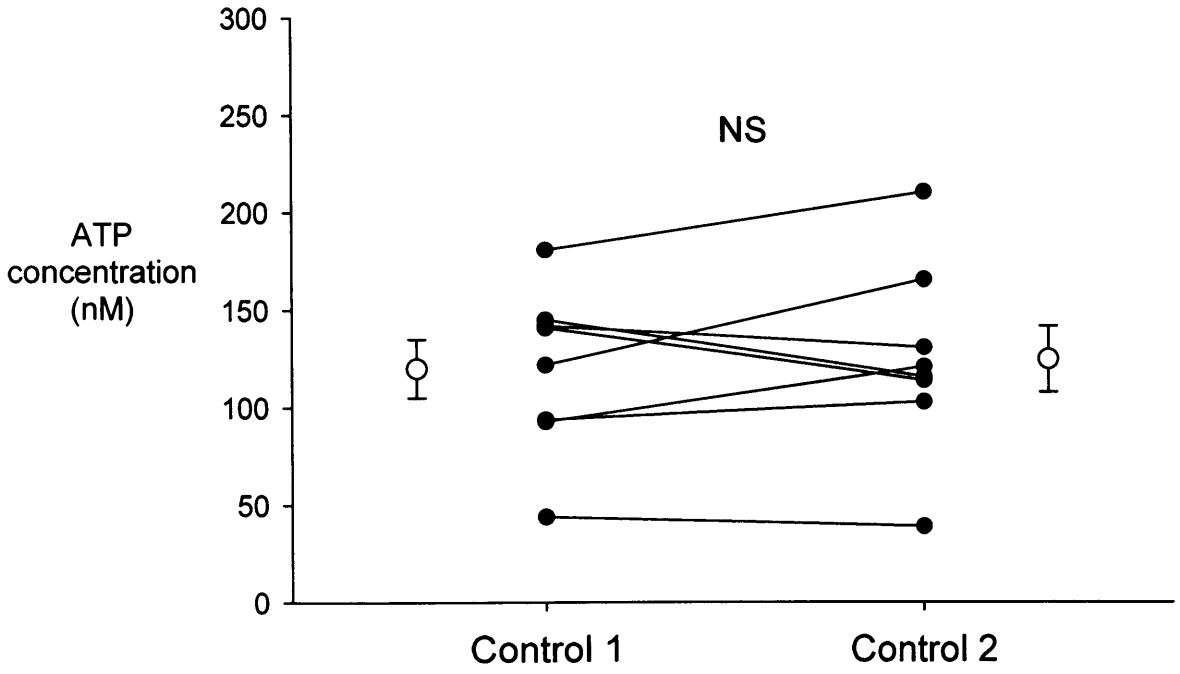

Fig. 3.7.2: Time controls: Intraluminal ATP concentrations in mid-proximal convoluted tubule during the first control period (control 1) and during the second control period 30-90 min later (control 2). Each point represents a single pooled collection, made up of 7-10 samples. Values in each rat are linked by solid lines. Means ± SEM are also shown.

3.7.2.3 Discussion

In these rats, Na^+ and water excretion rates were stable and comparable to those found in earlier experiments. The blood pressure was also stable and well within the normal range for Sprague-Dawley rats. Finally, despite considerable variation in proximal tubular ATP concentration between animals, in a given animal the value changed very little between the first and second control periods.

3.7.3 EXTRACELLULAR VOLUME EXPANSION

3.7.3.1 Introduction

Na^+ is the major solute of extracellular fluid. As such, it is also the major determinant of extracellular fluid (ECF) osmolality; thus changes in Na^+ balance are almost always associated with changes in ECF. It is because of this that increased Na^+ consumption is generally associated with extracellular volume expansion (ECVE). During this state, however, a number of physiological changes (including increased GFR and urinary Na^+ and water output) occur in the kidney in an attempt to restore euvolaemia. The mechanisms by which euvolaemia is achieved and the known physiological changes that occur during ECVE are outlined below (extracted from Koeppen and Stanton, 2001; Lote, 2000):

(i) Because of stimulation of atrial volume receptors, there is a reflex decrease in renal sympathetic nerve activity. This leads to dilation of afferent and efferent arterioles. Because the effect is greater in the afferent arteriole, the hydrostatic pressure within the glomerular capillaries increases, causing a rise in GFR and an increase in the filtered load of Na^+. In addition, activation of sympathetic nerves innervating the proximal tubule and Henle's loop is known to stimulate Na^+ reabsorption; therefore, the decreased sympathetic activity observed during ECVE should also decrease Na^+ reabsorption in these regions of the nephron.

(ii) During ECVE, renin secretion is reduced (largely because of reduced sympathetic nervous activity); consequently, angiotensin II levels are significantly reduced. A reduction in angiotensin II production reduces NaCl reabsorption in the proximal tubule.

(iii) The increased hydrostatic pressure within the glomerular capillaries can also lead to an increment of hydrostatic pressure in the peritubular capillaries. This alteration in the Starling forces within capillaries results in reduced absorption of solutes (including NaCl) and water from the lateral intercellular space, which ultimately acts to reduce net tubular reabsorption along the proximal tubule.

(iv) Because of reduced angiotensin II concentrations, aldosterone levels are also reduced during ECVE, resulting in reduced NaCl reabsorption in the thick ascending limb of Henle's loop and the distal tubule and collecting duct.

(v) In response to ECVE, dopamine, released from the cells of the proximal tubule, also acts on the proximal tubule where it directly inhibits NaCl reabsorption.

(vi) Plasma atrial natriuretic peptide (ANP; released from the cardiac atria following distension) and tubular urodilatin (secreted by the distal tubule and collecting duct) levels are also increased during ECVE. Both ANP and urodilatin act on the medullary regions of the collecting duct to inhibit NaCl reabsorption. ANP also acts to inhibit the action of ADH-stimulated water reabsorption in the collecting duct.

The increased hydrostatic pressure within the peritubular capillaries, the increased filtered load of Na^+ into the nephron, and the effects of reduced sympathetic nerve activity and angiotensin II levels on the reabsorption of NaCl in the proximal tubule, result in increased NaCl delivery to the distal segments of the nephron. This increase in distal delivery not only overwhelms the reabsorptive capacity in these regions, but in addition the hormonal and neuronal influences specifically targeting the loop of Henle, distal tubule and collecting duct augment the increase in Na^+ and water excretion during ECVE, in an attempt to restore euvolaemia.

Thus, in ECVE, the control of sodium excretion is not limited to the collecting duct (as seen in the euvolaemic state), but rather it involves the entire nephron. As indicated in the Introduction (see Section 2.4), ATP appears to have an inhibitory action on solute reabsorption throughout the nephron. It seemed possible, therefore, that an increase in intraluminal ATP concentration in the tubule might contribute to the reduction in fractional reabsorption seen during ECVE.

The aim of the present study was to test this possibility by determining any changes in the intraluminal ATP concentration in the proximal tubule during this state.

3.7.3.2 Methods

Eight male Sprague-Dawley rats were anaesthetised and prepared surgically for micropuncture in accordance with the protocol described above (see Section 3.2.2.1). Tubular fluid collections (n = 7-10; each collection lasting 4 min) were made from mid-proximal tubules (as described above, see Section 3.3.2.1) over a one-hour period and were pooled in 50 µl of ice-cold water and frozen immediately. The infusion rate of the isotonic saline was then increased from 4ml/hr to 24ml/hr. After 30 minutes, further tubular fluid collections (n = 7-10; each collection lasting 4 min) from the same region of another set of proximal convoluted tubules were made and the samples pooled in a separate vial of ice-cold water and frozen immediately. All tubular fluid pooled samples were later assayed for ATP (as described above, see Section 3.3.2.2). Fig. 3.7.3 shows an outline of the experimental protocol. Urine from the micropunctured and contralateral kidneys was collected throughout the tubular fluid collections. The urine samples were assayed for Na^+ and K^+ content using the protocol described above in Section 3.2.2.4. Mean arterial blood pressure (MABP) was monitored throughout the control and experimental periods via the cannulated right femoral artery (as described above, see Section 3.7.2.1).

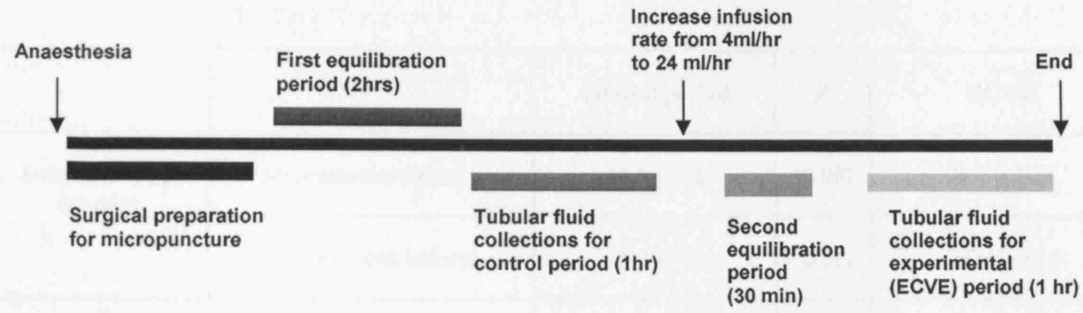

Fig. 3.7.3: Experimental protocol for ECVE

3.7.3.3 Results

(i) Urinary flow rate and Na^+ and K^+ output

Table 3.7.2 shows urinary flow rate and Na^+ and K^+ outputs from both micropunctured and contralateral kidneys during the control period and following volume expansion. A significant increase in urine flow rate was observed in both the micropunctured and contralateral kidney between the control period and ECVE. Similarly, significant increases in Na^+ output were observed in the micropunctured and contralateral kidneys. However, no significant change was observed in K^+ output for either the micropunctured or contralateral kidney.

None of these variables differed between the micropunctured and contralateral kidney, with the sole exception of urine flow rate during the control period (P = 0.022).

		Control period	*P*	ECVE
Urine flow rate (µl/min)	Micropuncture kidney	15.3 ± 5.2	<0.001	78.2 ± 10.4
	Contralateral kidney	25.2 ± 7.3	<0.001	100.4 ± 10.1
Na^+ output (µmol/min)	Micropuncture kidney	3.0 ± 0.7	0.001	14.2 ± 1.6
	Contralateral kidney	3.8 ± 0.7	0.004	18.3 ± 2.4
K^+ output (µmol/min)	Micropuncture kidney	1.1 ± 0.1	0.738	1.2 ± 0.1
	Contralateral kidney	1.2 ± 0.1	0.476	1.3 ± 0.2

Table 3.7.2: Urine flow rate and Na^+ and K^+ outputs in the micropunctured and contralateral kidney during the control and experimental (ECVE) period (means ± SEM: n= 7).

(ii) Mean arterial blood pressure

MABP was 109 ± 4 mmHg during the control period and 106 ± 4 mmHg during ECVE (NS).

(iii) Tubular flow rates

The tubular flow rate in the mid-proximal tubule during the control period was 30 ± 1 nl/min (mean ± SEM; n = 8). Following ECVE, a significant increase ($P < 0.01$) in tubular flow rate (36 ± 2 nl/min) was observed. These mean values were calculated from the average tubular flow rates per rat, which were themselves derived from 7-10 collections.

(iv) Intraluminal ATP concentrations

Intraluminal ATP concentrations are shown in Fig. 3.7.4. The ATP concentration in the proximal tubule during the control period was 168 ± 15 nmol/l (mean ± SEM; n =

8). After volume expansion, the intraluminal ATP concentration in the same rats was 145 ± 31 nmol/l. The difference in ATP concentration between control and ECVE states was not statistically significant. ($P = 0.541$).

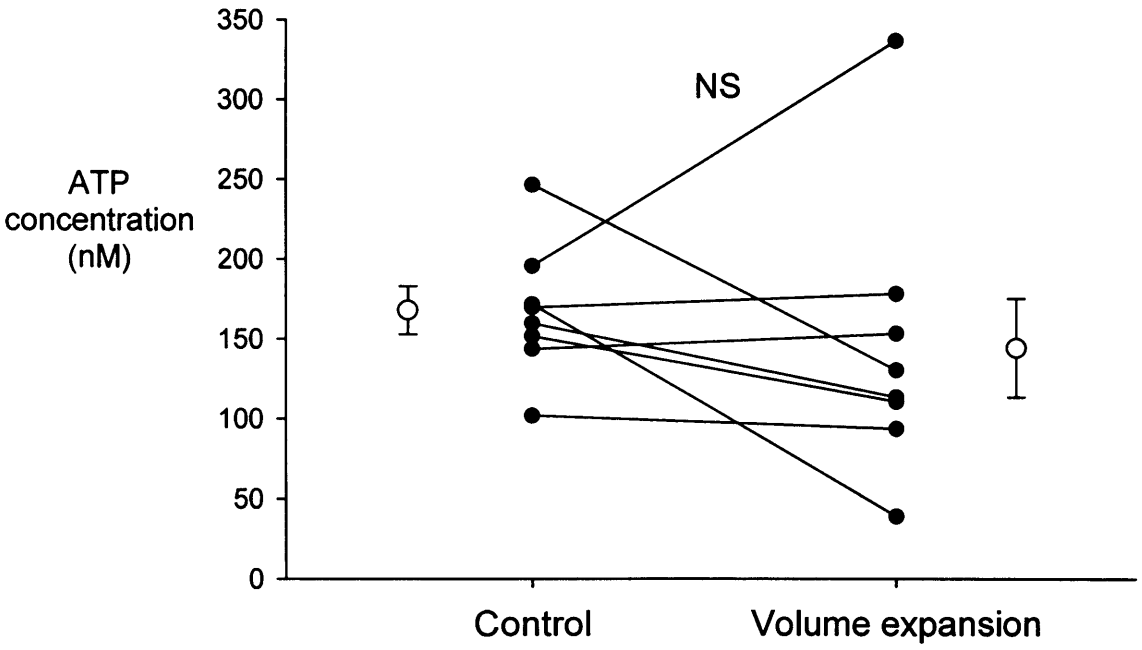

Fig. 3.7.4: Volume expansion: Intraluminal ATP concentrations in mid-proximal convoluted tubule during the control period and during the period 30-90 min after the start of an intravenous saline infusion of 24 ml/min ("volume expansion"). Each point represents a single pooled collection, made up of 7-10 samples. Values in each rat are linked by solid lines. Means ± SEM are also shown.

3.7.3.4 Discussion

Given that ATP can have an inhibitory effect on solute reabsorption, it might be expected to act as a signalling molecule to promote/augment a natriuretic response. Furthermore, previous studies have reported that ATP release is increased significantly following mechanical/shear-stress stimulation in endothelial and

epithelial cell lines (Bodin and Burnstock, 2001; Guyot and Hanrahan, 2002; Srinivas et al, 2002). In this context, increased tubular flow rates following ECVE might be expected to increase the intraluminal pressure in the proximal tubule sufficiently to mechanically stimulate the release of ATP from tubular epithelial cells.

In the present study, a natriuretic effect was observed when the rats were exposed to ECVE, indicating that both the micropunctured and contralateral kidneys responded to the physiological change. In addition, tubular flow rates increased significantly (presumably resulting from increased GFR and decreased tubular solute and water reabsorption). However, despite this normal physiological response, there was no significant change in intraluminal ATP concentration in the proximal tubule following volume expansion.

The most obvious conclusion from these findings is that stimulation of ATP release does not occur during ECVE and that ATP has no role to play in the observed natriuresis. Before dismissing such a role, however, the possibility should be considered that an increased release of ATP during ECVE might have been masked by the concomitant release of soluble nucleotidases originating from the same or adjacent cells. An example of this phenomenon has been demonstrated in postganglionic sympathetic nerves isolated from the vas deferens in the guinea-pig, where stimulation of the nerve evokes the concomitant release not only of ATP and noradrenaline, but also of soluble nucleotidases (Kennedy et al, 1997). The same group has also demonstrated that stimulated nerves were able to degrade exogenously applied ATP at a higher rate than could non-stimulated nerves. The soluble enzymes released from stimulated nerves have not been identified. However, at least two enzymes are believed to be involved: an ATPase (possibly a C- and N-terminal truncated form of a NTPDase family member) and an AMPase that closely resembles ecto-5'-nucleotidase (Westfall et al, 2002; Mihaylova-Todorova et al, 2002). Similarly, non-neuronal cells, such as vascular endothelial cells, have also been shown to release soluble nucleotidase and ATP concomitantly when exposed to shear stress stimuli (Yegutkin et al, 2000).

3.7.4 HAEMORRHAGIC HYPOTENSION

3.7.4.1 Introduction

During severe haemorrhage there are significant reductions in MABP and extracellular volume (ECV). These are accompanied by reductions in GFR and urinary excretion rates. As with ECVE, the renal changes are induced by volume (and pressure) sensors that detect the fall in ECV and, through various signalling and hormonal cascades, elicit responses opposite to those observed during ECVE, as outlined below:

Increased renal sympathetic activity, which induces constriction in the afferent and (to a lesser extent) the efferent arteriole, results in partial renal ischaemia and a reduction in the hydrostatic pressure in the glomerular capillaries, causing GFR and the filtered load of Na^+ to fall. The reduced filtered load of Na^+ causes a reduction in the amount of Na^+ delivered to the distal regions of the nephron. Increased sympathetic nerve activity and aldosterone levels will also stimulate Na^+ reabsorption in the thick ascending limb of Henle's loop, distal tubule and collecting duct. The rise in aldosterone levels, together with the absence of ANP and urodilatin, causes the small amount of Na^+ delivered to the collecting duct to be virtually all reabsorbed in this region of the nephron. ADH levels also increase in response to haemorrhage, which enhances water reabsorption in the collecting duct. In addition to these responses, fractional proximal reabsorption would be expected to be enhanced due to the increased renal sympathetic nerve activity and increased angiotensin II levels. However, direct micropuncture studies show this to be the case only for a very limited period after haemorrhage (Shirley and Walter, 1995). This suggests that the stimulatory effects of these systems are offset by an inhibitory effect of unknown source.

Because intraluminal ATP has been shown to have an inhibitory effect on solute transport (Section 2.4), it has been proposed that a rise in luminal ATP concentration may occur during renal ischaemia in an attempt to inhibit energy-consuming transport

processes (Leipziger, 2003). This proposal is strengthened by the above observation that fractional proximal reabsorption is little affected after haemorrhage. The present study was therefore conducted to test the hypothesis that partial renal ischaemia following haemorrhagic hypotension leads to increased intraluminal ATP concentrations.

3.7.4.2 Methods

Eight male Sprague-Dawley rats were anaesthetised and prepared surgically for micropuncture in accordance with the protocol described above (see Section 3.2.2.1). Tubular fluid collections (n = 7-10; each collection lasting 4 min) were made from the mid-proximal tubule (as described above, see Section 3.3.2.1) over a one-hour period and were pooled in 50µl of ice-cold water and frozen. Immediately after this control period, the rat was bled 15 ml/kg of its body weight via the femoral artery catheter and then given a partial recovery period of 30 minutes. Mid-proximal tubular fluid collections were then made (n = 7-10, each collection lasting 4 mins) from another set of proximal convoluted tubules and the samples pooled in a separate vial of ice-cold water and frozen. All tubular fluid pooled samples were later assayed for ATP (as described above, see Section 3.3.2.2). Fig. 3.7.5 shows an outline of the experimental protocol. Urine from the micropunctured and contralateral kidneys was collected throughout the tubular fluid collections. The urine samples were assayed for Na^+ and K^+ content using the protocol described above in Section 3.2.2.4. MABP was also monitored (as described above see Section 3.7.2.1) throughout the control and experimental periods.

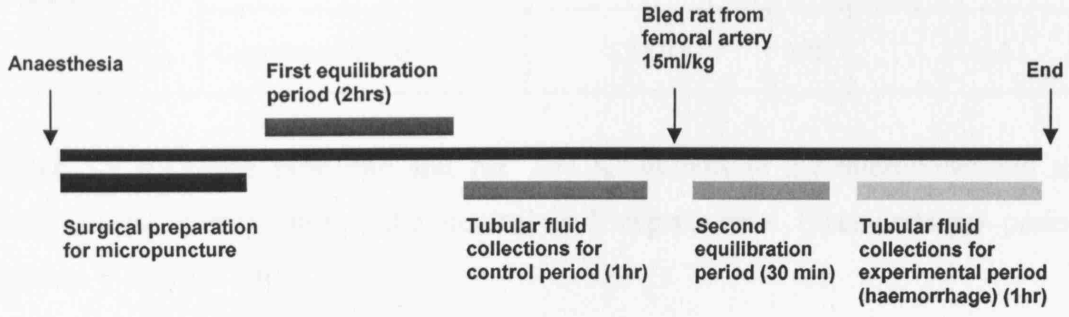

Fig. 3.7.5: Experimental protocol for hypotensive haemorrhage

3.7.4.3 Results

(i) Urinary flow rate and Na^+ and K^+ output

Table 3.7.3 shows urinary flow rate and Na^+ and K^+ outputs from both micropunctured and contralateral kidneys during the control period and following haemorrhage. A significant decrease in urine flow rate was observed in both the micropunctured and contralateral kidneys between the control and experimental periods. Similarly, a significant decrease in Na^+ output was observed in the micropunctured and contralateral kidneys. However, no significant change was observed in K^+ output for either the micropunctured or contralateral kidney.

There were no significant differences in these variables between the micropunctured and contralateral kidney, with two exceptions: urine flow rate during the experimental period ($P = 0.033$) and Na^+ output during the control period ($P = 0.026$).

		Control period	*P*	Haemorrhage
Urine flow rate output (µl/min)	Micropuncture kidney	19.4 ± 6.2	0.032	4.1 ± 1.2
	Contralateral kidney	24.1 ± 0.5	0.014	5.2 ± 1.3
Na^+ output (µmol/min)	Micropuncture kidney	2.7 ± 0.4	0.009	0.6 ± 0.2
	Contralateral kidney	3.5± 0.5	0.010	1.0 ± 0.3
K^+ output (µmol/min)	Micropuncture kidney	1.4 ± 0.3	0.182	0.8 ± 0.1
	Contralateral kidney	1.2 ± 0.1	0.261	1.0 ± 0.1

Table 3.7.3: Urine flow rate and Na^+ and K^+ outputs in the micropunctured and contralateral kidney during the control and experimental (haemorrhage) periods (means ± SEM; n = 6).

(ii) Mean arterial blood pressure

In rats subjected to haemorrhage (15 ml/kg), MABP was 112 ± 4 mmHg during the control period, fell significantly to 42 ± 3 mmHg immediately after bleeding, and recovered partially to 92 ± 2 mmHg during the period 30-90 min after bleeding (experimental period).

(iii) Tubular flow rates

The tubular flow rate in the mid-proximal tubule during the control period was 34 ± 2 nl/min (mean ± SEM; n = 8). Following haemorrhage, a significant decrease (P < 0.001) in mid-proximal tubular flow rate (17 ± 2 nl/min) was observed. These mean values were calculated from the average tubular flow rates per rat, which were themselves derived from 7-10 collections.

(iv) Intraluminal ATP concentrations

Intraluminal ATP concentration in the proximal tubule during the control period was 120 ± 22 nmol/l (mean ± SEM; n = 8). During the experimental period, intraluminal ATP concentration was 153 ± 38 nmol/l (Fig. 3.7.6). Although in two animals the post-haemorrhage ATP concentration was strikingly higher than the pre-haemorrhage value, taking the group as a whole there was no statistically significant effect (P = 0.412) on intraluminal ATP concentration.

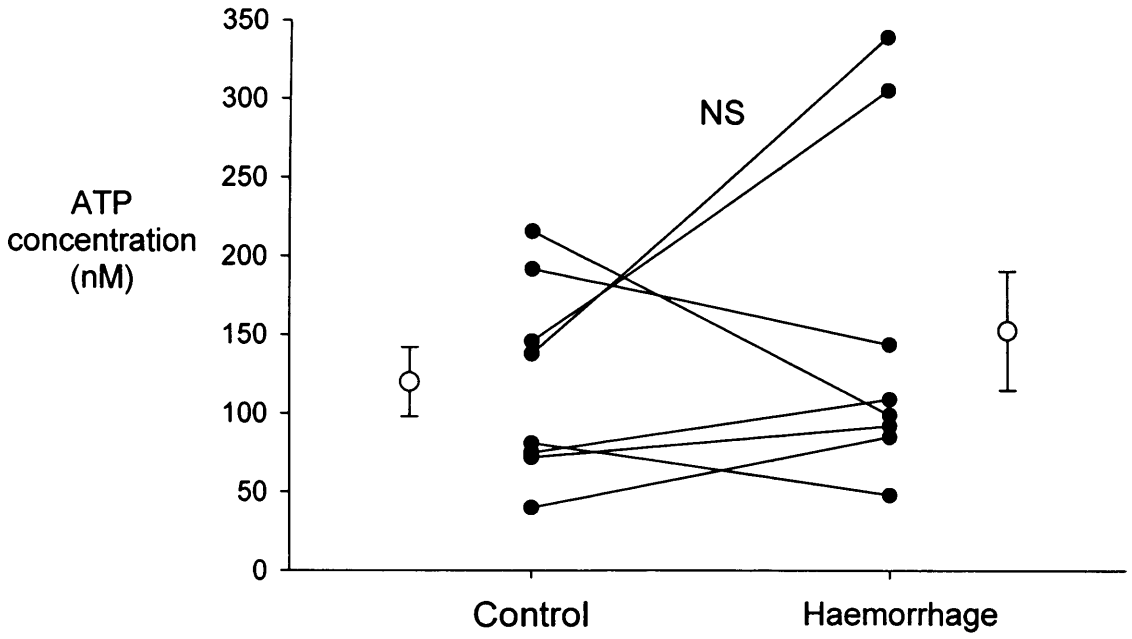

Fig. 3.7.6: Hypotensive haemorrhage: Intraluminal ATP concentrations in mid-proximal convoluted tubule during the control period and during the period 30-90 min after a blood loss of 15 ml/kg ("haemorrhage"). Each point represents a single pooled collection, made up of 7-10 samples. Values in each rat are linked by solid lines. Means ± SEM are also shown.

3.7.4.4 Discussion

There is evidence that ischaemia induces ATP release in a number of non-renal tissues (Dutta et al, 2004), and it has been proposed that intraluminal ATP serves to protect the renal tubular epithelium under ischaemic conditions by inhibiting energy-consuming transport processes (Leipziger, 2003). Moreover, Kribben et al (2003) examined the effect of ATP on hypoxia-induced injury in freshly isolated rat renal proximal tubules and concluded that the addition of stable ATP analogues reduced the extent of cellular damage. Using the agonists ATPγS and 2-MeSATP, the same report suggested that the protective effects of ATP were mediated by a member of the P2Y family, although the mechanism by which P2Y receptor activation protects the

cell remains unknown. Furthermore, Paller et al (1998) reported the beneficial effects of ATP in promoting new DNA synthesis and augmenting the expression of genes (namely, c-fos and c-jun) critical to cell proliferation when given shortly after ischaemia, suggesting that ATP contributes to cell regeneration in this situation.

The above *in vitro* studies indicate that ATP may have a protective role during ischaemia and/or may contribute to cell regeneration after hypoxia. In this context, it has been shown that the partial renal ischaemia that follows haemorrhage has little effect on fractional proximal tubular reabsorption despite enhanced activity of the renal sympathetic nerves and the renin-angiotensin system (Shirley and Walter, 1995). A plausible explanation is that the stimulatory effects of these systems are offset by an inhibitory effect of unknown source; possibly ATP. The question then arises: is ATP release into the intraluminal environment of the tubule increased during this condition?

In the present study, significant reductions in MABP, tubular flow rate and urinary Na^+ and water output were observed during hypotensive haemorrhage. These observations are consistent with normal responses to haemorrhage, which are effectively orchestrated by hormonal and neuronal activity (as described in the Introduction). The above observations indicate that the degree of haemorrhage used in the present study was sufficient to incite the physiological cascade of events expected to occur after haemorrhage. Thus, it is believed that an adequate stimulus was given for the potential release of ATP into the tubular lumen. However, although hypotensive haemorrhage appeared to cause a marked increase in intratubular ATP concentration in two animals (contrasting with the stability seen in time controls), in the group as a whole there was no statistically significant change. One possible explanation for the lack of change in intraluminal ATP concentration in the present study might be an instantaneous or short-duration release of ATP following haemorrhage. Tubular fluid was taken 30-90 minutes after haemorrhage (the earliest time in which tubular fluid could feasibly be taken following a bleed of this volume). Thus, intraluminal ATP concentrations might have normalized by the time tubular samples were taken. Alternatively, the release of ATP and subsequent rise in intraluminal ATP concentration may have been 'masked' through the concomitant release of soluble nucleotidases, as discussed for the volume expansion study.

3.8 SECTION 8: Summary and conclusions

In the present study, the concentration of ATP in proximal tubular fluid was found to average ~ 150 nmol/l. Although the concentration of ATP did not vary significantly between the early, mid and late regions of the S2 segment, ATP levels in distal tubular fluid (~ 30 nmol/l) were found to be consistently and significantly lower than those found in proximal tubular fluid.

Owing to the presence of (soluble and membrane-bound) nucleotidases (Beliveau et al 1983; Gandhi et al 1990; Kishore et al 2005; see Chapter 5 and Section 5), the ATP concentrations measured in the present study are likely to underestimate significantly those in the tubular micro-environment. Although membrane-bound nucleotidase activity could not be assessed, due to inaccessibility of the cell surface *in vivo* and lack of effective ectonucleotidase inhibitors, soluble nucleotidase activity was assessed by incubating an excess of exogenous ATP for varying time periods in collected proximal and distal tubular fluid. These experiments not only showed that soluble nucleotidases were active in proximal and distal tubular fluid, but that these enzymes caused similar rates of hydrolysis for ATP in the two regions of the nephron (16 and 15 fmol/min respectively).

When the half-life of endogenous ATP was assessed in proximal tubular fluid (by varying the duration of tubular fluid collections), ATP concentration fell exponentially as "processing time" increased and the half-life was found to be 3.4 min. Extrapolation back to zero time (i.e. before any degradation by soluble nucleotidases had occurred) gave a value of 275 nmol/l. Because of the presence of ectonucleotidases, it is highly likely that the concentration of ATP immediately in the vicinity of apical P2 receptors may be substantially higher than those measurable with the present methodology.

Nevertheless, ATP levels in the proximal and distal tubules were measurable. The next question addressed was the source of this luminal ATP. Was it merely filtered at the glomerulus or was it secreted by the proximal tubular cells? Experiments performed on Munich-Wistar rats showed that the ATP concentration in mid-proximal

tubule was, on average, more than 4-fold higher than that in Bowman's space. The modest fractional water reabsorption between the two sites (as indicated by TF/P_{In} measurements) could not account for this increase in ATP concentration, strongly suggesting that the proximal tubule secretes it into the lumen. Although the mechanism by which ATP secretion occurs in tubular epithelial cells is unknown, several possibilities exist; these will be discussed in the next chapter.

In any study of this nature, care must be taken to exclude possible artifacts and potential sources of contamination. It could be argued, for example, that disturbances of intraluminal pressure caused by the oil column distal to the point of collection might induce mechanical stress and stimulate ATP release by the proximal tubular cells, or that damage to the tubular cells caused by insertion of the collection pipette might itself lead to release of intracellular ATP into the lumen. More fundamentally, contamination of the pipette tip by ATP as the pipette traverses the tubular cells might also lead to artifactual intraluminal ATP concentrations (intracellular ATP concentrations being several orders of magnitude greater than those measured in the lumen). These possibilities were all assessed and no difference in luminal ATP concentrations were found whether or not an oil block was used, nor when a 4-min delay was interposed between insertion of the pipette and initiation of collection. Clearly, any pulse of ATP released on insertion of the pipette must have been washed away/metabolized within seconds, before tubular fluid collections began. Finally, some experiments in which a pipette was repeatedly inserted into a number of tubules were performed, but without tubular fluid collection, and the pipette tip then washed in de-ionized water. No trace of ATP could be detected. In conclusion, it can be assumed that the ATP measured in the proximal tubular lumen was not simply a consequence of the experimental manipulations employed. Parenthetically, the fact that lower ATP concentrations were measured in the distal tubule (and in Bowman's space) is further circumstantial evidence that the intraluminal ATP levels found in the proximal tubule in the present investigation were not simply the consequence of injury-induced release of ATP.

Finally, an attempt was made to address the question of whether intratubular ATP concentrations are altered by (patho)physiological manoeuvres that affect tubular reabsorptive processes. Given the inhibitory effects of intraluminal nucleotides on

tubular reabsorption (see Section 2.4), it could be speculated that the reduction in fractional proximal reabsorption that accompanies acute volume expansion might result partly from enhanced ATP secretion. However, despite a marked natriuresis and significant increase in mid-proximal tubular flow rate, volume expansion had no systematic effect on measured intratubular ATP concentrations. Another situation in which ATP secretion might be expected to increase is renal ischaemia, where it has been proposed that intraluminal ATP might serve to protect the renal tubular epithelium under ischaemic conditions by inhibiting energy-consuming transport processes (Leipziger, 2003). In the event, although hypotensive haemorrhage appeared to cause a marked increase in intratubular ATP concentration in two animals (contrasting with the stability seen in time controls), in the group as a whole there was no statistically significant change.

Although at first glance these negative findings suggest that proximal tubular ATP release is "constitutive", lacking physiological control, there is some evidence that such a view may be over-simplistic. Individually, there did appear to be a greater variation in intratubular ATP concentration amongst the rats that were exposed to ECVE or haemorrhage than seen either in the same rats before the manoeuvre or in time controls. Although there is no ready explanation for this observation, there are at least two possibilities arising from the multifactorial physiological changes associated with ECVE or haemorrhage. The first is that ATP secretion may have been affected to differing extents between animals. The second possibility is that ATP concentrations in glomerular plasma, and therefore in glomerular filtrate, varied considerably between animals. This possibility was assessed in a separate group of Munich-Wistar rats (n = 6) subjected to haemorrhage (data not shown). Similar results were obtained to those seen in Sprague-Dawley rats, *i.e.*, no significant haemorrhage-induced change in proximal tubular ATP concentration, with a wide spread of post-haemorrhage values. However, there was no correlation between ATP concentrations in Bowman's space and proximal tubules; indeed, in only one animal did the ATP concentration in Bowman's space alter after haemorrhage.

The overall lack of change in ATP concentration following ECVE or haemorrhage may involve variation in the activity of nucleotidases to ultimately 'mask' the release of additional ATP. This has been demonstrated in guinea-pig vas deferens, where

stimulation of sympathetic nerves evokes the release not only of ATP but also of soluble nucleotidases (Mihaylova-Todorova, 2001); a similar phenomenon has been described when vascular endothelial cells are exposed to shear stress (Yegutkin et al, 2000). It is therefore feasible that enhanced ATP release during these pathophysiological manoeuvres could have been masked by its immediate partial degradation by both ecto- and soluble nucleotidases. In this context, it should be noted that the inhibitory effects of apically applied nucleotide on proximal tubular NHE3 activity (Bailey, 2004) and Na^+K^+ATPase (Jin and Hopfer, 1997) are mediated by the $P2Y_1$ receptor subtype, which has a much greater sensitivity to ADP than to ATP (King and Townsend-Nicholson, 2003). It would make physiological sense, therefore, for locally released ATP to be rapidly converted to its diphosphate form.

CHAPTER 4

VESICULAR STORAGE AND RELEASE OF ATP IN A RAT PROXIMAL TUBULE CELL LINE

4.1 Introduction

As indicated in earlier chapters, the physiological release of ATP from healthy, intact cells is increasingly being recognised. The debate now lies in the mechanism by which ATP is transported, as a molecule the size and charge of ATP cannot cross the cell membrane by simple diffusion, despite there being a highly favourable electrochemical gradient (Bodin and Burnstock, 2001). Various mechanisms by which ATP is released from cells have been proposed. These include transport via ATP binding cassette (ABC) proteins, which include CFTR and the MDR-1 gene product P-glycoprotein; connexin hemichannels; large anion channels; and exocytotic vesicular release.

As far as the renal tubule is concerned, previous in *vitro* studies have demonstrated ATP secretion by renal epithelial cells (Wilson et al, 1999) and the previous chapter confirmed this *in vivo*. However, to date, the only study of the mechanism(s) of ATP secretion in the tubule has been in the macula densa, where maxi-anion channels mediate its release across the basolateral membrane (Bell et al, 2003). It is important to note that the mechanisms of ATP transport may differ not only between various cell types but also between apical and basolateral membranes.

4.1.2 ATP binding cassette (ABC) transporters

ABC transporters are a superfamily of transport proteins, thought to bind and/or hydrolyze ATP intrinsically. Various workers have speculated that members of the ABC family, in particular the CFTR and the product of the MDR-1 gene, P-glycoprotein, are involved in ATP transport across the cell membrane. Both structures have 12 alpha-helical transmembrane domains, with intracellular N- and C-termini and two intracellular nucleotide binding folds/domains involved in nucleotide hydrolysis to provide the driving force required for substrate transport.

(i) Cystic fibrosis transmembrane regulator

CFTR is a chloride channel found predominantly on the apical membrane of secretory and absorptive epithelia. Mutations in this transporter result in defective chloride secretion, causing cystic fibrosis (CF). Its mRNA has been detected in all segments

of the nephron, and at the protein level the transporter has been found in the proximal tubule, the distal convoluted tubule, the cortical collecting duct (restricted to principal cells) and the inner medullary collecting duct (Morales et al, 2000). Despite its high expression in the kidney, patients with CF display no major renal dysfunction: they have enhanced proximal tubular reabsorption and a decreased capacity to dilute and concentrate urine (Morales et al, 2000). In addition to chloride transport, a number of studies using CFTR-transfected membrane preparations and patch clamp techniques have implicated CFTR in ATP transport in a variety of cell lines (Reisin et al, 1994; Cantiello, 2001). However, other studies, using CFTR-transfected and CFTR-free cell lines, reported no significant difference in ATP release between the two preparations; furthermore, inhibitors of CFTR (such as glibenclamide) appeared to have no effect on ATP release (Reddy et al, 1996, Sabirov et al, 2001; Dutta et al, 2004). In addition, the estimated maximum pore size of the CFTR channel was reported to be 1.38nm in diameter, which is similar to the diameter of an ATP anion (1.16 – 1.30nm), thus questioning the feasibility of ATP movement through this channel (Sabirov and Okada, 2004). An alternative suggestion is that CFTR is not an ATP channel itself but might regulate a separate ATP-permeable channel (Sugita et al, 1998), possibly a plasma membrane form of a voltage-dependent anion channel (pl-VDAC) (see below); in this context, CFTR and pl-VDAC have been shown to colocalize, but the mechanism by which CFTR might regulate this channel is unknown (Reymann et al, 1995).

(ii) P-Glycoprotein

Another candidate for ATP transport is the MDR-1 gene product, P-glycoprotein, which conventionally transports hydrophobic drugs and has also been implicated in the regulation of Cl^- channel transport. In the rat, MDR-1 mRNA has been detected in the glomeruli, proximal tubules, thin limbs of Henle's loop, cortical and medullary thick ascending limbs, and inner medullary collecting ducts; its abundance was 35% less in the renal cortex than in the medulla (Morales et al, 2000). At the protein level, P-glycoprotein was expressed in the glomerular mesangium, the proximal tubule, the thick ascending limb of Henle's loop and the collecting ducts (Ernest et al, 1997). Studies in other polarized epithelial cells suggest that the expression of P-glycoprotein is localized to the apical membrane (Borst et al, 1999). It has been shown that over-expression or transfection of the MDR-1 protein into NIH 3T3 cells (a fibroblast cell

line derived from the mouse) and CHO cells transiently increases ATP release several fold; and that single amino acid substitution at the nucleotide binding site blocks this effect (Roman et al, 2001; Cantiello, 2001). Furthermore, Roman et al (2001) demonstrated that non-selective MDR-1 inhibitors, such as verapamil and cyclosporine, significantly attenuated ATP release. These results suggest that this protein is involved in ATP release. However, the latter group also demonstrated that alteration of the MDR-1 substrate specificity by mutation of the MDR-1 protein had no effect on ATP release, and concluded that MDR-1 is not likely to function as an ATP channel but instead may act as a regulator/modulator of other ATP release mechanisms.

4.1.2 Large-conductance anion channels/maxi-anion channels

At physiological pH, most intracellular ATP is present in anionic form (Okada et al, 2004). Therefore it is plausible that large-conductance anion channels, or maxi-anion channels, are involved in the conductance of ATP across the plasma membrane. Maxi-anion channels comprise a variety of anion channels, such as the volume-sensitive outwardly rectifying (VSOR) anion channel and the voltage-dependent anion channel (VDAC) (as well as CFTR – see above). Due to the lack of selective inhibitors of these channels, distinguishing between them has not always been feasible.

Maxi-anion channels have been implicated in ATP transport in a number of cell types. Studies performed on a mammary cell line (C127i cells) (Sabirov et al, 2001) and on primary cultures of neonatal cardiomyocytes (Dutta et al, 2004) showed that maxi-anion channel blockers, namely 5-nitro-2-(3-phenylpropylamino)-benzoate (NPPB), 4-acetamido-4'-isothiocyanostilbene (SITS) and Gd^{3+}, significantly inhibited ATP release from these cells following hypotonic stimulation; but that the CFTR blocker glibenclamide had no effect on ATP release. With respect to the kidney, Bell and colleagues (2003) reported that macula densa cells also expressed Gd^{3+}-inhibitable maxi-anion channels, which were shown to transport ATP across the basolateral membrane in response to increased luminal NaCl concentrations. These channels are therefore strongly implicated in the transduction of signals from the macula densa to the adjacent afferent arteriole and mesangial cells during the TGF response (see Section 1.2.2).

Using various inhibitors (namely verapamil, tamoxifen and fluoxetine) of the VSOR anion channel, Hisadome and colleagues (2002) implicated this channel in the release of ATP from primary cultures of bovine aorta endothelial cells. However, Ternovsky et al (2002) reported the pore radius of this channel to be 0.63nm, which would make the transport of ATP (which, as indicated above, has a radius of 0.58 – 0.65nm) theoretically difficult, although not impossible. Furthermore, Hazama et al (1999) reported that no significant reduction in ATP release occurred when either glibenclamide or arachidonate (non-specific inhibitors of VSOR anion channels) was used on an epithelial cell line of the human intestine, suggesting that this channel does not mediate ATP release in this epithelium. A similar finding was made using a murine mammary cell line (Hazama et al, 2000).

Voltage-dependent anion channels (VDAC) are porins in the outer mitochondrial membrane, where they are believed to transport purine nucleotides such as ATP and ADP. A variant of the first exon in the VDAC-1 gene was first identified in the mouse. This variant of the VDAC-1 gene, having a 'signal' peptide at its N-terminus, enables the porin protein to be targeted to the plasma membrane via the Golgi apparatus; the signal peptide is eventually cleaved away to produce a plasmalemmal VDAC (pl-VDAC) protein that is identical to the mitochondrial one (Sabirov and Okada, 2004). These pl-VDAC porins have been implicated in mediating ATP translocation across the cell membrane. One study, using NIH 3T3 cells, reported that ATP release in response to hypotonic shock was significantly higher in cells transfected with pl-VDAC-1 than in non-transfected cells (Okada et al, 2004). Similarly, ATP release was significantly lower from fibroblasts isolated from VDAC-1 knockout mice compared with wild-type mice. These results suggest that this channel contributes to ATP release in murine cells. However, the fact that a significant amount of ATP was still released from VDAC-1 knockout cells following hypotonic stimuli suggests that this channel is not the only mechanism of ATP release (Okada et al, 2004). Recent electrophysiological studies have suggested that a maxi-anion channel (possibly VDAC) may exist in the macula densa (as indicated above) and also in rabbit cortical collecting duct (Okada et al, 2004). However, the role of maxi-anion channels in the translocation of ATP in the latter cells has not been examined.

4.1.3 Connexin hemichannels

Gap junctions are intercellular contacts between plasma membranes of adjacent cells. They mediate the passage of ions and small molecules through a narrow hydrophilic core connecting the cytoplasm of the two cells. Formation of the gap junction involves each of the neighbouring cells contributing half of the intercellular channel; each moiety, known as a hemichannel or connexon (itself made up of connexin sub-units), migrates to the plasma membrane and eventually associates with its opposite number in the narrow space between adjacent plasma membranes. In addition to constituting the gap junctions, hemichannels or connexons are also functional as single subunits, displaying permeability to small molecules (<1 KDa) (Bahima et al, 2005).

In vitro evidence suggests that hemichannels are permeable to ATP, as cells transfected with connexins (specifically connexins 26, 32, 38 and 43) showed a marked increase in the level of ATP released compared with non-transfected cells (Cotrina et al, 1998; Bahima et al, 2005). Moreover, in most cases release of ATP was significantly reduced by the application of connexin channel blockers such as flufenamic acid and octanol (Bahima et al, 2005; Stout et al, 2004).

Immunohistochemical studies have shown the expression of connexin 32 (Cx32) in both foetal and adult kidneys in hamsters, localized on the lateral cell membrane of the cells lining the developing and adult proximal tubules. No immunopositive staining for Cx32 was observed in the distal or collecting tubules (Udaka et al, 1995). Other connexins found in the (mouse) kidney include Cx45, localised to the glomeruli and distal tubule, and Cx26, in the proximal tubule (Butterweck et al, 1994).

It is worth noting that whilst these channels may be plausible candidates for ATP translocation across the cell membrane, their large pore size and lack of specificity begs the question of the consequences of the activation of such channels, in that they could rapidly cause dramatic and potentially detrimental changes in cytoplasmic ionic concentrations. If these channels were involved in ATP translocation across the cell membrane, their activity must be highly regulated.

4.1.4 Exocytotic release of ATP

Rather than use one of the above transporters/channels, there is evidence that in a variety of situations ATP may traverse the cell membrane via the release of intracellular stores of ATP from acinar vesicles or secretory granules. Exocytotic release of ATP has been more commonly reported in excitable tissues such as neuronal cells, where the storage and release of ATP occurs in conjunction with neurotransmitters such as acetylcholine and noradrenaline from sympathetic neurones (Van der Kloot, 2003; Silinsky and Redman, 1996; Burnstock and Knight, 2004). However, vesicular release of ATP has also been demonstrated in non-neuronal cells.

4.1.4.1 Quinacrine and its interaction with ATP

The antimalarial drug quinacrine (Fig. 4.1) has a high affinity for ATP (Irvin and Irvin, 1954) which, upon binding, fluoresces under exposure to UV light. Many studies have made use of these properties by incubating a variety of cells, including human endothelial cells (Bodin and Burnstock, 2001), guinea pig inner ear cells (Suzuki et al, 1997), ocular ciliary epithelial cells (Mitchell et al, 1998) and rat pancreatic acinar cells (Sorensen and Novak, 2001) with quinacrine for labelling intracellular stores of ATP. In all these studies, granular-like fluorescent staining was found in the cytoplasm. Moreover, many of the above studies also reported reduced granular fluorescence together with marked increases in extracellular ATP, in response to various stimuli, providing evidence for vesicular release of ATP from these cells.

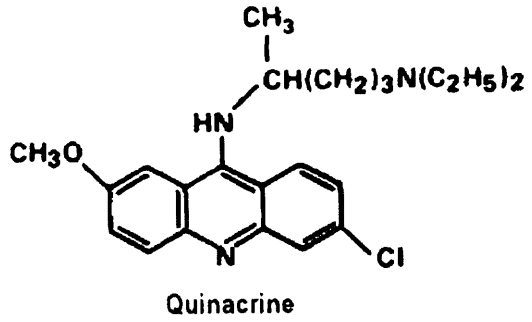

Fig. 4.1: Molecular structure of the anti-malarial drug quinacrine, used to visualize intracellular stores of ATP.

In one of the above studies, granular staining in the cytoplasm of endothelial cells was found to be reduced when cells were pre-incubated with the drug monensin, which prevents vesicle formation at the Golgi apparatus; this decrease in fluorescence was associated with a significant reduction in ATP release (compared with controls) following shear-stress stimulation (Bodin and Burnstock, 2001). In the same study, cells incubated with the drug N-ethylmaleimide (NEM), which inhibits the docking of vesicles to the plasma membrane, showed abundant granular fluorescence, and low extracellular ATP levels following shear-stress/mechanical stimulation. These results strongly suggest that release of ATP from these cells was indeed mediated via vesicles.

Other studies have used hypotonic shock or mechanical stimulation, rather than shear-stress, to elicit ATP secretion. In each case it is hypothesized that distortion of the plasma membrane leads to activation of stretch-sensitive channels that may ultimately lead to ATP release (Wang et al, 1996).

4.1.6 Aim of the present study

To date, no study has examined intracellular stores or vesicular release of ATP in renal epithelial cells. The present investigation has therefore used quinacrine to visualise intracellular stores of ATP in an immortalized proximal tubular cell line (WKPT-0293). This cell line was originally derived from the S1 segment of the proximal tubule of Wistar-Kyoto rats by Woost et al (1996). These cells, which have numerous mitochondria, rough and smooth endoplasmic reticulum, Golgi apparati and clathrin-coated vesicles, also display similar features to proximal cells such as tight junctional complexes and convolutions in basolateral membranes forming intracellular spaces. The cells absorb sodium, a process that was shown to be angiotensin II sensitive; they possess an apical Na^+/H^+ exchanger; and they actively absorb succinate via an apical sodium-dicarboxylate co-transporter ($3Na^+$ to 1 dicarboxylate coupling ratio). They continue to thrive in a glucose-free environment, demonstrating their ability for gluconeogenesis (Woost et al, 1996).

In addition to visualizing intracellular stores of ATP using quinacrine, an attempt was made to induce ATP release from the same cells using hypotonic shock as a stimulus. By directly comparing extracellular ATP levels and intracellular stores of ATP under

control conditions and hypotonic conditions, the possibility that ATP is stored in vesicles and released via exocytosis in this cell line was investigated.

4.2 Methods

4.2.1 Cell culture

Immortalized cells (WKPT-0293 C1.2) derived from the S1 segment of the proximal tubule of normotensive Wistar-Kyoto rats were cultured as described by Woost et al (1996). These cells were maintained and grown as monolayers in Dulbecco's modified Eagle's medium (DMEM) nutrient mixture F-12 (1:1) (GibCo, Paisley, UK) supplemented with: foetal bovine serum (FBS) 10%; penicillin (100 units/ml); streptomycin (100μg/ml) (GibCo, Paisley, UK); $NaHCO_3$ (1.2mg/ml); insulin (5μg/ml) (Sigma, Poole, UK), dexamethasone (4μg/ml) (Sigma, Poole, UK), epidermal growth factor (0.01μg/ml) (Sigma, Poole, UK) and apo-transferrin (5μg/ml) (Sigma, Poole, UK) in $25cm^2$ standard tissue flasks at 37°C in a humidified incubator with 5% CO_2/95% air.

Upon reaching confluence, cells were passaged twice per week. Cell growth media were discarded and cells were submerged in 1 x trypsin-EDTA (Sigma, Poole, UK) for 10 min at 37°C. Once cells were successfully suspended, culture medium was added to dilute the trypsin solution 1/5. Cells were then spun for 2 min at 1200 rpm in a sterile tube, the supernatant discarded and seeded at 1:10 or 1:20 dilutions, into $25cm^2$ standard tissue flasks and sterile Falcon petri-dishes, respectively. All media and solutions introduced to cells were preheated to 37°C in a water bath.

4.2.2 Incubation of cells in isotonic or hypotonic solution

Cells grown to confluence in sterile Falcon dishes were rinsed in Dulbecco-phosphate buffered saline (D-PBS) (Sigma, Poole, UK). Cultures were then incubated with 1 ml of either 'isotonic' (280 mosmol/kg H_2O) or hypotonic (140 mosmol/kg H_2O) D-PBS for 15 min at 37°C. The osmolality of the buffers had been previously confirmed using a cryoscopic osmometer. Although the cell numbers used varied between each set of experiments (since the number of cells seeded varied), for any given experiment

(where isotonic and hypotonic incubations were directly compared), the number of cells was approximately the same. This was because, for a given experiment, following re-suspension of cells from a single tissue flask, the volume aliquoted (and therefore the number of cells seeded) into the two Falcon dishes was identical. In addition, the cells grew to confluence for the same time period and under identical conditions.

During incubation, 50µl samples of the medium were taken at 1, 5 and 15 min, immediately centrifuged, and the supernatant transferred to fresh vials. These vials were immediately snap frozen in liquid nitrogen and kept frozen at -80°C for later determination of ATP content using the luciferin-luciferase assay.

4.2.3 Quinacrine fluorescence studies

Immediately after the 15 min incubation period with isotonic or hypotonic D-PBS, the same cells were incubated with quinacrine (2mmol/l) in isotonic D-PBS for 10 min at room temperature. The cells were then rinsed with isotonic D-PBS, viewed with a microscope (Zeiss Axioplan, Oberkochen, Germany) fitted with a 'FITC' filter, and photographed (Leica DC200; Leica, Heerbrugg, Switzerland). Quinacrine requires a wavelength of 420nm for excitation and 500nm for emission.

4.2.4 Measurement of ATP

Samples previously isolated and frozen from the cell media during isotonic or hypotonic exposure were quickly thawed and loaded onto a 96-well plate. Immediately after this, the samples were assayed for ATP using the luciferin-luciferase assay as previously described (see Section 3.3.2.2)

4.2.5 Procedure for freezing cells

Cell culture medium was aspirated from flasks that had reached approximately 80% confluency in cellular monolayers. Subsequently, cells were bathed and incubated with preheated (37°C) 1 x trypsin-EDTA (Sigma, Poole, UK) for 10 min in a 37°C humidified incubator with 5% CO_2/95% air. Once cells were successfully trypsinised,

culture medium was added to dilute the trypsin solution 1/5 to inhibit the action of the trypsin enzyme. Cells were harvested through centrifugation (1200 rpm for 2 min). The supernatant containing the cell culture medium and trypsin solution was then discarded and cells were resuspended in 500µl of fresh cell culture medium. This cell suspension was subsequently transferred to a cryovial that contained 400µl of FBS and 100µl of dimethyl sulfoxide (DMSO) (Sigma, Poole, UK) and carefully mixed using a sterile 10ml pipette. The vial was then stored at -20 °C for 4-6 hours and then at -80 °C overnight. Long term storage was achieved by later transferring the vials into liquid nitrogen.

4.2.6 Recovery of cells from freezing

A cryovial stored at -80 °C or in liquid nitrogen was isolated and quickly thawed to 37°C using a water bath. The cell suspension was then transferred to 25cm^2 standard sterile tissue flasks and gently resuspended in 8ml of cell culture medium (pre-heated to 37°C), then immediately placed into a 37°C humidified incubator with 5% CO_2/95% air. The cell culture medium was replaced after 24 hours with 8ml of fresh medium. Cells were then left to grow to confluence, which routinely took 2-3 days. All reagents were pre-heated to 37°C prior to contact with cells.

4.2.7 Statistics

Results are expressed as means ± standard error of the means (SEM). Changes in ATP concentration with time were assessed with Student's Newman Keules paired *t* test. Differences between treatments at a given interval were compared using Student's unpaired *t* test. The difference between two mean values was considered statistically significant when $P < 0.05$.

4.3 Results

WKPT cells maintained under isotonic conditions had extracellular ATP concentrations of 4.0 ± 1.5, 4.6 ± 1.3 and 4.4 ± 1.5 nmol/l (mean ± SEM; $n = 7$) in samples taken at 1, 5 and 15 min, respectively, as shown in Fig. 4.2. No significant changes in ATP concentrations were observed between the times at which samples

were taken. Subsequent incubation of the same cells with quinacrine resulted in a high level of fluorescence, which, upon high magnification, appeared to be granular and exclusive to the cytoplasm (Fig. 4.3A; 4.4A).

Cells that were subjected to hypotonic stimulation had extracellular ATP concentrations of 15.6 ± 6.0, 19.1 ± 5.8 and 25.4 ± 7.2 nmol/l (mean ± SEM; $n = 7$) in samples taken at 1, 5 and 15 min, respectively, as shown in Fig. 4.2. Significant changes in ATP concentrations were observed as the duration of incubation increased ($P = 0.009$). At all times, ATP concentrations in the hypotonic medium were significantly higher than corresponding values in isotonic medium. Subsequent incubation of the same cells with quinacrine resulted in fluorescence; however, this was profoundly reduced compared with that seen in cells subjected to isotonic conditions. (Fig. 4.3B; 4.4B).

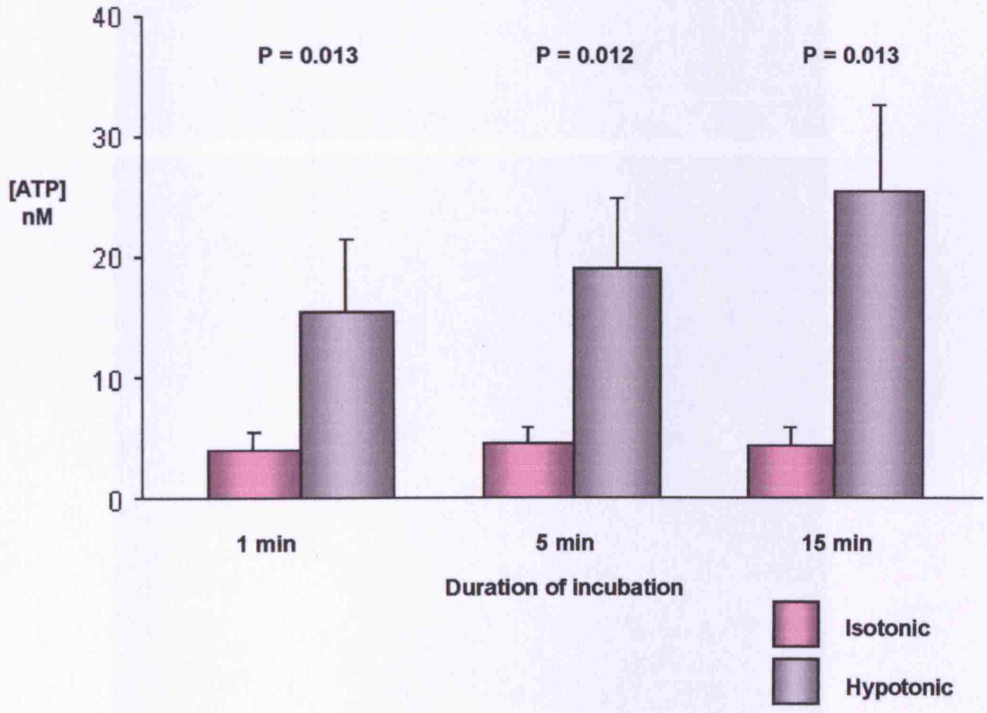

Fig. 4.2: Extracellular concentrations of ATP (means ± SEM; $n = 7$) at 1, 5 and 15 minutes in medium bathing WKPT cells subjected to isotonic (pink columns) or hypotonic (grey columns) conditions. ATP levels did not vary significantly between the times at which the samples were taken in isotonic conditions. However, ATP concentrations increased with time under hypotonic conditions. Significant

differences in ATP concentrations were observed between isotonic and hypotonic conditions at each time interval.

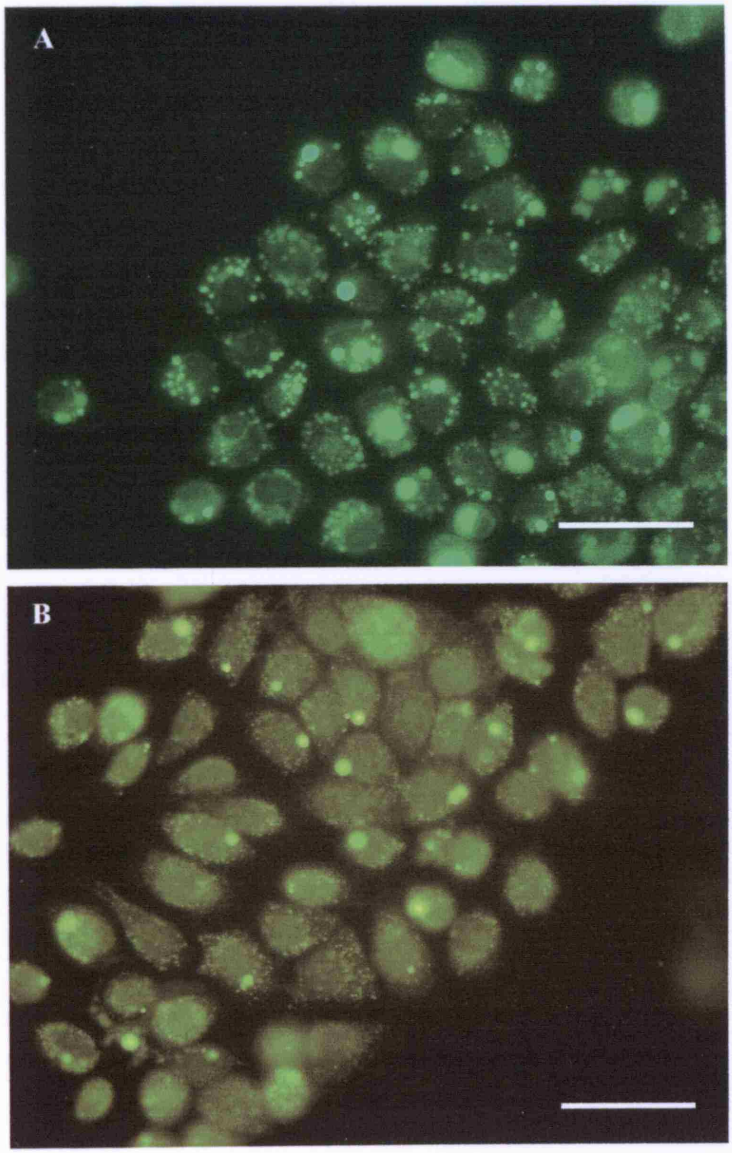

Fig. 4.3: Appearance of WKPT cells following incubation with quinacrine. (A) Granular fluorescent staining in the cytoplasm of WKPT cells subjected to isotonic conditions. (B) Pronounced reduction in granular fluorescence staining in the cytoplasm of WKPT cells subjected to hypotonic conditions (scale bar = 50μm).

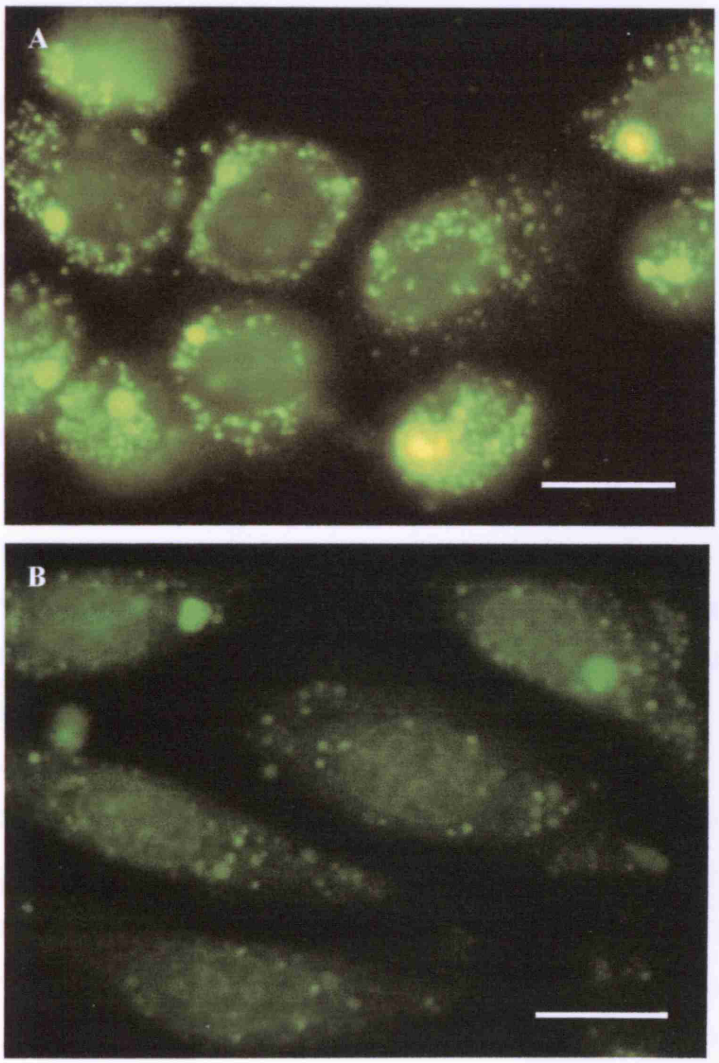

Fig. 4.4: Magnified appearance of WKPT cells following incubation with quinacrine. (A) Granular fluorescent staining in the cytoplasm of WKPT cells subjected to isotonic conditions. (B) Pronounced reduction in granular fluorescence staining in the cytoplasm of WKPT cells subjected to hypotonic conditions (scale bar = 20μm).

4.4 Discussion

Many studies have demonstrated the release of ATP from resting and stimulated epithelial and non-epithelial cells. In the previous chapter, ATP concentrations in the tubular lumen of the proximal convoluted tubule were shown to be markedly higher than in fluid being filtered at the glomeruli, strongly suggesting that ATP was being released from proximal tubular epithelial cells *in vivo*. The mechanism by which cellular release of ATP occurs may vary between cell types. Evidence for a variety of mechanisms has been obtained in a variety of epithelia, as described in the Introduction above. In the present study, quinacrine was used to visualize intracellular stores of ATP in the cytoplasm of a proximal convoluted tubule cell line. Although a number of other studies have used quinacrine to locate intracellular stores of ATP in a variety of different cells, no study has ever examined vesicular storage of ATP in renal epithelial cells.

By combining intracellular labelling of ATP (with quinacrine) and the luciferin-luciferase ATP assay, the present investigation examined whether exocytosis is one of the mechanisms by which ATP is released from a cell line originally derived from the S1 region of the proximal convoluted tubule.

In these proximal cell lines, quinacrine fluorescence was granular and was localized exclusively to the cytoplasm. Under control conditions, levels of ATP in the extracellular milieu were only just measurable. Upon hypotonic stimulation, the granular fluorescence in the cytoplasm was greatly reduced. This decreased granular fluorescence was coupled with a significant rise in extracellular ATP concentration. These findings suggest that ATP is stored in these cells in compartments, possibly in vesicles, and is released upon hypotonic exposure. Although the possibility of cell damage cannot be ruled out, it would be reasonable to assume that the release occurs via exocytosis of ATP-containing vesicles.

4.4.1 Hypotonic stimulation

Many *in vitro* investigations, in addition to the present study, have used hypotonic stimuli as a mechanism to induce ATP release. This release of ATP during cell swelling may have implications for cell volume regulation. Studies by other

laboratories have shown that cell volume is maintained and restored by adaptive responses such as the opening of K^+ and Cl^- channels that allow the efflux of these ions to restore cell volume.

The mechanisms linking cell volume expansion to ion channel opening are not completely understood. Various studies have demonstrated that application of extracellular ATP induces Cl^- secretion in many epithelial cell lines (Simmons 1981; Cressman et al, 1999), including renal epithelial cells (Cuffe et al, 2000). Further studies have concluded that upon hypotonic exposure cell swelling induces deformation of the plasma membrane which activates stretch-sensitive channels; this may induce, directly or indirectly, the release of ATP into the extracellular milieu (Bodin and Burnstock 2001; Jans et al, 2002). The rise in extracellular ATP concentration could then stimulate P2 receptors expressed on the same cell to open Cl^- channels (Wang et al, 1996).

4.4.2 Mechanism of ATP transport into vesicles

Vesicular release of ATP has already been described in a variety of cells and cell lines, and, as revealed in the present investigation, is a likely mechanism for ATP release in the proximal tubule. It has been reported that intravesicular concentrations of ATP can reach as high as 150mM in other cells (Lazarowski et al, 2003a), so the next question would be: how does ATP become so concentrated inside these vesicles? Bankston and Guidotti (1996) have proposed that movement of the ATP anion is driven by the electrochemical force created by the vacuolar-type H^+-ATPase located on the vesicular membrane (which acidifies the vesicle's interior). Although the mechanism by which ATP moves down the electrochemical gradient across the vesicular membrane is still unknown, it is likely that ATP-conductive channels and transporters have an important role (Schwiebert et al, 2003). The transporter or channel in question, in addition to its ability to transport ATP, also allows the movement of other nucleotides such as GTP and UTP, suggesting that it is not the mitochondrial ATP/ADP exchanger (GTP and UTP being unsuitable substrates for this exchanger) (Bankston and Guidotti, 1996). Interestingly, it has been suggested that should ATP transporters exist on these membranes, the fusion of the vesicle to the plasma membrane would not only release its quanta of ATP but would also permit

these transporters to be inserted into the plasma membrane, to potentially drive ATP release further (Schwiebert et al, 2003); but this is mere speculation.

4.4.3 Basal and stimulated release of ATP from WKPT cells

The levels of ATP documented in the present study in the isotonic/hypotonic solutions surrounding the cells do not represent real-time release of ATP from this proximal cell line. This is at least partly because of dilution and diffusion, where the concentration of ATP close to the cell surface is expected to be greater than that in the bulk solution from which measurements are made. Indeed, this has been shown in a recent study by Okada and colleagues (2005), where ATP measurements were made from Calu-3 airway epithelial cells, at the cell surface (using membrane-bound luciferase) and ~12 μm and ~2.6 mm from the cell surface. This study showed that measurements made 2.6 mm away from the cell surface were markedly lower than those measured 12 μm from the cell surface or at the cell surface (the latter two values being similar when the cells were stimulated to secrete ATP).

Furthermore, in the present study the cell number was unknown and varied between each set of experiments. This was because of variation in the number of cells seeded. However, it should be emphasized that, despite this variation between each set of experiments, the cell number did not vary significantly between compared *pairs*. (That is, only cells that were identically seeded, and grown to confluence for the same time period, were directly compared with respect to fluorescence intensity and extracellular ATP concentrations following isotonic and hypotonic exposure.) The variation in cell numbers between experiments may explain the large standard error bars observed. Despite this, the extracellular ATP levels found when cells were incubated in hypotonic solution were significantly greater than when the cells were incubated in isotonic solution.

Interestingly, the concentration of ATP in the medium did not change significantly between the time intervals at which the samples were taken (i.e., at 1, 5 and 15 minutes) when the cells were exposed to isotonic conditions. One possible explanation for this stability is that ATP released from the cells may have been hydrolysed continuously by ectonucleotidases expressed on the cell surface, a balance being set between the amount of ATP released and the amount hydrolysed.

Under hypotonic conditions, where ATP secretion was stimulated, a significant rise in ATP concentration in the medium was found to occur with time. This suggests that surface ectonucleotidases were unable to hydrolyze ATP at a rate that matched the rate of its release.

4.4.4 Specificity of quinacrine as a marker for ATP

As mentioned above, other studies have previously used quinacrine as a marker to visually identify ATP granules in cultured cells. In one study using primary cultures of endothelial cells and adopting a similar protocol to that used here, similar observations were also found (i.e., granular fluorescent staining of the cytoplasm, which, following mechanical stimulation, decreased markedly and was coupled with a rise in extracellular ATP levels) (Bodin and Burnstock, 2001). In that study, as indicated in the Introduction, further evidence for the identification of intracellular stores of ATP was achieved through the use of monensin and NEM, which interfere with the formation and release of vesicles, respectively. Pre-incubation with each of these drugs caused significant inhibition of the release of ATP during shear-stress stimulation. Although these drugs have other properties, monensin being a monovalent selective ionophore and NEM a potent alkylating agent, they inhibit vesicular transport by two different mechanisms. The fact that *both* drugs were able to inhibit ATP release makes it unlikely that their effect on vesicular ATP release was due to their other actions.

In addition to its interaction with ATP, quinacrine can also interact with polyanions such as RNA and DNA (Irvin and Irvin, 1954). Quinacrine has also been used in other studies to visualize intracellular stores of renin (Peti-Peterdi et al, 2004; Casellas et al, 1993). Some studies have reported renin to be present in proximal tubular cells (Moe et al, 1993; Henrich et al, 1996), and Skøtt and Taugner (1987) reported that superfusion with hypo-osmotic solutions stimulated renin release from rat epithelioid cells (modified macrophages that are adapted for secretion as opposed to phagocytosis). Thus, the possibility that at least some of the fluorescent granular staining observed in the cytoplasm of the proximal cell line in the present study was due to renin granules cannot be excluded.

4.4.5 Use of cell line

It must be acknowledged that cells grown in culture could change their phenotype and lose their ability to synthesize ATP transport proteins. The use of a primary cell line might have been a better option; even so, native characteristics in a primary culture cannot always be guaranteed. Another caveat is that the cell line used in this study was originally derived from the S1 region of the proximal tubule of the rat and may not represent other regions of the proximal tubule, let alone other segments of the nephron.

4.5 Conclusion

The granular fluorescence observed in the cytoplasm following incubation with quinacrine suggests that ATP is compartmentalised, possibly stored as vesicles in these cells. The medium bathing cells subjected to hypotonic exposure had significantly higher levels of ATP compared to that bathing cells maintained in isotonic saline; this finding, together with reduced granular fluorescence in hypotonic-treated cells, suggests that ATP release occurs following hypotonic shock and that that this release occurs via exocytosis from ATP-containing vesicles.

Whilst the mechanisms of ATP transport across the plasma membrane (discussed in the Introduction above) all seem plausible, and have in many cases been supported by experimental evidence, vesicular release would provide a highly controlled mechanism for the release of ATP from cells. The present study, although confined to a cell line, has provided evidence that vesicular release is at least one of the possible mechanisms for ATP release by proximal tubule cells.

CHAPTER 5

IMMUNOLOCALISATION OF ECTONUCLEOTIDASES ALONG THE RAT NEPHRON

5.1 Introduction

The extent of activation of purinoceptors is influenced by the existence of ectonucleotidases located on the surface membranes of epithelial and endothelial cells. Four families are known to exist: ectonucleoside triphosphate diphosphohydrolases 1-8 (NTPDases 1-8), ectonucleotide pyrophosphatase phosphodiesterases 1-3 (NPPs 1-3), ecto-5'-nucleotidase and alkaline phosphatase. These families of enzymes and their respective members differ in their hydrolysis pathways and/or in their affinities for nucleotides. The presence of ectonucleotidases in specific segments of the nephron may have a significant and regulatory influence on the stimulation of tubular purinoceptor subtypes, not only because nucleotide agonists are hydrolysed but also because, in some cases, the generation of their hydrolysis products (in particular ADP and adenosine) will preferentially activate ADP-sensitive P2 and P1 receptors.

5.1.1 Ectonucleoside triphosphate diphosphohydrolase (NTPDase) family

The NTPDase family consists of eight members. The topology of NTPDases 1-6 is shown in Fig. 5.1. NTPDases 1-4 have two membrane spanning regions, whereas NTPDases 5 and 6 have single transmembrane domains, which may be cleaved close to the membrane to release a soluble form of the enzyme. The topologies of the newly discovered NTPDases 7 and 8 have not been defined. Four of these members, namely NTPDase1, NTPDase2 NTPDase3 and NTPDase8, are primarily concerned with the hydrolysis of adenine-based nucleotides (although they may also hydrolyze other nucleotides such as UTP, GTP, ITP and CTP and their respective diphosphates). NTPDases 4-7 are believed to be localized to intracellular membranes such as the Golgi apparatus and the endoplasmic reticulum; these ectonucleotidases are primarily concerned with the hydrolysis of uridine-based nucleotides but may also hydrolyse other nucleotides such as GTP, ITP and/or CTP, albeit with a lower affinity (Zimmermann, 2001a; Kukulski et al, 2005). Table 5.1 shows details of the hydrolysis pathways.

5.1.1.1 NTPDases 1-3

NTPDase1 hydrolyses ATP and ADP with almost equal preference (Zimmermann 2001a). However, hydrolysis of ATP by this enzyme largely proceeds directly to AMP (i.e., no ADP intermediate is released). This occurs most likely because ADP remains bound to the enzyme, and is dephosphorylated at the same or a nearby catalytic site. In the vasculature there is strong evidence that endothelial NTPDase1 limits the extent of intravascular platelet aggregation by hydrolysing pro-aggregatory ADP. Furthermore, NTPDase1 knock-out mice developed systemic hypertension, highlighting the potential physiological significance of this ectonucleotidase in the vasculature (Kishore et al, 2005).

In contrast to NTPDase1, NTPDase2 has a significantly higher (approximately 30-fold) preference for the hydrolysis of ATP over ADP (Zimmermann, 2000), whereas NTPDase3, which shares the same hydrolytic pathway, has only an approximately 3-fold preference for the hydrolysis of ATP (Zimmermann 2001a). NTPDases 1-3 have all been found in the kidney at the protein and/or mRNA level (Kishore et al, 2005; Chadwick and Fischauf, 1998).

5.1.1.2 NTPDases 4-8

NTPDase 4 has been found in most tissues including the kidney, and in transfected cell lines (COS-7 cells) was reported to be located intracellularly, more specifically, expressed on the membrane of the Golgi apparatus (Wang and Guidotti, 1998). The same study found the mRNA for this enzyme in human kidney tissue as well as other tissues. The substrates of NTPDase 4 primarily include UDP and other nucleoside 5' di- and triphosphates except ATP and ADP. NTPDase 5 and NTPDase 6 follow a similar catalytic pathway, preferentially hydrolysing UDP, GDP and IDP over ADP. Using northern blot analysis, the mRNA for NTPDase 5 has been found in human kidney (Chadwick and Frischauf, 1998) and that for NTPDase 6 in rat kidney (Braun et al, 2000). Their catalytic pathways, together with their location, suggest that these

intracellular ectonucleotidases may have a role in importing nucleotide sugars into the Golgi cisternae (Zimmermann, 2000).

NTPDases 7 and 8 have been characterised recently; and the mRNA transcripts for both enzymes have been found in a variety of tissues including the kidney. NTPDase7, located on intracellular membranes such as the Golgi apparatus and endoplasmic reticulum, has a substrate preference for nucleoside triphosphates such as UTP, GTP and CTP, with little or no activity on their respective diphosphates or indeed other nucleoside triphosphates (Shi et al, 2001). Unlike NTPDase7, NTPDase8 is located on the plasma membrane. This enzyme is involved in the hydrolysis of adenine- and uridine-based tri- and dinucleotides and so, like NTPDases1-3, may influence purinoceptor activation, (Bigonnesse et al, 2004).

5.1.1.3 K_m and catalytic properties

The effectiveness or potency of these enzymes in influencing purinoceptor activation has been demonstrated in studies where the use of stable analogues of ATP has often had a very potent effect, eliciting contractions in smooth muscles up to a hundred times greater than those caused by the same dose of ATP itself.

The catalytic activity of the enzyme for a particular substrate is strongly influenced by the affinity of the enzyme for that substrate, which is represented by the K_m-value. A high affinity of the enzyme for its substrate would be shown by a low K_m-value, as a low concentration of substrate would be required to half saturate the enzyme (to reach half maximal velocity [1/2 V_{max}] for the reaction). The converse is true for a high K_m-value. However, the V_{max} itself is also a major determinant of enzyme activity, as an enzyme with a high K_m and high V_{max} might have the same activity as one with a low K_m and low V_{max}.

The K_m-values of the ectonucleotidases vary not only between the various members, but also differ between the membrane-bound and soluble forms of enzyme. The K_m is also

influenced by the type of nucleotide-based substrate and the species in which the enzyme is expressed. For example, NTPDase1 isolated from bovine aorta has a K_m for ATP of 10μmol/l, whereas human NTPDase1 expressed on COS-7 cells was reported to have a K_m of 75μmol/l for the same substrate. Furthermore, soluble recombinant human NTPDase1 lacking the N- or C-terminal domains had K_m-values of 220μmol/l and 2.1μmol/l, respectively. K_m is also strongly influenced by pH and by the presence of divalent cations such as Ca^{2+}, Mg^{2+} and Zn^{2+}. The ranges of K_m-values for the families of enzymes have been summarized in Table 5.1.

5.1.2 Ectonucleotide pyrophosphatase/phosphodiesterase (NPP) family

The ectonucleotide pyrophosphatase/phosphodiesterase (NPP) multigene family comprises three members. NPPs 1-3 have been structurally characterized, having a small intracellular domain (10-80 residues) and a large extracellular domain (~830 residues) that harbours the catalytic site (Gijsbers et al, 2001). As well as being membrane bound by a single transmembrane domain at the N-terminus, these enzymes may also be proteolytically cleaved and released as a soluble form (Fig. 5.1). Indeed, soluble forms of these enzymes have been found in serum.

Like NTPDases, NPPs 1-3 are also able to catalyze ATP and ADP to AMP, but vary in their affinities for the nucleotide substrates. NPP2 has the widest catalytic capacity, being able to hydrolyze AMP to adenosine in addition to hydrolyis of ATP to ADP and ADP to AMP.

The catalytic activity of these enzymes is positively influenced in the presence of divalent cations such as Mg^{2+} and Ca^{2+}, and is also influenced by pH (working optimally at pH 9). The K_m-values are similar to those of the NTPDase family (ranging over 10-150 μmol/l) and are similarly subject to a variety of influences. For instance, rat C6 glioma cells expressing NPP1 were reported to have a K_m-value for ATP of 17μmol/l, whereas a soluble form of the same enzyme had a K_m- value of 50μmol/l for the same substrate.

Based on sequence homology of the catalytic site, additional members of this family, designated NPP4 and NPP5, have been identified. Distinctly smaller than their other family counterparts, NPP4 and NPP5 are made up of 453 and 477 residues respectively. Genetic analysis by Gijsbers et al, (2001) suggested that these enzymes had a broad tissue distribution; however, their presence in the kidney was not indicated.

5.1.3 Ecto-5'-nucleotidase

Ecto-5'-nucleotidase catalyses the hydrolysis of AMP to adenosine. The enzyme, which exists as a dimer, is attached to the membrane via a glycosylphosphatidyl inositol (GPI) anchor, which may be cleaved to release a soluble form of the enzyme (Fig. 5.1). The K_m- value for AMP is in the low micromolar range (10 – 50μmol/l) but is influenced by competitive inhibition by ATP and ADP. Ecto-5'-nucleotidase is a zinc-binding metalloenzyme, and chelators such as EDTA can inhibit enzyme activity.

5.1.4 Alkaline phosphatase

This enzyme has a broad substrate specificity, capable of metabolizing ATP, ADP and AMP down to the nucleoside, adenosine. Therefore, expression of this enzyme would enable the complete hydrolysis of ATP to adenosine to occur. However, the K_m- values for these substrates are in the low millimolar range. Like ecto-5'-nucleotidase, alkaline phosphatase shares the feature of being glycosyl phosphatidyl inositol (GPI)-anchored and so may also exist as a soluble form. The significance of this enzyme in purinoceptor signalling and extracellular nucleotide metabolism has received little attention.

Table 5.1 summarizes the hydrolysis pathways of the ectonucleotidases described above.

Table 5.1: The hydrolysis pathways and the apparent K_m values for the four families of ectonucleotidases.

Members	K_m Value (µmol/l)	Hydrolysis pathway
NTPDase1	10 -200	ATP to AMP + 2P_i * ADP to AMP + P_i (ATP = ADP)
NTPDase2		ATP to ADP + P_i * ADP to AMP + P_i (ATP >> ADP)
NTPDase3		ATP to ADP + P_i * ADP to AMP + P_i (ATP > ADP)
NTPDase4		UDP to UMP + P_i UTP to UDP + P_i
NTPDase5		UDP to UMP + P_i UDP > GDP, IDP >>> ADP, CDP
NTPDase6		GDP to GMP + P_i GDP > IDP >>> UDP, CDP >>>ADP
NTPDase7		UTP to UDP + P_i GTP to GDP + P_i CTP to CDP + P_i
NTPDase8		ATP to ADP + P_i UTP to UDP + P_i ADP to AMP + P_i UDP to UMP + P_i
NPP1	10 -150	ATP to AMP + 2P_i ADP to AMP + P_i 3',5'-cAMP to AMP
NPP2		ATP to AMP + 2P_i ATP to ADP + P_i ADP to AMP + P_i GTP to GDP + P_i 3',5'-cAMP to AMP AMP to Adenosine + P_i
NPP3		ATP to AMP + 2P_i ADP to AMP + P_i 3',5'-cAMP to AMP
Ecto-5'-nucleotidase	10 – 50	AMP to Adenosine + P_i
Alkaline phosphatase	1 – 4 x 10^3	ATP to ADP + P_i ADP to AMP + P_i AMP to Adenosine + P_i

* Denotes that UTP, GTP,ITP, CTP, UDP, GDP, IDP and CDP can also be substrates.

(Compiled from Kukulski et al, 2005; Zimmermann, 2001a ; Zimmermann, 2001b; Zimmermann, 2000)

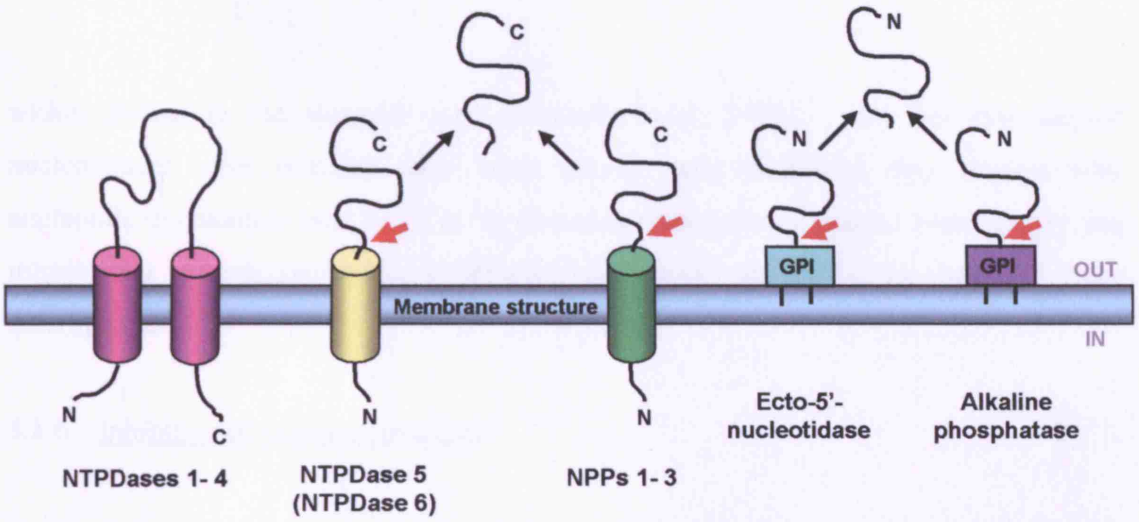

Fig. 5.1: Topological structure of ectonucleotidases. NTPDases 1, 2, 3 and 8 are expressed on the plasma membrane. NTPDases 4, 5, 6 and 7 are believed to have an intracellular location, expressed on either the Golgi apparatus or endoplasmic reticulum membrane, but also have the potential to be released as soluble forms. NTPDases 1-4 have two membrane-spanning regions, with intracellular N- and C-termini, whilst NTPDases5 and 6, as well as NPPs 1-3, have a single membrane-spanning region. The topological structures of NTPDases 7 and 8 have not been fully characterized. Both ecto-5'-nucleotidase and alkaline phosphatase are GPI-anchored with an extracellular N terminus. With the exception of NTPDases 1- 4 (and possibly NTPDase 6), ectonucleotidases have the potential to be cleaved at the cleavage site (denoted by a red arrow) and released as a soluble form. (Bigonesse et al, 2004; Kukulski et al, 2005; Mulero et al, 1999; Wang et al, 1998). These ectonucleotidases may exist as homo-oligomers of dimers, trimers or even tetramers.

5.1.5 Soluble nucleotidases

Not all of the ectonucleotidases exist as membrane-bound enzymes; some soluble forms also exist. Soluble nucleotidases have been found to be released from nerve endings following stimulation, and the latency of the postsynaptic effects of adenosine derived from ATP released at hippocampal synapses suggests that complete hydrolysis can occur

within 200ms in the synaptic cleft (Kennedy et al, 1997). The fact that soluble nucleotidases were released only when nerves were stimulated may explain why nucleotide degradation was found to be slower in resting neural tissue. Interestingly, the intracellular membrane-bound NTPDase5 has been shown to be released from macrophages.

5.1.6 Inhibitors of ectonucleotidases

A diverse group of compounds has been shown to inhibit the catabolism of ATP and/or ADP. However, many of these compounds only display mild inhibition and/or are non specific. Others, such as suramin, are effective not only in inhibiting ectonucleotidase activity but also in inhibiting P2 receptor activation and may interact with other types of membrane proteins. The activity of many ectonucleotidases is augmented in the presence of divalent cations; thus, ion chelators such as EDTA may significantly reduce or possibly inhibit the activity of these enzymes.

Although other inhibitors such as ARL 67156, azide and heparin have been found to inhibit nucleotidase activity in several tissues including human red blood cells, rat and guinea-pig vas deferens, chicken oviduct and rat kidney and liver (Todorov et al, 1997; Knowles and Nagy, 1999; Vieira et al, 2001), the specificity of these inhibitors remains undefined.

5.1.7 Distribution of ectonucleotidases along the nephron – current knowledge

Ecto-5'nucleotidase has been shown to be present in the brush-border membrane of the rat proximal tubule, and in the apical membrane and apical cytoplasm of intercalated cells in the connecting tubule and collecting duct, as well as in the peritubular space (Gandhi et al, 1990; Le Hir and Kaissling, 1989). Alkaline phosphatase has been shown to be confined to the brush-border membrane of the proximal tubule (Beliveau et al, 1983).

Current knowledge of the distribution of other ectonucleotidases along the nephron is fragmentary and incomplete. Some laboratories have detected mRNA for a number of ectonucleotidases in kidney tissue homogenates (Chadwick et al, 1998; Fuss et al, 1997; Kegal et al, 1997). Others have demonstrated their expression at the protein level; these findings, however, have usually been confined to the renal vasculature, with little or no mention of the tubular expression of the enzymes (Lemmens et al, 2000; Kishore et al, 2005).

NTPDases1 and 2 have recently been identified in the thin limbs of Henle, but not investigated elsewhere (Kishore et al, 2005). Of the NPP family, the intrarenal distribution of NPP1 has previously been examined in the mouse (Harahap and Goding, 1988), but no information is available on NPP2 or NPP3. The present study has therefore used immunohistochemistry to examine the expression of five major ectonucleotidases along the rat nephron. The enzymes examined were NTPDase1, NTPDase2, NTPDase3, NPP3 and, for comparative purposes, ecto-5'-nucleotidase. Using antibodies to well-defined segments of the nephron, the distribution of these five enzymes was examined in the proximal tubule, the TAL, the distal tubule and the collecting duct.

5.2 Methods

5.2.1 Ectonucleotidase antibodies

NB: These experiments were performed by Dr Jean Sévigny and colleagues at Centre de Recherche en Rhumatologie et Immunologie, Université Laval, Sainte-Foy, Québec, Canada

Polyclonal antibodies for NTPDases 1, 2 and 3 and ecto-5'-nucleotidase were raised in rabbit by direct intramuscular or subcutaneous injection of the encoding cDNA ligated into the plasmid pcDNA3, using the same protocol as described previously (Koszalka et

al, 2004; Sévigny et al, 2002). NPP3 antibody was also raised in rabbit, against affinity-purified native protein as described previously (Maurice et al, 1994). The use and specificity of antibodies to NTPDases 1 and 2 (Kishore et al, 2005, Sévigny et al, 2002), ecto-5'-nucleotidase (Koszalka et al, 2004) and NPP3 (Meerson et al, 2000; Meerson et al, 1998) have been extensively described in previous studies.

5.2.1.1 Specificity of NTPDase3 antibodies - transfection and western blotting procedures

NB: These experiments were performed by Dr Jean Sévigny and colleagues at Centre de Recherche en Rhumatologie et Immunologie, Université Laval, Sainte-Foy, Québec, Canada

Preparation of human embryonic kidney (HEK 293) cells and transient transfection with NTPDase3 cDNA constructs were prepared as described previously for NTPDase1 in COS-7 cells (Kaczmarek et al, 1996). Protein samples of NTPDase3 transfected cells and untreated HEK 293 cells were resuspended in NuPAGE LDS Sample Buffer (Invitrogen, Burlington, Ontario, Canada) under nonreducing conditions and separated on a NuPAGE 4-12% Bis-Tris gel. The separated proteins were then transferred to an Immobilon-P membrane (Millipore, Bedford, MA, USA) by electroblotting according to the manufacturer's recommendation (Invitrogen) and then blocked with 2.5% non-fat milk in PBS-T (10.1 mM Na_2HPO_4, 1.8 mM KH_2PO_4, 136.9 mM NaCl, 2.7 mM KCl, 0.15% Tween 20, pH 7.4) overnight at 4°C. The membrane was subsequently probed for NTPDase3 through incubation with rabbit anti-NTPDase polyclonal antibody (RN3-1) for 90min at a dilution of 1/2000 and the bands visualized using horseradish peroxidase-conjugated goat anti-rabbit IgG (Amersham Biosciences, Baie d'Urfé, Québec, Canada) for 1 hour at a dilution of 1/10,000, followed by Lightning Western Blot Chemiluminescence Reagent Plus (Perkin Elmer Life Sciences, Boston, MA, USA). Positively stained bands were only detected in NTPDase3 transfected cell lines (Fig. 5.2).

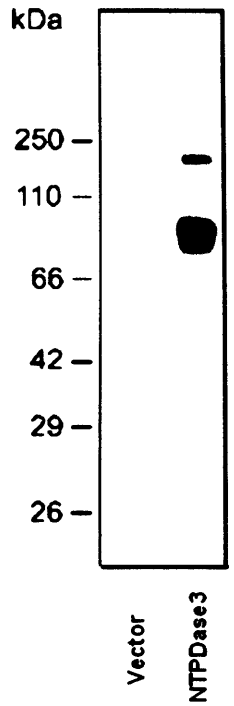

Fig. 5.2: Western blot showing cell lysates from HEK 293 cells transiently transfected (NTPDase3) or non-transfected (Vector; negative control) with rat NTPDase3 cDNA constructs. Proteins were fractionated on NuPAGE 4-12% Bis-Tris gel under nonreducing conditions, transferred to an Immobilon-P membrane and subsequently incubated with NTPDase3 (RN3-1) primary antibody or its preimmune control (not shown). Stained bands were exclusively detected in NTPDase3 transfected cell extracts.

5.2.1.2 Specificity of NTPDase3 antibodies – immunocytochemistry

NB: These experiments were performed by Dr Jean Sévigny and colleagues at Centre de Recherche en Rhumatologie et Immunologie, Université Laval, Sainte-Foy, Québec, Canada

COS-7 cells were fixed in 10% phosphate-buffered formalin mixed with cold acetone. Briefly, cells were incubated in a blocking solution of 7% normal goat serum in phosphate-buffered saline (PBS) for 30 min and then incubated overnight at 4°C with primary antibodies. The cells were then incubated with 0.15% hydrogen peroxide in PBS

for 10 min, incubated with avidin/biotin blocking kit (Vector Laboratories, Burlington, Ontario, Canada) and then with a biotin-labelled goat anti-rabbit secondary antibody. The complex avidin/biotinylated horseradish peroxidase (Vector laboratories) was added to optimize the reaction. Peroxidase activity was revealed using 3, 3'-diaminobenzidine (DAB; Sigma, St. Louis, MO, USA) as a substrate. Cells were counterstained with aqueous haematoxylin (Biomeda, Foster City, CA, USA) in accordance with the manufacturer's protocol (see Fig. 5.3).

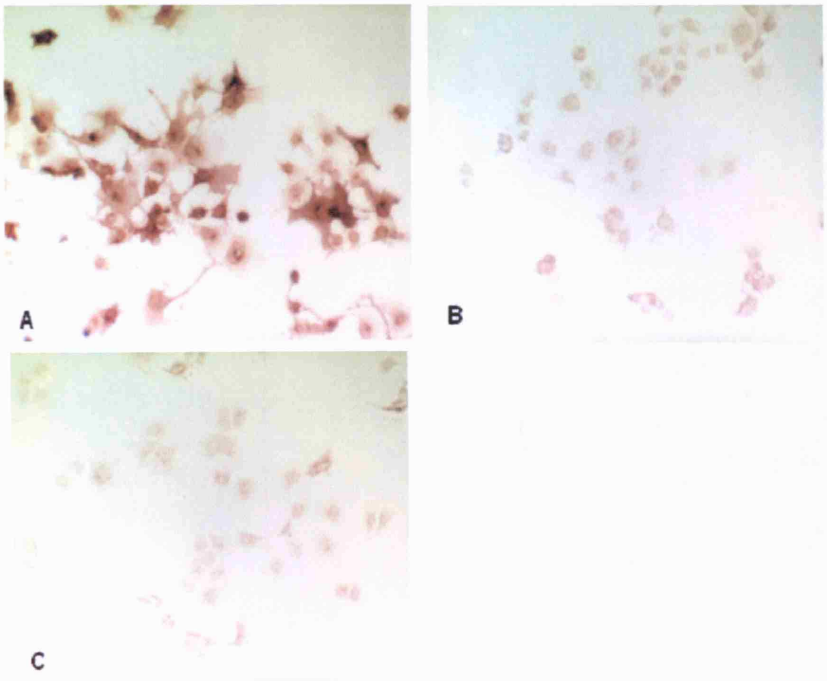

Fig. 5.3: Immunocytochemistry of intact COS-7 cells transfected (A and C) or non-transfected (B) with NTPDase3 cDNA constructs. Cells were incubated with NTPDase3 (RN3-1) antibody (A and B) or pre-immune serum (C). A positive signal could be seen only with NTPDase3 transfected cells incubated with NTPDase3 antibody (A). No staining was seen in the negative controls (B and C).

5.2.2 Other markers

The proximal tubule marker *phaseolus vulgaris* erythroagglutinin (PVE) was purchased from Vector Laboratories, Burlingame, CA, USA. The proximal tubule marker for the S3 segment, neutral endopeptidase (NEP) antibody, was a gift from Prof. P Ronco and has been previously characterized (Ronco et al, 1988); the thick ascending limb marker Tamm-Horsfall protein antibody was purchased from Biogenesis, Poole, UK; the distal tubule marker Calbindin D-28k antibody was purchased from Swant, Bellinzona, Switzerland; and the collecting duct marker aquaporin2 (AQP2) was a gift from Dr. D Marples. The specificity of this AQP2 antibody has been previously demonstrated by immunocytochemistry (D. Marples, personal communication). Secondary antibodies for donkey anti-sheep CY3, donkey anti-rabbit CY3, biotinylated donkey anti-rabbit and goat anti-mouse FITC were purchased from Jackson Immunoresearch Laboratories, West Grove, PA, USA. Streptavidin-fluorescein . FITC was purchased from Amersham Biosciences, Chalfont St Giles, Bucks, UK.

5.2.3 Tissue preparation

Male Sprague-Dawley rats were anaesthetized with sodium thiopentone (Link Pharmaceuticals, Horsham, UK; 100mg/kg, intraperitoneally). The left kidney was perfused via the abdominal aorta, first with Hanks' balanced salt solution and then with a periodate-lysine paraformaldehyde fixative containing 2% paraformaldehyde, 0.075 M lysine and 0.01 M sodium periodate solution, pH 7.4 (McLean et al, 1974). The perfusion-fixed kidney was then isolated and left overnight in 7% sucrose at 4°C. Subsequently, it was embedded in Tissue-Tek® compound and snap frozen in pre-chilled isopentane followed by liquid nitrogen. Sections 10μm thick were cut serially using a Leica cryostat cutter (Oberkochen, Germany) and mounted onto gelatinized glass slides.

5.2.4 Immunofluorescence

Frozen cryostat sections were allowed to air dry for several minutes at room temperature and were then washed three times for 5 min in 0.1M PBS. Tissue sections were then incubated in 10% normal horse serum (NHS) prepared in PBS containing 0.05% merthiolate (NHS-PBS merthiolate) for 30 min at room temperature. Sections were then incubated overnight at room temperature with antibody raised against NTPDase1 (1/600), NTPDase2 (1/1000), NTPDase3 (1/50), NPP3 (1/400) or ecto-5'-nucleotidase (1/400), each diluted in 10% NHS-PBS merthiolate. They were then incubated with either CY3-conjugated donkey anti-rabbit (1/400) immunoglobulin antibody (labelled red) or biotinylated donkey anti-rabbit antibody (1/500) for 60 min at room temperature. Sections that had been incubated with biotinylated donkey anti-rabbit antibody were then incubated with streptavidin-fluorescein (FITC-green fluorophore) (1/200) diluted in 1% NHS-PBS merthiolate for 30 min at room temperature.

(i) Proximal tubule staining

Sections that had been incubated with CY3-conjugated donkey anti-rabbit antibody (as described above) were incubated overnight with the biotinylated lectin PVE (specific to the proximal tubule) diluted 1/1500 in 10% NHS-PBS merthiolate, followed by a 30 min incubation with streptavidin-fluorescein (FITC-green fluorophore) diluted in 1% NHS-PBS merthiolate.

(ii) Proximal tubule S3 segment staining

Sections that had been incubated with CY3-conjugated donkey anti-rabbit antibody (as described above) were incubated overnight with antibody specific to NEP (specific for the S3 segment of the rat proximal tubule), diluted 1/1000 in 10% NHS-PBS merthiolate

followed by a 1 hr incubation with FITC-green-conjugated goat anti-mouse antibody diluted 1/200 in 1% NHS-PBS merthiolate.

(iii) Thick ascending limb (TAL) staining

Sections that had been previously incubated with the biotinylated donkey anti-rabbit antibody followed by streptavidin-fluorescein (FITC-green fluorophore) were incubated overnight with antibody specific to Tamm-Horsfall protein (specific for the TAL) diluted 1/1500 in 10% NHS-PBS merthiolate, followed by a 1 h incubation with CY3-conjugated donkey anti-sheep (1/400) diluted in 1% NHS-PBS merthiolate.

All incubations were separated by 3 x 5 min washes in 0.1M PBS. Slides were then mounted in Citifluor (Citifluor, London, UK) solution. Tissue sections were then viewed using a microscope (Zeiss Axioplan, Oberkochen, Germany) fitted with a 'rhodium' and 'FITC' filter to view CY3 and FITC fluorescence, respectively, and photographed with a microscope-mounted digital camera (Leica DC 200; Heerbrugg, Switzerland)

5.2.5 Double-immunofluorescence labelling of ectonucleotidases and tubular markers using unconjugated primary antibodies raised in the same species

The method of Tyramide Signal Amplification (TSA) immunohistochemistry was adopted under circumstances where the marker antibody used to identify tubular segments (Calbindin D-28k, a marker for the distal tubule, and AQP2, a marker for the principal cells of the collecting duct) was raised in the same host species (rabbit) as the ectonucleotidase antibody. If the conventional method had been adopted (as described above for labelling the proximal tubule and the TAL), the secondary antibody (i.e., CY3 conjugated donkey anti-rabbit IgG) would have been unable to differentiate between the ectonucleotidase and marker antibody due to cross reactivity.

Frozen sections were rinsed in 0.1M PBS (3 x 5 min), incubated with 10% NHS-PBS merthiolate for 30 min and then incubated overnight at room temperature with antibody specific to NTPDase1 (1/9000), NTPDase2 (1/12000), NTPDase3 (1/1200), NPP3 (1/4000) or ecto-5'-nucleotidase (1/4000), prepared at a dilution (in 10% NHS-PBS merthiolate) that could not be detected by the conventional immunofluorescence protocol described above, but could be detected using the TSA protocol.

The sections were subsequently incubated with biotinylated donkey anti-rabbit antibody for 60 min at room temperature. In accordance with the manufacturer's protocol, the sections were incubated with the supplied horseradish peroxidase-conjugated streptavidin (diluted 1/100 with 1% NHS-PBS merthiolate) for 30 min at room temperature and then incubated with the supplied fluorophore tyramide (PerkinElmer, Boston, MA, USA), prepared diluted 1/50 with the supplied amplification reagent at room temperature for 3-7 min.

The same sections were then incubated overnight at room temperature with a marker antibody: Calbindin D28k (1/1500) or AQP2 (1/1000) antibody diluted with 10% NHS-PBS merthiolate. This marker antibody was then labelled using CY3-conjugated donkey anti-rabbit immunoglobulin antibody (labelled red) and incubated for 60 min at room temperature.

Again, all incubations were separated by 3 x 5-min washes in 0.1M PBS. Slides were then mounted in Citifluor solution, and viewed using a microscope (Zeiss Axioplan, Oberkochen, Germany) fitted with a 'rhodium' and 'FITC' filter to view CY3 and TSA fluorophore fluorescence, respectively, and photographed with a microscope-mounted digital camera (Leica DC 200; Heerbrugg, Switzerland)

5.2.6 Secondary antibody control experiments

Control experiments in which each secondary antibody was directly incubated with kidney tissue sections (i.e without prior incubation with primary antibodies) were performed. No positive staining was observed (Fig. 5.4A/B).

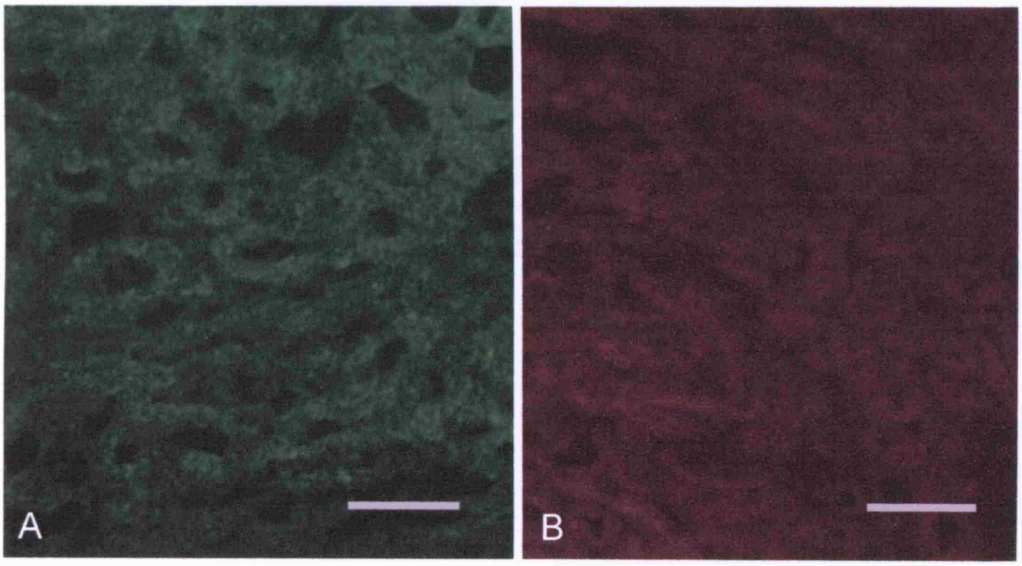

Fig. 5.4: Cortical sections from control experiments in which each secondary antibody FITC (A) or Cy3 (B) was directly incubated with kidney tissue sections (without prior incubation with primary antibodies). No positive staining was observed (Magnification x20; scale bar = 50μm).

5.3 Results

5.3.1 Glomerulus

Prominent immunostaining was found in the glomerulus for NTPDase1 (Fig. 5.5A) and NPP3 (Fig. 5.8A). No fluorescence was found for any other ectonucleotidase.

5.3.2 Proximal tubule

Indirect immunofluorescence labelling with antibodies specific to ectonucleotidases and the proximal tubule marker (PVE) showed prominent staining for NPP3 and ecto-5'-nucleotidase, but not for NTPDases 1, 2 or 3. Staining for both NPP3 (Fig. 5.8B/C) and ecto-5'-nucleotidase (Fig. 5.9A/B) was found to be predominantly on the apical side of the tubules, although staining in the peritubular space was also seen for ecto-5'-nucleotidase. Notably, not all positively stained proximal tubular segments stained for NPP3 or ecto-5'-nucleotidase, suggesting that these enzymes are localized to specific proximal tubular sub-segments.

To investigate this further, the monoclonal antibody to neutral endopeptidase (NEP), which in the rat is localized to the S3 segment of the proximal tubule (Ronco et al, 1988), was used in conjunction with the NPP3 and ecto-5'-nucleotidase antibodies. NPP3 staining was found to co-localize with NEP (Fig. 5.8D/F), suggesting that NPP3 is either exclusively or predominantly expressed in the S3 segment of the proximal tubule. In contrast, co-staining for ecto-5'-nucleotidase and NEP was found in some, but not all, positively stained S3 segments (Fig. 5.9C/D).

5.3.3 Thick ascending limb of Henle

Staining of the TAL using Tamm-Horsfall protein as a marker revealed expression of NTPDase2 (Fig. 5.6A/B) and NTPDase3 (Fig. 5.7A/B). This staining was not exclusive to the apical surface; some staining, particularly for NTPDase2, was also found on the basolateral surface. No immunoreactivity for NTPDase1, NPP3 or ecto-5'-nucleotidase was observed in this nephron segment.

5.3.4 Distal tubule

This segment stained for NTPDase2 (Fig. 5.6C/D) and NTPDase3 (Fig. 5.7C/D), predominantly on the apical side, and showed no staining for NPP3 or NTPDase1. Staining for NTPDase2 was variable: not every positively stained distal tubular segment expressed this enzyme. Very low-level apical expression was also observed for ecto-5'-nucleotidase in some, but not all, segments of positively stained distal tubules (Fig. 5.9E/F).

5.3.5 Collecting duct

Cortical and outer medullary collecting ducts displayed sparse staining for NTPDase3, which did not co-localize with AQP2-stained cells, suggesting that the enzyme is confined to intercalated cells (Fig. 5.7 E-G). A similar pattern of low-level staining was also observed for ecto-5' nucleotidase (Fig. 5.9 G-I). No other ectonucleotidases were identified in these regions.

5.3.6 Inner medullary collecting duct

In this segment, ecto-5'-nucleotidase was found again in intercalated cells (Fig. 5.9 J-L), whereas low-level staining for NTPDase3 was found in most 'principal' cells (Fig. 5.7 H-J). In addition to these two enzymes, some 'principal' and intercalated cells of the inner medullary collecting duct showed sparse expression of NTPDases 1 (Fig. 5.5C/D) and 2 (Fig. 5.6 E-G).

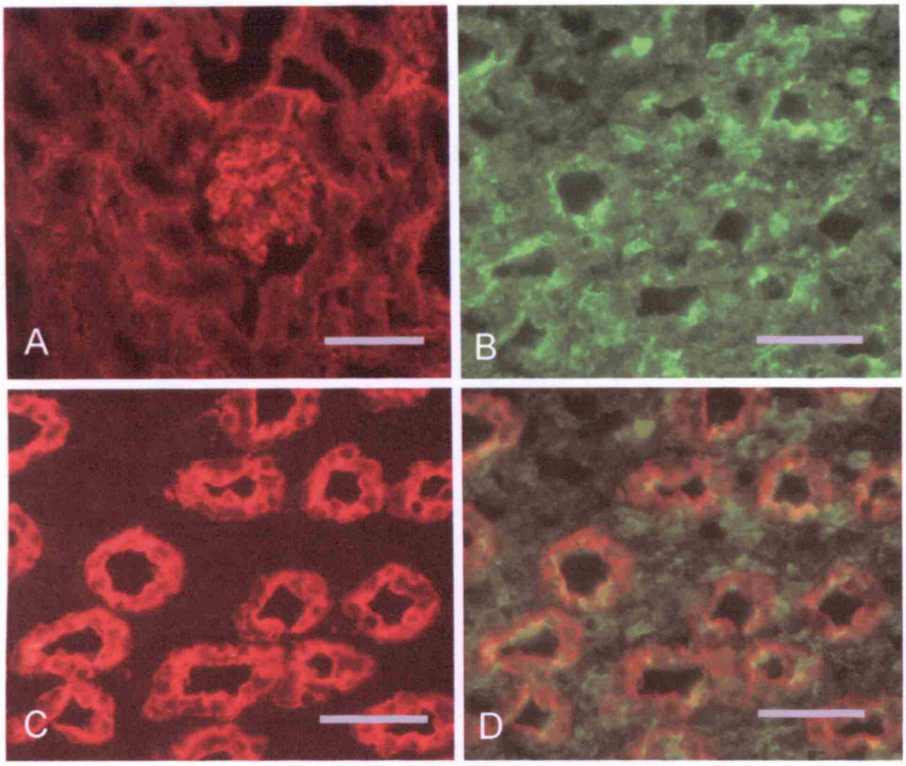

Fig. 5.5: A. Staining for NTPDase 1 in the glomerulus. (Magnification x20; scale bar = 100μm). B. Staining for NTPDase 1 in inner medullary collecting ducts. C. Same section as B, stained for aquaporin 2. D. Merged image of B and C stained for both NTPDase1 (green) and AQP2 (red). Co-localized staining of NTPDase1 and AQP2 is yellow. (Magnification x20; scale bar = 25μm).

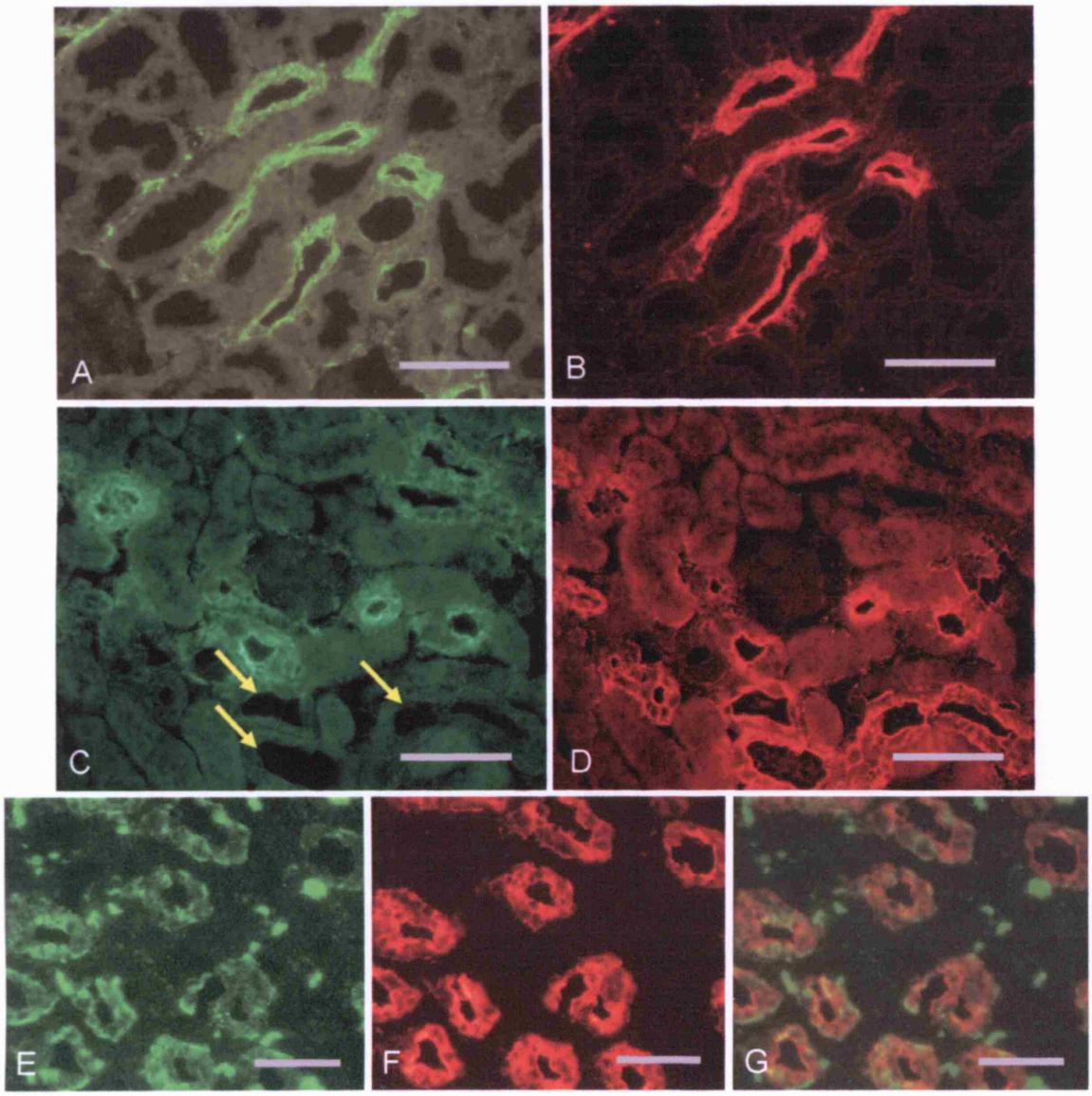

Fig. 5.6: A. Staining for NTPDase 2 in thick ascending limbs. B. Same section as A, stained for Tamm-Horsfall protein. (Magnification x20; scale bar = 100μm). C. Staining for NTPDase 2 in distal tubules. D. Same section as C, stained for Calbindin-D28k. Arrows denote positively stained distal tubules lacking expression of NTPDase 2. (Magnification x20; scale bar = 100μm). E. Staining for NTPDase 2 in inner medullary collecting ducts. F. Same section as E, stained for AQP2. G. Merged image of E and F stained for both NTPDase2 (green) and AQP2 (red). Co-localized staining of NTPDase1 and AQP2 is yellow. (Magnification x20; scale bar = 25μm).

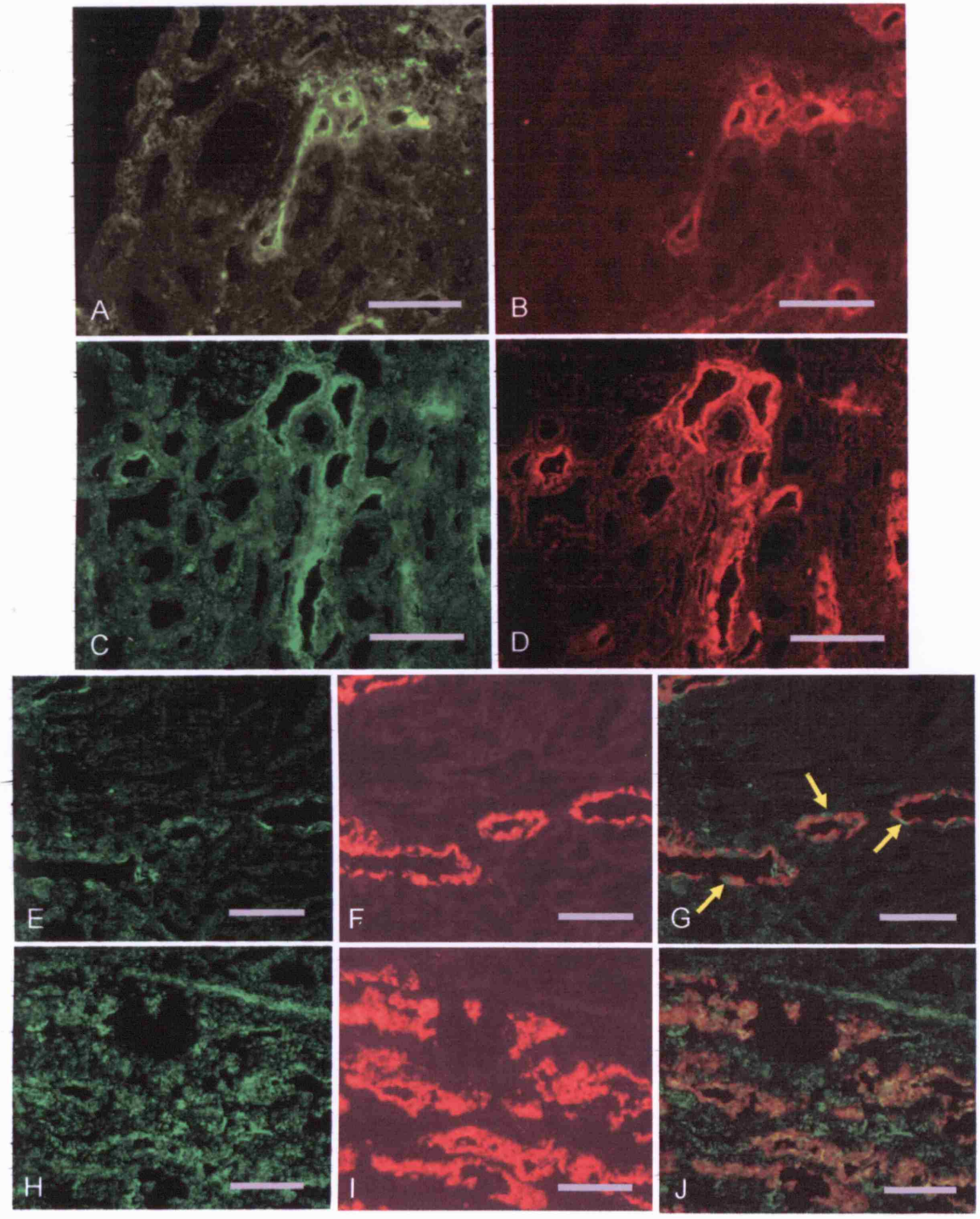

Fig. 5.7: A. Staining for NTPDase 3 in thick ascending limbs. B. Same section as A, stained for Tamm-Horsfall protein. (Magnification x20; scale bar = 100μm). C. Staining for NTPDase 3 in distal tubules. D. Same section as C, stained for Calbindin-D28k. (Magnification x20; scale bar = 100μm). E. Staining for NTPDase3 in outer medullary

collecting ducts. F. Same section as E, stained for AQP2. G. Merged image of E and F stained for both NTPDase3 (green) and AQP2 (red). Arrows denote presumed intercalated cells. (Magnification x10; scale bar = 50μm). H. Staining for NTPDase 3 in inner medullary collecting ducts. I. Same section as H, stained for AQP2. J. Merged image of H and I stained for both NTPDase3 (green) and AQP2 (red). Co-localized staining of NTPDase1 and AQP2 is yellow. (Magnification x10; scale bar = 800μm).

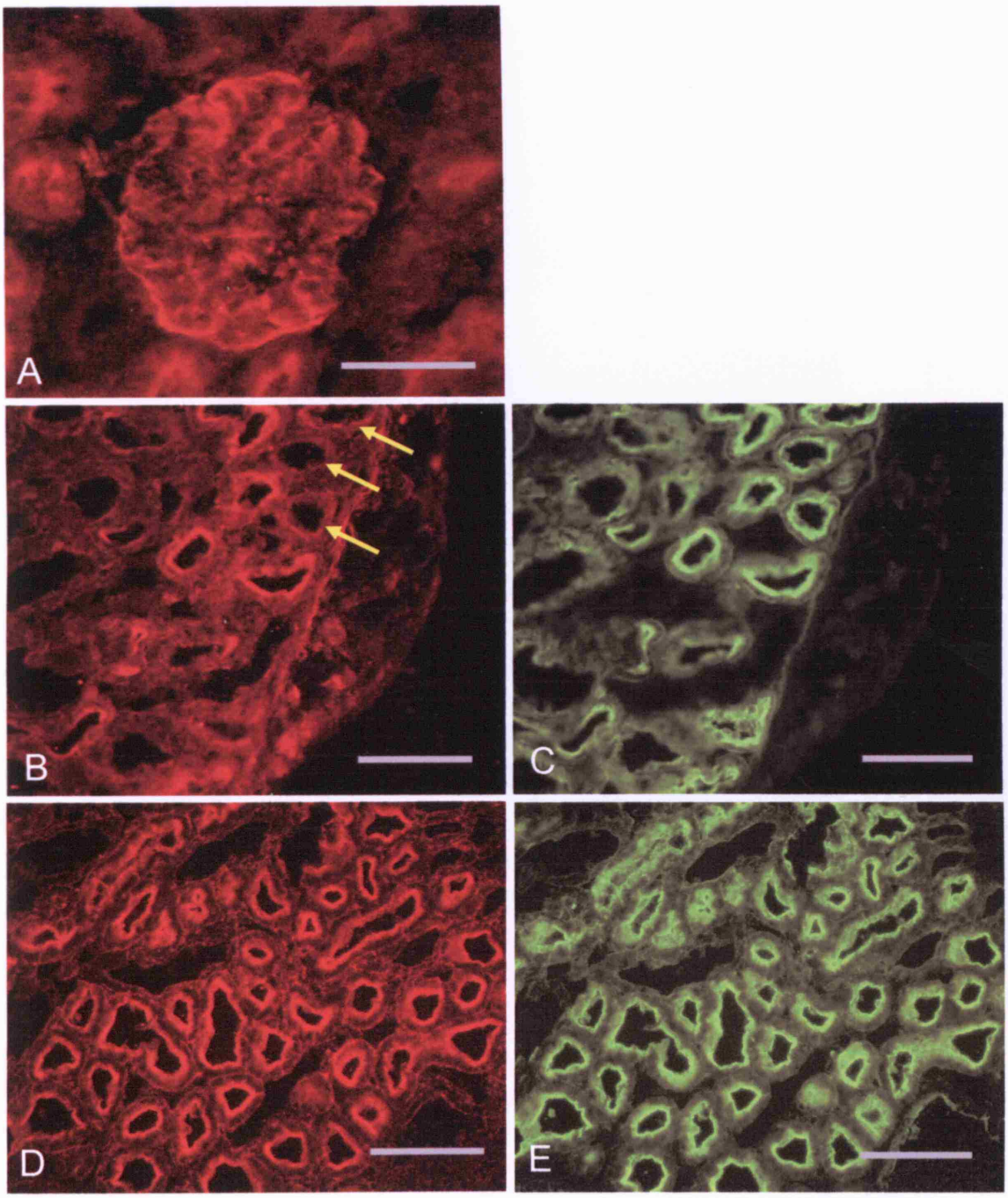

Fig 5.8: A. Staining for NPP3 in the glomerulus. (Magnification x20; scale bar = 50μm). B. Staining for NPP3 in proximal tubules. C. Same section as B, stained for PVE. Arrows denote positively stained proximal tubules lacking expression of NPP3. (Magnification x20; scale bar = 100μm). D. Staining for NPP3 in pars recta. E. Same section as D, stained for NEP. (Magnification x20; scale bar = 100μm).

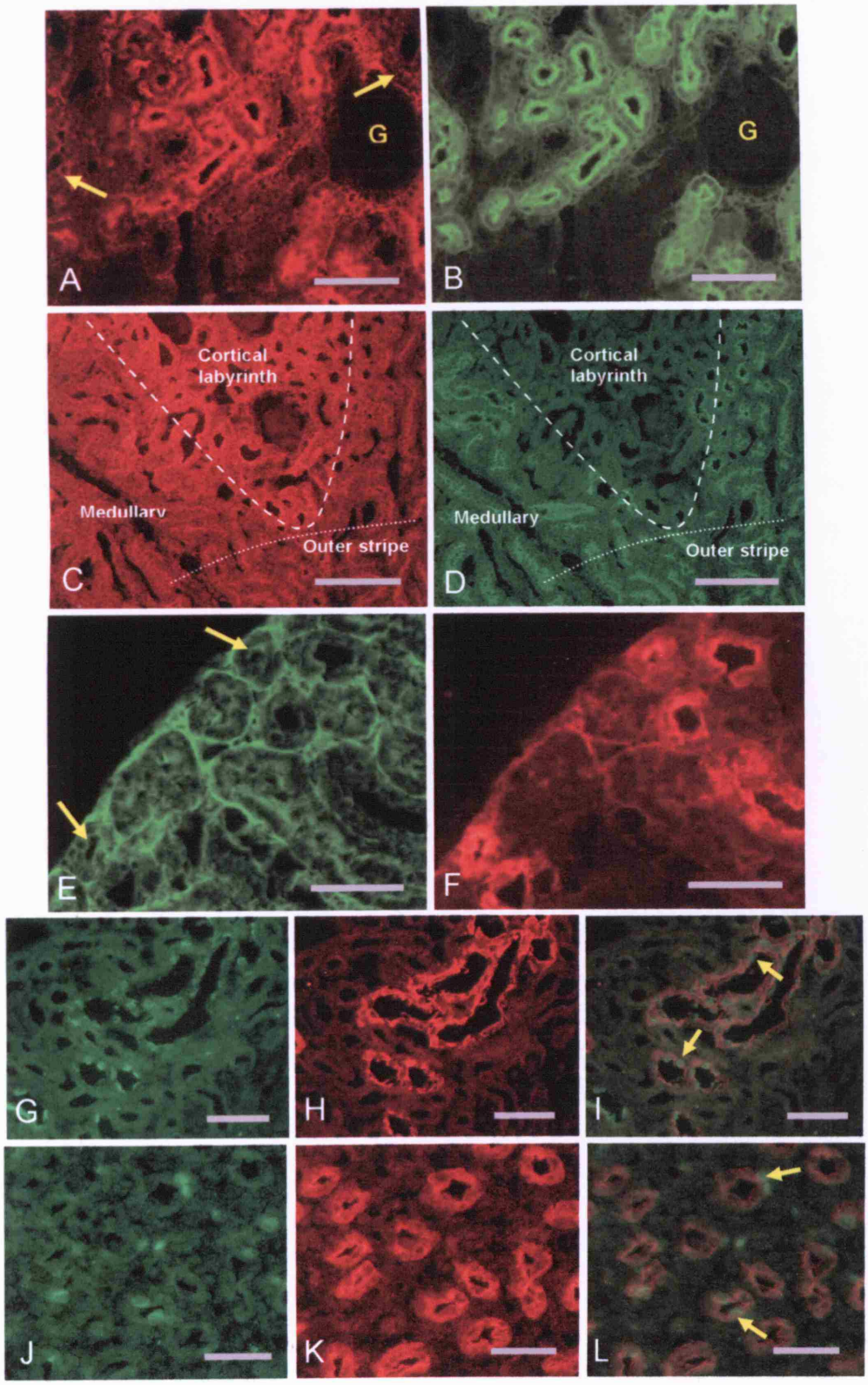

Fig. 5.9: See next page for legend

Fig. 5.9: A. Staining for ecto-5'-nucleotidase in proximal tubules. B. Same section as A, stained for PVE. Arrows denote positively stained proximal tubules lacking expression of ecto-5'-nucleotidase. G denotes glomerulus. (Magnification x20; scale bar = 100μm). C. Staining for ecto-5'-nucleotidase in the cortical labyrinth and outer stripe of outer medulla. D. Same section as C, stained for NEP. Note staining in medullary rays and outer stripe. (Magnification x10; scale bar = 200μm). E. Staining for ecto-5'-nucleotidase in distal tubules. F. Same section as E, stained for Calbindin-D28k. Arrows denote low-level expression of ecto-5'-nucleotidase in positively stained distal tubules. (Magnification x10; scale bar = 50μm). G. Staining for ecto-5'-nucleotidase in outer medullary collecting ducts. H. Same section as G, stained for AQP2. I. Merged image of G and H stained for both ecto-5'-nucleotidase (green) and AQP2 (red). Arrows denote presumed intercalated cells. (Magnification x20; scale bar = 25μm). J. Staining for ecto-5'-nucleotidase in inner medullary collecting ducts. K. Same section as J, stained for AQP2. L. Merged image of J and K stained for ecto-5'-nucleotidase (green) and AQP2 (red). Arrows denote presumed intercalated cells. (Magnification x20; scale bar = 25μm).

5.4 Discussion

The lack of uniformity in the distribution of ectonucleotidases along the nephron, together with their co-expression with purinoceptors (P1 and P2), makes it probable that these enzymes have a role in influencing the activation of different purinoceptor subtypes. This concept is illustrated by *in vitro* studies examining the effect of ectonucleotidases on ADP-sensitive platelet aggregation (Alvarado-Castillo et al, 2005). These studies demonstrated that in the presence of extracellular ATP, expression of NTPDase1 (which hydrolyses both ATP and ADP with almost equal preference) reduced platelet aggregation, whereas expression of NTPDase2 (which preferentially hydrolyses ATP) had the opposite effect. Thus a detailed knowledge of the types of ectonucleotidase present in each nephron segment is essential to our understanding of purinoceptor function.

To date, the only ectonucleotidases whose distribution along the nephron has been described in detail are alkaline phosphatase and ecto-5'-nucleotidase. Alkaline phosphatase has broad substrate specificity, capable of metabolizing ATP, ADP and AMP to adenosine. It is glycosyl phosphatidyl inositol (GPI) anchored and so may also exist in a soluble form. In the kidney, alkaline phosphatase is exclusively expressed in the brush-border membrane of the proximal tubule (Beliveau et al, 1983). Ecto-5'-nucleotidase dephosphorylates AMP to adenosine and is also GPI anchored. It has been shown previously to be present in the brush-border membrane of the proximal tubule, and in the apical membrane and apical cytoplasm of intercalated cells in the connecting tubule and collecting duct, as well as in the peritubular space (Gandhi et al, 1990; Le Hir and Kaissling 1989).

The present study examined the intraluminal distribution of the ectonucleotidases NTPDases 1-3, NPP3 and, for purposes of comparison, ecto-5'-nucleotidase. A key feature of this investigation was the use of specific markers to identify each nephron

segment. Figure 5.10 is a summary of the main findings. In the discussion that follows, each of the enzymes will be dealt with in turn.

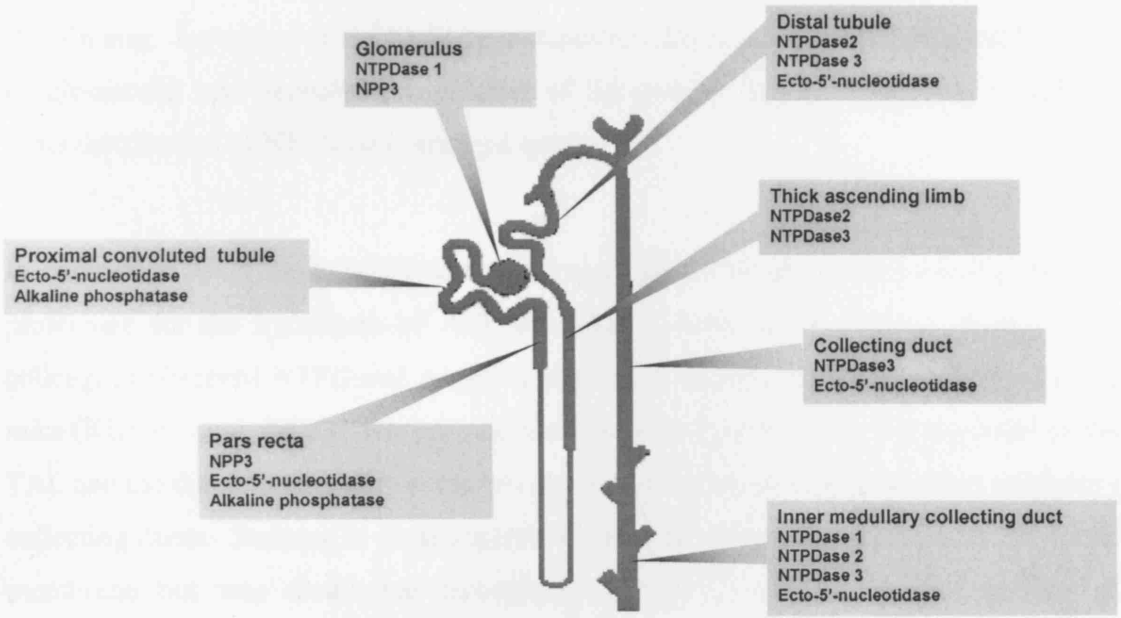

Fig. 5.10: Summary of the distribution of ectonucleotidases along the rat nephron.

5.4.1 Ectonucleoside triphosphate diphosphohydrolases 1-3

All members of the NTPDase family hydrolyse ATP and ADP to AMP, but they differ in their preferences for these substrates (Kukulski et al, 2005). As indicated above, NTPDase1 hydrolyses ATP and ADP with almost equal preference (Zimmermann 2001a). However, hydrolysis of ATP by rat NTPDase1 largely proceeds directly to AMP (Zimmermann, 2000). In the present study, NTPDase1 was prominently expressed in the glomerulus and peritubular space, with some low-level staining in the inner medullary collecting ducts; this enzyme was not present in any of the other nephron segments

examined. These results are consistent with those of a recent study in rat and mouse in which glomerular mesangial cells and/or glomerular capillary membranes, as well as peritubular capillaries, stained for NTPDase1 (Kishore et al, 2005). The same study also identified NTPDase1 in thin ascending limb of the loop of Henle, but, owing to the lack of a suitable marker for this nephron segment, the present study was unable to confirm this finding. Lemmens et al (2000) have identified this enzyme in the blood vessel walls of glomerular and peritubular capillaries of the porcine kidney, suggesting conserved renal distribution of NTPDase1 amongst species.

In contrast to NTPDase1, NTPDase2 has a significantly higher (approximately 30-fold) preference for the hydrolysis of ATP over ADP (Zimmermann, 2000). Kishore and colleagues observed NTPDase2 labelling in tubular structures in kidneys from rats and mice (Kishore et al, 2005). The present study has identified these tubular segments as the TAL and the distal tubule, with some low-level enzyme expression in the inner medullary collecting ducts. Staining in these regions of the nephron was not confined to the apical membrane but was distributed throughout the cell cytoplasm. Co-localization of NTPDase2 with the distal tubular marker (Calbindin D28k) was variable. This variation in distribution might be explained by the fact that Calbindin D28k is present in both the distal convoluted tubule and the connecting tubule (Bindels et al, 1991); given its prominent expression in the TAL, it seems possible that NTPDase2 is expressed only in the distal convoluted tubule and not the connecting tubule.

NTPDase3 was found in all of the post-proximal segments of the nephron examined, including the TAL, the distal tubule and the collecting duct. In the cortical and outer medullary collecting duct, this enzyme appeared to be confined to intercalated cells, whereas in the inner medullary collecting ducts it was found in 'principal' cells. Catalytically, this ectonucleotidase has a higher preference (approximately 3-fold) for the hydrolysis of ATP over ADP (Zimmermann, 2000) .

Currently, the functional significance of the distribution of NTPDases 2 and 3 is unclear. However, the presence of NTPDase1 in the glomerulus and peritubular space raises a number of possibilities. In the glomerulus, ATP induces relaxation of pre-contracted mesangial cells. NTPDase1 (and other ectonucleotidases such as NPP3) may modulate this activity (Jankowski et al, 2001), thereby influencing the capillary surface area available for filtration. These enzymes may also influence other glomerular purinoceptor responses such as P2Y-dependent cell proliferation of mesangial cells, or may serve in the protection of these cells by preventing ATP levels reaching concentrations that activate the apoptotic $P2X_7$ receptor (Harada et al, 2000).

It is also possible that NTPDase1, along with ecto-5'-nucleotidase, is involved in tubulo-glomerular feedback (TGF), whereby changes in renal perfusion pressure, or other causes of altered NaCl delivery to the macula densa, ultimately cause compensatory changes in afferent arteriolar resistance so that glomerular filtration rate is regulated (see section 1.2.2). ATP concentrations in renal interstitial fluid increase in response to elevations in renal arterial perfusion pressure (Nishiyama et al, 2001), and ATP can act directly on $P2X_1$ receptors on the afferent arteriole to induce constriction (Inscho et al, 2003). However, strong evidence also exists for adenosine (acting via A_1 receptors) being the chemical mediator in this response (Osswald et al, 1991; Schnermann et al, 1997). In this context, it is possible that NTPDase1, expressed in the peritubular space, might convert any unbound or excess ATP into AMP. The latter, being a suitable substrate for the enzyme ecto-5'-nucleotidase, also expressed in the peritubular space (see below), could then be converted to adenosine to cause or augment the vasoconstrictive response in TGF.

5.4.2 Ectonucleotide pyrophosphatase phosphodiesterases 1-3

NPPs 1-3 are also able to catalyze ATP and ADP to AMP, but vary in their affinities for the nucleotide substrates. Of these three well-characterized members, only NPP1 has been identified previously in the kidney. Using immunohistochemistry, Harahap and

Goding, (1988) showed strong expression of this enzyme in the basal epithelium of the distal tubule of the mouse, with low-level staining in the proximal convoluted tubule. The significance of its tubular expression in the nephron was not mentioned in their study; however, its basolateral expression in the distal nephron, together with its catalytic activity, suggests that this enzyme may also contribute to the signalling in the TGF mechanism by producing the end-hydrolysis product AMP; which together with ecto-5'nucleotidase (expressed in peritubular connective tissue) would form the TGF signalling mediator adenosine. Although northern blot data have indicated the presence of NPP2 mRNA in rat kidney (Fuss et al, 1997), lack of a suitable antibody precluded my mapping the expression of either NPP1 or NPP2 along the rat renal tubule.

In the present study, prominent staining for NPP3 was observed in the brush-border membrane of the proximal tubule. However, its expression in this part of the nephron varied, as some positively identified proximal segments displayed little or no staining for the enzyme. Subsequent co-localisation studies, using neutral endopeptidase (NEP) antibody as a specific marker of the S3 segment in the rat (Edwards et al, 1999; Ronco et al, 1988), showed prominent expression of NPP3 in every case, indicating that those segments of the proximal tubule not staining for NPP3 are likely to be within S1 or S2 regions and that NPP3 is expressed predominantly in the S3 segment of the proximal tubule. In addition to the proximal tubule, NPP3 expression was also found in glomeruli. A unique feature of the NPP ectonucleotidases is their ability to hydrolyse the phosphodiester bonds of nucleic acids, suggesting a protective role against blood-borne DNA- or RNA-based viruses; alternatively, they may serve to salvage purines liberated during injury or cell death (Zimmermann 2001a).

5.4.3 Ecto-5'-nucleotidase

Prominent immunostaining of ecto-5'-nucleotidase was identified in the apical membrane of the proximal tubule. However, as with NPP3, staining was variable: not all positively stained proximal tubular segments expressed ecto-5'-nucleotidase. Further investigation,

again using the NEP antibody specific to the S3 segment of the rat proximal tubule, showed that in contrast to NPP3 there was only modest and variable co-staining with NEP. This suggests that the expression of ecto-5'-nucleotidase in the proximal tubule is restricted mainly to the S2 and, possibly, S1 segments.

Kaissling's group has reported high ecto-5'-nucleotidase activity in the S1 segment of the proximal tubule of the rat, decreasing progressively in the S2 segment. In the outer stripe of the outer medulla the S3 segment showed expression of ecto-5'- nucleotidase in most but not all rats, whereas staining in the S3 segments of the medullary rays was either weak or absent (Le Hir and Kaissling, 1989); this is consistent with the observations made in the present investigation (Fig. 5.9C/D). If adenosine were to be produced by either ecto-5'-nucleotidase or alkaline phosphatase in the proximal tubule, it would be expected to activate the adenosine (A_1) receptors also found in the proximal tubule (Smith et al, 2001), resulting in increased sodium and water reabsorption (Wilcox et al, 1999).

In the present study, low-level staining for ecto-5'-nucleotidase was also seen in the cortical and medullary collecting ducts. Some low-level staining of this enzyme was also found in some, but not all, parts of positively stained distal tubular segments. As previously indicated, Calbindin D28k is expressed in both the distal convoluted tubule and the connecting tubule. Given that ecto-5'-nucleotidase is expressed in the collecting duct, it seems possible that it is present in the connecting tubule, rather than the distal convoluted tubule. Gandhi *et al* (1990) have attributed the sparse staining of this enzyme in the connecting tubule and the collecting duct to intercalated cells, which accords with the observations made in the present study.

If adenosine were produced in the distal tubule or connecting tubule, its functional significance in these segments is not clear. In the collecting duct, Jackson et al (2003) reported that adenosine formation was reduced when ecto-5'-nucleotidase activity was inhibited, suggesting that, despite its low expression, this enzyme is functionally active in

this nephron segment. Adenosine produced in the collecting duct may act to stimulate A_1 receptors (which have been identified in the medullary collecting ducts) (Smith et al, 2001). Contrary to their effects in the proximal tubule, stimulation of collecting duct A_1 receptors reduces sodium reabsorption (Yagil et al, 1994). Overall, renal A_1 receptor inhibition is natriuretic and diuretic, because the effect on proximal tubular reabsorption predominates (Wilcox et al, 1999).

Prominent ecto-5'-nucleotidase staining was also observed outside the tubule, in the peritubular space. In an extensive previous study (Le Hir and Kaissling, 1989), this peritubular staining was attributed to interstitial fibroblasts. Located between tubules, peritubular capillaries and arteriolar smooth muscle cells, these fibroblasts may serve to convert nucleotides (released from nerve endings and tubules) into adenosine. This would affect nearby adenosine-sensitive tissues such as the renin-producing granular cells and erythropoietin-producing cells (Le Hir and Kaissling, 1993). The possible role of ecto-5'-nucleotidase in TGF has already been discussed. In this connection, ecto-5'-nucleotidase knockout mice have been shown to have a blunted TGF response (Castrop et al, 2004).

5.4.3.1 *Nucleoside transporters*

Adenosine produced in the nephron might travel downstream or, alternatively, be removed from the lumen to be taken into renal epithelial cells via nucleoside transporters. Nucleosides are hydrophilic and require facilitated transport in order to enter renal epithelial cells. Sodium-dependent concentrative nucleoside transporters (Le Hir and Dubach, 1984; Thorn and Jarvis, 1996) and equilibrative nucleoside transporters are believed to be located on the proximal tubular apical and basolateral membranes, respectively (Mangrative et al, 2003). Once inside the cell, adenosine can either traverse the basolateral membrane or be converted into inosine. Further studies need to be conducted to establish the existence of these nucleoside transporters in other tubular sites.

Overall, it seems as though expression of adenosine receptors in the nephron coincides with the presence of adenosine-producing ectonucleotidases, allowing the possibility that these enzymes serve to produce adenosine to activate adjacent receptors. In addition, co-expression of nucleoside transporters with these adenosine-producing enzymes in the proximal tubule suggests an alternative function for the ectonucleotidases in recycling/scavenging nucleotides released from cells or filtered at the glomerulus. Moreover, the existence of nucleoside transporters on both the apical and basolateral membranes on the same cell allows the transepithelial movement of adenosine, raising the possibility that adenosine produced in the lumen of the tubule may move transcellularly to stimulate adenosine receptors expressed on the basolateral membrane.

5.4.4 Renal ectonucleotidase expression under pathophysiological conditions

The expression of these enzymes can be up- or down-regulated under pathological situations. For instance, Kaissling et al (1993), have reported glomerular ecto-5'-nucleotidase activity following hypoxia in the rat kidney, whereas the enzyme was undetected under normal conditions. Using immunohistochemistry, increased expression of glomerular ecto-5'-nucleotidase has also been shown in patients with chronic allograft nephropathy (clinically characterized by a slow, progressive decline in GFR, usually in conjunction with proteinuria) (Mui et al, 2003). The same study also showed decreased glomerular expression of NTPDase1 in these patients.

The up-regulation of ecto-5'-nucleotidase under pathophysiological conditions would increase adenosine which, since it prevents platelet aggregation, is a vasodilator and a reactive oxygen species (ROS) scavenging agent, may serve to counteract the effects of ischaemic damage (Kaissling et al, 1993). Okusa (2002) reported that stimulation of A_{2A} receptors on renal endothelial cells significantly reduced the expression of endothelial intracellular adhesion molecule-1 (ICAM-1) (required for binding and activating neutrophils, a key mechanism for pathogenesis during ischaemia-reperfusion injury). Thus, under these conditions the increased levels of adenosine might serve to prevent

inflammatory responses in the renal endothelium. Other adenosine receptors (namely A_3) have been identified on mesangial cells of the glomerulus, the activation of which resulted in apoptosis (Zhao et al, 2002). During pathophysiological conditions, apoptosis would be favoured over necrosis, as the latter may augment inflammatory responses, resulting in further tissue damage.

It is not clear why ATP-hydrolyzing ectonucleotidases (ecto-ATPases) are downregulated in patients with chronic allograft nephropathy, particularly when studies have implicated their having an anti-inflammatory role. In this context, *in vivo* experiments performed on glomerular ectonucleotidase impaired mice demonstrated increased platelet aggregation in glomeruli of nephritic kidneys (Poelstra et al, 1991). Similarly, platelet aggregation was also increased when poorly hydrolysable ATP or ADP analogues were applied to the glomeruli of nephritic kidneys of wild-type mice (Poelstra et al, 1992). It is worth noting that an (unidentified) ecto-ATPase was shown to be highly sensitive to ROS generated during tissue injury (Barbey et al, 1989), which might explain why these enzymes are downregulated during these conditions. If so, this could contribute to the progression of diseases like glomerulonephritis.

However, the converse is true in other tissues as mRNA transcripts for NTPDase1 and ecto-5'-nucleotidase were up-regulated in the brain of the rat following cerebral ischaemia. This was mirrored by a rise in extracellular nucleotide hydrolysis. Under this circumstance the up-regulation of these enzymes may serve several purposes, such as (i) increasing the production of adenosine (a neuroprotective agent), (ii) increasing the salvation of purines, and/or (iii) preventing the activation of cytolytic $P2X_7$ receptors by high concentrations of ATP.

5.5 Conclusion

Although the mRNA of many ectonucleotidases has been identified previously in the kidney, the segmental distribution of the enzymes along the nephron remained largely undefined. The present study showed that the distribution of the ectonucleotidases varied significantly along the different regions of the nephron. Reasons for this pattern of distribution are still unclear, but their varying hydrolysis pathways suggest that the enzymes may be strategically placed so as to influence the activity of P2 and P1 purinoceptors through the generation, or hydrolysis, of agonists such as ATP, ADP or adenosine.

It is interesting that the hydrolysis pathway for some of these ectonucleotidases can proceed directly from ATP to AMP (without releasing ADP as an intermediate); and that the segmental distribution of these enzymes along the nephron is highly specific. For instance, NTPDase1 and NPP3 were found in the glomeruli, and NPP3 was found in the pars recta; because both these enzymes (in addition to hydrolysing ADP) hydrolyse ATP directly to AMP, it could be proposed that in these regions insufficient ADP is produced to activate adjacent P2 receptor subtypes. In particular, the ADP-sensitive $P2Y_1$ receptor is expressed in both these regions.

It is also interesting how AMP-producing ectonucleotidases are either co-expressed or expressed immediately before the adenosine-producing ecto-5'-nucleotidase; and ecto-5'-nucleotidase is predominantly found in the proximal tubule, where adenosine stimulates Na^+ reabsorption, and in the collecting duct, where the opposite is the case.

On the basis of the above, it could be proposed that under basal/normal conditions, ectonucleotidases function to prevent or limit the extent to which P2 receptors are activated, thereby limiting the inhibiting effects of these receptors on electrolyte reabsorption. Conversely, under pathological or other stimulatory conditions, release of ATP may overwhelm the regulatory ectonucleotidases, and may in turn activate P2

receptors, to reduce energy-consuming ion reabsorption. Future studies may use ectonucleotidase knockout models, which, in conjunction with micropuncture techniques, could be used to investigate the influence of ectonucleotidase expression on ion transport in the kidney under physiological and pathophysiological circumstances.

CHAPTER 6

FINAL DISCUSSION

Over recent years, many studies have shown that activation of purinoceptors in the kidney can influence renal functions such as glomerular haemodynamics, TGF and tubular water and electrolyte reabsorption. In addition to these physiological actions, extracellular nucleotides have also been implicated in pathophysiological conditions by augmenting or inhibiting inflammatory responses, apoptosis and cell proliferation. Although *in vitro* evidence suggests that ATP release does occur from renal epithelial cells, no attempts have previously been made to quantify intraluminal ATP levels *in vivo*; the extent to which apical P2 receptors are activated in the renal tubule was therefore unknown. Renal epithelial cells in culture are often placed in a static environment and are not exposed to the shear-stressed environments found *in vivo*; as a result, in an attempt to adapt to the surrounding conditions, cultured cells may lose or change their characteristic features/phenotypes. The present study, using micropuncture has been the first to measure intraluminal ATP levels *in vivo*. It was shown that not only are ATP levels detectable in the proximal and distal convoluted tubule, but, in the case of the proximal convoluted tubule at least, are high enough to activate some P2 receptor subtypes.

In a further investigation, using Munich-Wistar rats (which display surface glomeruli), Bowman's space fluid was sampled and assayed for ATP to assess whether the ATP in the proximal tubule originated from plasma being filtered at the glomerulus. Because the ATP concentration in filtered fluid was markedly lower (more than 4 fold) than that in mid-proximal tubular fluid (a difference that could not be attributed to water reabsorption), it was concluded that proximal tubular epithelial cells secrete ATP into their luminal environment.

Although a number of mechanisms for ATP release have been suggested by studies using a variety of cells and cell lines, no attempt has previously been made to examine the mechanism by which ATP is released from proximal tubular cells. In the present study, the potential for ATP release to occur via exocytosis was examined in a proximal epithelial cell line originally derived from the S1 segment of the rat, using an intracellular marker of ATP, quinacrine. In these cells, quinacrine fluorescence was granular and

localized exclusively to the cytoplasm. This intracellular fluorescence was reduced markedly following exposure to a hypotonic medium, while extracellular ATP concentrations increased. These findings suggest that ATP is stored within the cytoplasm, possibly in vesicles, and is released by exocytosis upon hypotonic exposure. However, it should be emphasized that, because the current study used a tubular cell line, there is no certainty that the findings represent ATP release mechanisms in native tissue. Moreover the possibility of additional release mechanisms mediating ATP release in proximal tubular epithelial cells cannot be ruled out.

Interestingly, the concentrations of ATP in distal tubular fluid were found to be markedly lower than those in the proximal tubular lumen. There are several possible explanations for this. First, the distal tubular ATP may simply be proximally secreted ATP that has travelled down the nephron in the tubular fluid. Secondly, the distal tubule may secrete ATP, but at a lower rate than the proximal tubule. Thirdly, the distal tubule may secrete ATP at a similar rate to the proximal tubule, but may have a greater rate of degradation due to higher ectonucleotidase activity compared with that of the proximal convoluted tubule. Although the latter possibility was not directly assessed, immunohistological analysis of ectonucleotidases at the protein level, showed strong expression of the ATP-hydrolysing NTPDases 2 and 3 in the distal convoluted tubule; these ectonucleotidases are known to have lower K_m values than the ATP-hydrolysing ectonucleotidase found in the proximal convoluted tubule, namely alkaline phosphatase. In addition, other studies have reported that distal tubular epithelial cells in culture do release ATP into the extracellular environment (albeit at lower rates than those found for the proximal tubules). Taken together, these data suggest that ATP in the distal convoluted tubule is not derived from that released upstream in the proximal convoluted tubule, but instead, either distal tubular cells secrete less ATP than proximal tubular cells or distal tubules exhibit higher ectonucleotidase activity. Unless ectonucleotidase activity could be selectively inhibited, these two possibilities cannot be distinguished.

The present study assessed soluble nucleotidase activity within proximal tubular fluid as a means of extrapolating ATP concentrations at time zero, before any degradation by

soluble nucleotidases had occurred. Although their activity was not assessed *in vivo*, this study nevertheless provided evidence that soluble nucleotidases are indeed active in tubular fluid, and that the hydrolysis rates in fluids derived from proximal and distal tubules are similar. It is possible that the soluble nucleotidase in proximal tubular fluid is a cleaved soluble form of alkaline phosphatase. Because NTPDases 2 and 3 (identified in distal tubule) do not have the potential to be cleaved and released as a soluble form, it is possible that alkaline phosphatase, together with NPP3 (which is found in the pars recta of the proximal tubule and also has the potential to be cleaved into a soluble form), is responsible for the soluble nucleotidase activity observed in distal tubular fluid. However, a contribution from intracellular nucleotidases (namely NTPDases 4-7) released from intracellular compartments of renal epithelial cells, or indeed additional ectonucleotidases which have the potential to be cleaved into a soluble form, cannot be ruled out. Although the expression of five major ectonucleotidases, namely NTPDases 1-3, NPP3 and ecto-5'-nucleotidase was examined by immunohistochemistry and found to be differential along the major regions of the nephron, other newly discovered ectonucleotidases are continually being identified; thus previously unknown ectonucleotidases may contribute significantly to influencing ATP levels, and ultimately purinoceptor activation.

Finally, the present investigation showed that two pathophysiological manoeuvres, namely haemorrhage and ECVE, caused no significant change to intraluminal ATP concentrations. As discussed earlier, it is possible that ATP levels may have increased during these conditions, but that the concomitant release of soluble nucleotidases may have masked these changes.

Conclusion

It is clear from the present investigation that ATP is secreted from proximal epithelial cells into the intraluminal environment of the tubule and that one of the potential release mechanisms may involve exocytosis from ATP-containing vesicles stored in the cytoplasm of these cells. Although the ATP levels found in the present study do not represent those at the cell surface, the concentrations are nevertheless believed to be high

enough to activate some P2 receptor subtypes (known from other studies to be expressed along the nephron). In addition, an array of ectonucleotidases was found to be differentially expressed along the nephron and may serve to influence activation of tubular purinoceptors.

The release of ATP, presence of apical P2 receptors and expression of nucleotide hydrolyzing enzymes strongly suggest a physiological role for extracellular nucleotides acting from the lumen of the kidney. Although other studies have reported inhibitory effects of intraluminal ATP on tubular reabsorption, its precise physiological role in the nephron will be a matter for future investigations.

REFERENCES

Alvarado-Castillo C, Harden TK and Boyer JL. Regulation of $P2Y_1$ receptor-mediated signaling by the ectonucleoside triphosphate diphosphohydrolase isozymes NTPDase1 and NTPDase2. *Mol Pharmacol* 67: 114-122, 2005.

Anderson CM and Parkinson FE. Potential signalling roles for UTP and UDP: sources, regulation and release of uracil nucleotides. *Trends Pharmacol Sci* 18: 387-392, 1997.

Aschrafi A, Sadtler S, Niculescu C, Rettinger J and Schmalzing G. Trimeric architecture of homomeric $P2X_2$ and heteromeric $P2X_{1+2}$ receptor subtypes. *J Mol Biol* 342: 333-343, 2004.

Atherton JC and Jammaz I. Renal tubular effects of Inactin anaesthesia in Sprague-Dawley rats. *Renal Physiol* 9: 107-108, 1986.

Atherton JC, Mahendran D and Mannan M. Effect of Inactin anaesthesia on kidney function in Sprague-Dawley rats. *J Physiol* 342: 75P-76P: 1983.

Auger R, Motta I, Benihoud K, Ojcius DM and Kanellopoulos JM. A role for mitogen-activated protein kinase(Erk1/2) activation and non-selective pore formation in $P2X_7$ receptor-mediated thymocyte death. *J Biol Chem* 280: 28142-28151, 2005.

Bahima L, Aleu J, Elias M, Martin-Satue M, Muhaisen A, Blasi J, Marsal J and Solsona C. Endogenous hemichannels play a role in the release of ATP from *Xenopus* oocytes. *J Physiol* 567P: PC152, 2005.

Bailey MA, Imbert-Teboul M, Turner C, Marsy S, Srai K, Burnstock G and Unwin RJ. Axial distribution and characterization of basolateral P2Y receptors along the rat renal tubule. *Kidney Int* 58: 1893-1901, 2000a.

Bailey MA, Hillman KA and Unwin RJ. P2 receptors in the kidney. *J Auton Nerv Syst* 81: 264-270, 2000b.

Bailey MA, Imbert-Teboul M, Turner C, Srai SK, Burnstock G and Unwin RJ. Evidence for basolateral $P2Y_6$ receptors along the rat proximal tubule: functional and molecular characterization. *J Am Soc Nephrol* 12: 1640-1647, 2001.

Bailey MA. Inhibition of bicarbonate reabsorption in the rat proximal tubule by activation of luminal $P2Y_1$ receptors. *Am J Physiol Renal Physiol* 287: F789-F796, 2004.

Bankston LA and Guidotti G. Characterization of ATP transport into chromaffin granule ghosts. Synergy of ATP and serotonin accumulation in chromaffin granule ghosts. *J Biol Chem* 271: 17132-17138, 1996.

Barbey MM, Fels LM, Soose M, Poelstra K, Gwinner W, Bakker W and Stolte H. Adriamycin affects glomerular renal function: evidence for the involvement of oxygen radicals. *Free Radic Res Commun* 7: 195-203, 1989.

Baricordi OR, Melchiorri L, Adinolfi E, Falzoni S, Chiozzi P, Buell G and Di VF. Increased proliferation rate of lymphoid cells transfected with the $P2X_7$ ATP receptor. *J Biol Chem* 274: 33206-33208, 1999.

Baum D, Halter JB, Taborsky GJ, Jr. and Porte D, Jr. Pentobarbital effects on plasma catecholamines: temperature, heart rate, and blood pressure. *Am J Physiol* 248: E95-E100, 1985.

Beach RE and Good DW. Effects of adenosine on ion transport in rat medullary thick ascending limb. *Am J Physiol* 263: F482-F487, 1992.

Beigi R, Kobatake E, Aizawa M and Dubyak GR. Detection of local ATP release from activated platelets using cell surface-attached firefly luciferase. *Am J Physiol* 276: C267-C278, 1999.

Beliveau R, Brunette MG and Strevey J. Characterization of phosphate binding by alkaline phosphatase in rat kidney brush border membrane. *Pflügers Arch* 398: 227-232, 1983.

Bell PD, Lapointe JY, Sabirov R, Hayashi S, Peti-Peterdi J, Manabe K, Kovacs G and Okada Y. Macula densa cell signaling involves ATP release through a maxi anion channel. *Proc Natl Acad Sci U S A* 100: 4322-4327, 2003.

Bigonnesse F, Levesque SA, Kukulski F, Lecka J, Robson SC, Fernandes MJ and Sévigny J. Cloning and characterization of mouse nucleoside triphosphate diphosphohydrolase-8. *Biochemistry* 43: 5511-5519, 2004.

Bindels RJM, Timmermans JA, Hartog A, Coers W and van Os CH. Calbindin-D9k and parvalbumin are exclusively located along basolateral membranes in rat distal nephron. *J Am Soc Nephrol* 2: 1122-1129, 1991.

Bodin P and Burnstock G. ATP-stimulated release of ATP by human endothelial cells. *J Cardiovasc Pharmacol* 27: 872-875, 1996.

Bodin P and Burnstock G. Evidence that release of adenosine triphosphate from endothelial cells during increased shear stress is vesicular. *J Cardiovasc Pharmacol* 38: 900-908, 2001.

Born GV and Kratzer MA. Source and concentration of extracellular adenosine triphosphate during haemostasis in rats, rabbits and man. *J Physiol* 354: 419-429, 1984.

Borst P, Evers R, Kool M and Wijnholds J. The multidrug resistance protein family. *Biochim Biophys Acta* 1461: 347-357, 1999.

Braun N, Fengler S, Ebeling C, Servos J and Zimmermann H. Sequencing, functional expression and characterization of rat NTPDase6, a nucleoside diphosphatase and novel member of the ecto-nucleoside triphosphate diphosphohydrolase family. *Biochem J* 351: 639-647, 2000.

Briggs DR. The metaphosphoric acid-protein reaction. *J. Biol Chem* 134: 261-272, 1940.

Bulanova E, Budagian V, Orinska Z, Hein M, Petersen F, Thon L, Adam D and Bulfone-Paus S. Extracellular ATP induces cytokine expression and apoptosis through $P2X_7$ receptor in murine mast cells. *J Immunol* 174: 3880-3890, 2005.

Burnstock G. Purine-mediated signalling in pain and visceral perception. *Trends Pharmacol Sci* 22: 182-188, 2001.

Burnstock G and Knight GE. Cellular distribution and functions of P2 receptor subtypes in different systems. *Int Rev Cytol* 240: 31-304, 2004.

Butterweck A, Gergs U, Elfgang C, Willecke K and Traub O. Immunochemical characterization of the gap junction protein connexin 45 in mouse kidney and transfected human HeLa cells. *J Membr Biol* 141: 247-256, 1994.

Cantiello HF. Electrodiffusional ATP movement through CFTR and other ABC transporters. *Pflügers Arch* 443 Suppl 1: S22-S27, 2001.

Casavola V, Guerra L, Reshkin SJ, Jacobson KA, Verrey F and Murer H. Effect of adenosine on Na^+ and Cl^- currents in A6 monolayers. Receptor localization and messenger involvement. *J Membr Biol* 151: 237-245, 1996.

Casellas D, Dupont M, Kaskel FJ, Inagami T and Moore LC. Direct visualization of renin-cell distribution in preglomerular vascular trees dissected from rat kidney. *Am J Physiol* 265: F151-F156, 1993.

Castrop H, Huang Y, Hashimoto S, Mizel D, Hansen P, Theilig F, Bachmann S, Deng C, Briggs J and Schnermann J. Impairment of tubuloglomerular feedback regulation of GFR in ecto-5'-nucleotidase/CD73-deficient mice. *J Clin Invest* 114: 634-642, 2004.

Chadwick BP and Frischauf AM. The CD39-like gene family: identification of three new human members (CD39L2, CD39L3, and CD39L4), their murine homologues, and a member of the gene family from *Drosophila melanogaster. Genomics* 50: 357-367, 1998.

Chamberlain RM. The renal functional response to partial nephrectomy. PhD thesis, University of London. 1996.

Chan CM, Unwin RJ and Burnstock G. Potential functional roles of extracellular ATP in kidney and urinary tract. *Exp Nephrol* 6: 200-207, 1998.

Chapman E, Hussain S, Peppiatt CM, Marks J, Churchill LJ, Turner CM, King BF, Unwin RJ and Wildman SS. Immunohistochemical localisation of P2 receptors in the rat renal collecting duct: effects of altering dietary sodium intake. *Proc Physiol Soc.* April, 2006.

Cochrane JP. The aldosterone response to surgery and the relationship of the response to postoperative sodium retention. *Br J Surg* 65: 744-747, 1978.

Cole BR, Hays AE, Boylan JG, Burch HB and Lowry OH. Distribution of enzymes of adenylate and guanylate nucleotide metabolism in rat nephron. *Am J Physiol* 243: F349-F355, 1982.

Cortell S. Silicone rubber for renal tubular injection. *J Appl Physiol* 26: 158-159, 1969.

Cotrina ML, Lin JH, ves-Rodrigues A, Liu S, Li J, zmi-Ghadimi H, Kang J, Naus CC and Nedergaard M. Connexins regulate calcium signaling by controlling ATP release. *Proc Natl Acad Sci USA* 95: 15735-15740, 1998.

Cressman VL, Lazarowski E, Homolya L, Boucher RC, Koller BH, Grubb BR. Effect of loss of $P2Y_2$ receptor gene expression on nucleotide regulation of murine epithelial Cl^- transport. *J Biol Chem* 274: 26461-26468. 1999.

Cuffe JE, Bielfeld-Ackermann A, Thomas J, Leipziger J and Korbmacher C. ATP stimulates Cl^- secretion and reduces amiloride-sensitive Na^+ absorption in M-1 mouse cortical collecting duct cells. *J Physiol* 524: 77-90, 2000.

Dai LJ, Kang HS, Kerstan D, Ritchie G and Quamme GA. ATP inhibits Mg^{2+} uptake in MDCT cells via P2X purinoceptors. *Am J Physiol Renal Physiol* 281: F833-F840, 2001.

Deutsch S, Pierce EC, Jr. and Vandam LD. Cyclopropane effects on renal function in normal man. *Anesthesiology* 28: 547-558, 1967.

Diaz-Sylvester P, Mac LM and Amorena C. Peritubular fluid viscosity modulates H^+ flux in proximal tubules through NO release. *Am J Physiol Renal Physiol* 280: F239-F243, 2001.

Dutta AK, Sabirov RZ, Uramoto H and Okada Y. Role of ATP-conductive anion channel in ATP release from neonatal rat cardiomyocytes in ischaemic or hypoxic conditions. *J Physiol* 559: 799-812, 2004.

Edgecombe M, Craddock HS, Smith DC, McLennan AG and Fisher MJ. Diadenosine polyphosphate-stimulated gluconeogenesis in isolated rat proximal tubules. *Biochem J* 323: 451-456, 1997.

Edwards RM and Spielman WS. Adenosine A_1 receptor-mediated inhibition of vasopressin action in inner medullary collecting duct. *Am J Physiol* 266: F791-F796, 1994.

Edwards RM, Pullen M and Nambi P. Distribution of neutral endopeptidase activity along the rat and rabbit nephron. *Pharmacology* 59: 45-50, 1999.

Ernest S, Rajaraman S, Megyesi J and Bello-Reuss EN. Expression of MDR1 (multidrug resistance) gene and its protein in normal human kidney. *Nephron* 77: 284-289, 1997.

Ferrari D, Chiozzi P, Falzoni S, Hanau S and Di VF. Purinergic modulation of interleukin-1 beta release from microglial cells stimulated with bacterial endotoxin. *J Exp Med* 185: 579-582, 1997.

Filipovic DM, Adebanjo OA, Zaidi M and Reeves WB. Functional and molecular evidence for P2X receptors in LLC-PK1 cells. *Am J Physiol* 274: F1070-F1077, 1998.

Fromm M, Oelkers W and Hegel U . Time course of aldosterone and corticosterone plasma levels in rats during general anaesthesia and abdominal surgery. *Pflügers Arch* 399: 249-254, 1983.

Fuss B, Baba H, Phan T, Tuohy VK and Macklin WB. Phosphodiesterase 1, a novel adhesion molecule and/or cytokine involved in oligodendrocyte function. *J Neurosci* 17: 9095-9103, 1997.

Gagnon JA, Felipe I, Nelson LD and Butkus DE. Influence of thiopental anesthesia on renal sodium and water excretion in the dog. *Am J Physiol* 243: F265-F270, 1982.

Gandhi R, Le Hir M and Kaissling B. Immunolocalization of ecto-5'-nucleotidase in the kidney by a monoclonal antibody. *Histochemistry* 95: 165-174, 1990.

Gijsbers R, Ceulemans H, Stalmans W and Bollen M. Structural and catalytic similarities between nucleotide pyrophosphatases/phosphodiesterases and alkaline phosphatases. *J Biol Chem* 276: 1361-1368, 2001.

Gordon JL. Extracellular ATP: effects, sources and fate. *Biochem J* 233: 309-319, 1986.

Guerra L, Favia M, Fanelli T, Calamita G, Svetlo M, Bagorda A, Jacobson KA, Reshkin SJ and Casavola V. Stimulation of *Xenopus* $P2Y_1$ receptor activates CFTR in A6 cells. *Pflügers Arch* 449: 66-75, 2004.

Guyot A and Hanrahan JW. ATP release from human airway epithelial cells studied using a capillary cell culture system. *J Physiol* 545: 199-206, 2002.

Haines WR, Torres GE, Voigt MM and Egan TM. Properties of the novel ATP-gated ionotropic receptor composed of the $P2X_1$ and $P2X_5$ isoforms. *Mol Pharmacol* 56: 720-727, 1999.

Harada H, Chan CM, Loesch A, Unwin R and Burnstock G. Induction of proliferation and apoptotic cell death via P2Y and P2X receptors, respectively, in rat glomerular mesangial cells. *Kidney Int* 57: 949-958, 2000.

Harahap AR and Goding JW. Distribution of the murine plasma cell antigen PC-1 in non-lymphoid tissues. *J Immunol* 141: 2317-2320, 1988.

Hazama A, Fan HT, Abdullaev I, Maeno E, Tanaka S, ndo-Akatsuka Y and Okada Y. Swelling-activated, cystic fibrosis transmembrane conductance regulator-augmented ATP release and Cl^- conductances in murine C127 cells. *J Physiol* 523: 1-11, 2000.

Hazama A, Shimizu T, ndo-Akatsuka Y, Hayashi S, Tanaka S, Maeno E and Okada Y. Swelling-induced, CFTR-independent ATP release from a human epithelial cell line: lack of correlation with volume-sensitive Cl^- channels. *J Gen Physiol* 114: 525-533, 1999.

Henrich WL, McAllister EA, Eskue A, Miller T and Moe OW. Renin regulation in cultured proximal tubular cells. *Hypertension* 27: 1337-1340, 1996.

Hillman KA, Woolf AS, Johnson TM, Wade A, Unwin RJ and Winyard PJ. The $P2X_7$ ATP receptor modulates renal cyst development in vitro. *Biochem Biophys Res Commun* 322: 434-439, 2004.

Hisadome K, Koyama T, Kimura C, Droogmans G, Ito Y and Oike M. Volume-regulated anion channels serve as an auto/paracrine nucleotide release pathway in aortic endothelial cells. *J Gen Physiol* 119: 511-520, 2002.

Holstein-Rathlou NH, Christensen P and Leyssac PP. Effects of halothane-nitrous oxide inhalation anesthesia and Inactin on overall renal and tubular function in Sprague-Dawley and Wistar rats. *Acta Physiol Scand* 114: 193-201, 1982.

Hume DM, Bell CC and Bartter F . Direct measurement of adrenal secretion during operative trauma and convalescence. *Surgery* 52: 174-187, 1962.

Inscho EW. P2 receptors in regulation of renal microvascular function. *Am J Physiol Renal Physiol* 280: F927-F944, 2001.

Inscho EW, Cook AK, Imig JD, Vial C and Evans RJ. Physiological role for $P2X_1$ receptors in renal microvascular autoregulatory behavior. *J Clin Invest* 112: 1895-1905, 2003.

Insel PA and Snavely MD. Catecholamines and the kidney: receptors and renal function. *Annu Rev Physiol* 43: 625-636, 1981.

Irvin JL and Irvin EM. The interaction of quinacrine with adenine nucleotides. *J Biol Chem* 210: 45-56, 1954.

Jackson EK, Mi Z, Zhu C and Dubey RK. Adenosine biosynthesis in the collecting duct. *J Pharmacol Exp Ther* 307: 888-896, 2003.

Jankowski M, Szczepanska-Konkel M, Kalinowski L and Angielski S. The role of P2Y-receptors in the regulation of glomerular volume. *Med Sci Monit* 7: 635-340, 2001.

Jans D, Srinivas SP, Waelkens E, Segal A, Lariviere E, Simaels J and Van DW. Hypotonic treatment evokes biphasic ATP release across the basolateral membrane of cultured renal epithelia (A6). *J Physiol* 545: 543-555, 2002.

Jin W and Hopfer U. Purinergic-mediated inhibition of Na^+-K^+-ATPase in proximal tubule cells: elevated cytosolic Ca^{2+} is not required. *Am J Physiol* 272: C1169-C1177, 1997.

Joyce JT, Roizen MF and Eger EI. Effect of thiopental induction on sympathetic activity. *Anesthesiology* 59: 19-22, 1983.

Kaczmarek E, Koziak K, Sévigny J, Siegel JB, Anrather J, Beaudoin AR, Bach FH and Robson SC. Identification and characterization of CD39/vascular ATP diphosphohydrolase. *J Biol Chem* 271: 33116-33122, 1996.

Kaissling B, Spiess S, Rinne B and Le HM. Effects of anemia on morphology of rat renal cortex. *Am J Physiol* 264: F608-F617, 1993.

Kang HS, Kerstan D, Dai LJ, Ritchie G and Quamme GA. Adenosine modulates Mg^{2+} uptake in distal convoluted tubule cells via A_1 and A_2 purinoceptors. *Am J Physiol Renal Physiol* 281: F1141-F1147, 2001.

Kaufman JM, Siegel N, Lytton B and Hayslett JP. Compensatory renal adaptation after progressive renal ablation. *Invest Urol* 13: 441-444, 1976.

Kegel B, Braun N, Heine P, Maliszewski CR and Zimmermann H. An ecto-ATPase and an ecto-ATP diphosphohydrolase are expressed in rat brain. *Neuropharmacology* 36: 1189-1200, 1997.

Kennedy C, Todorov LD, Mihaylova-Todorova S and Sneddon P. Release of soluble nucleotidases: a novel mechanism for neurotransmitter inactivation? *Trends Pharmacol Sci* 18: 263-266, 1997.

Kimura N, Shimada N, Nomura K and Watanabe K. Isolation and characterization of a cDNA clone encoding rat nucleoside diphosphate kinase. *J Biol Chem* 265: 15744-15749, 1990.

King BF, Townsend-Nicholson A, Wildman SS, Thomas T, Spyer KM and Burnstock G. Coexpression of rat $P2X_2$ and $P2X_6$ subunits in *Xenopus* oocytes. *J Neurosci* 20: 4871-4877, 2000.

King BF and Townsend-Nicholson A. Nucleotide and nucleoside receptors. *Tocris Reviews*, 23: 1-11, 2003.

Kishore BK, Chou CL and Knepper MA. Extracellular nucleotide receptor inhibits AVP-stimulated water permeability in inner medullary collecting duct. *Am J Physiol* 269: F863-F869, 1995.

Kishore BK, Ginns SM, Krane CM, Nielsen S and Knepper MA. Cellular localization of $P2Y_2$ purinoceptor in rat renal inner medulla and lung. *Am J Physiol Renal Physiol* 278: F43-F51, 2000.

Kishore BK, Isaac J, Fausther M, Tripp SR, Shi H, Gill PS, Braun N, Zimmermann H, Sévigny J and Robson SC. Expression of nucleoside triphosphate diphosphohydrolase-1 (NTPDase1) and NTPDase2 in murine kidney: relevance to regulation of P2 receptor signaling. *Am J Physiol Renal Physiol* 288: F1032-F1043 2005.

Knight TF, Sansom S, Hawk L, Frankfurt SJ and Weinman EJ. The effects of anesthesia on the excretion of an isotonic saline load in the rat. *Pflügers Arch* 373: 139-143, 1978.

Knowles AF and Nagy AK. Inhibition of an ecto-ATP-diphosphohydrolase by azide. *Eur J Biochem* 262: 349-357, 1999.

Koeppen BA and Stanton BA. Renal Physiology, 3rd Edition. St Louis, Missouri, Mosby Inc, 2001

Komlosi P, Fintha A and Bell PD. Renal cell-to-cell communication via extracellular ATP. *Physiology* 20: 86-90, 2005.

Koszalka P, Ozuyaman B, Huo Y, Zernecke A, Flogel U, Braun N, Buchheiser A, Decking UK, Smith ML, Sévigny J, Gear A, Weber AA, Molojavyi A, Ding Z, Weber C, Ley K, Zimmermann H, Godecke A and Schrader J. Targeted disruption of cd73/ecto-5'-nucleotidase alters thromboregulation and augments vascular inflammatory response. *Circ Res* 95: 814-821, 2004.

Kribben A, Feldkamp T, Horbelt M, Lange B, Pietruck F, Herget-Rosenthal S, Heemann U and Philipp T. ATP protects, by way of receptor-mediated mechanisms, against hypoxia-induced injury in renal proximal tubules. *J Lab Clin Med* 141: 67-73, 2003.

Kukulski F, Levesque SA, Lavoie EG, Lecka J, Bigonnessee F, Knowles AF, Robson SC, Kirley TL, and Sévigny J. Comparative hydrolysis of P2 receptor agonists by NTPDases 1, 2, 3 and 8. *Pur Sig* 1: 193-204, 2005.

Lang MA, Preston AS, Handler JS and Forrest JN, Jr. Adenosine stimulates sodium transport in kidney A6 epithelia in culture. *Am J Physiol* 249: C330-C336, 1985.

Lazarowski ER Molecular and biological properties of P2Y receptors. Purinergic receptors and signaling (Current Topics in Membranes 54), edited by EM Schwiebert. Academic Press, 2003, p. 59-96.

Lazarowski ER and Boucher RC. UTP as an extracellular signaling molecule. *News Physiol Sci* 16: 1-5, 2001.

Lazarowski ER, Boucher RC and Harden TK. Mechanisms of release of nucleotides and integration of their action as P2X- and P2Y-receptor activating molecules. *Mol Pharmacol* 64: 785-795, 2003a.

Lazarowski ER and Harden TK. Quantitation of extracellular UTP using a sensitive enzymatic assay. *Br J Pharmacol* 127: 1272-1278, 1999.

Lazarowski ER, Homolya L, Boucher RC and Harden TK. Direct demonstration of mechanically induced release of cellular UTP and its implication for uridine nucleotide receptor activation. *J Biol Chem* 272: 24348-24354, 1997.

Lazarowski ER, Shea DA, Boucher RC and Harden TK. Release of cellular UDP-glucose as a potential extracellular signaling molecule. *Mol Pharmacol* 63: 1190-1197, 2003b.

Lazarowski ER, van Heusden C and Kreda S. Regulated release of nucleotides and UDP-sugars from the secretory pathway in epithelial cells. *J Physiol* 567P: SA23, 2005.

Le Hir M and Dubach UC. Sodium gradient-energized concentrative transport of adenosine in renal brush border vesicles. *Pflügers Arch* 401: 58-63, 1984.

Le Hir M and Kaissling B. Distribution of 5'-nucleotidase in the renal interstitium of the rat. *Cell Tissue Res* 258: 177-182, 1989.

Le Hir M and Kaissling B. Distribution and regulation of renal ecto-5'-nucleotidase: implications for physiological functions of adenosine. *Am J Physiol* 264: F377-F387, 1993.

Le KT, Babinski K and Seguela P. Central $P2X_4$ and $P2X_6$ channel subunits coassemble into a novel heteromeric ATP receptor. *J Neurosci* 18: 7152-7159, 1998.

Lehrmann H, Thomas J, Kim SJ, Jacobi C and Leipziger J. Luminal $P2Y_2$ receptor-mediated inhibition of Na^+ absorption in isolated perfused mouse CCD. *J Am Soc Nephrol* 13: 10-18, 2002.

Leipziger J. Control of epithelial transport via luminal P2 receptors. *Am J Physiol Renal Physiol* 284: F419-F432, 2003.

Lemmens R, Kupers L, Sévigny J, Beaudoin AR, Grondin G, Kittel A, Waelkens E and Vanduffel L. Purification, characterization, and localization of an ATP diphosphohydrolase in porcine kidney. *Am J Physiol Renal Physiol* 278: F978-F988, 2000.

Lote CJ. Principles of Renal Physiology, 4th Edition. Kluwer Academic Publishers, 2000.

Lu M, MacGregor GG, Wang W and Giebisch G. Extracellular ATP inhibits the small-conductance K channel on the apical membrane of the cortical collecting duct from mouse kidney. *J Gen Physiol* 116: 299-310, 2000.

Ma H and Ling BN. Luminal adenosine receptors regulate amiloride-sensitive Na^+ channels in A6 distal nephron cells. *Am J Physiol* 270: F798-F805, 1996.

Maddox DA and Brenner BM. Glomerular ultrafiltration: The kidney. 6th Edition, edited by Brenner BM and Rector FC. Philadelphia: W.B. Saunders Company, 2000, p. 340-370.

Maddox DA, Price DC and Rector FC, Jr. Effects of surgery on plasma volume and salt and water excretion in rats. *Am J Physiol* 233: F600-F606, 1977.

Mangravite LM, Badagnani I and Giacomini KM. Nucleoside transporters in the disposition and targeting of nucleoside analogs in the kidney. *Eur J Pharmacol* 479: 269-281, 2003.

Mathieson PW. The cellular basis of albuminuria. *Clin Sci* 107: 533-538, 2004.

Maurice M, Schell MJ, Lardeux B and Hubbard AL. Biosynthesis and intracellular transport of a bile canalicular plasma membrane protein: studies in vivo and in the perfused rat liver. *Hepatology* 19: 648-655, 1994.

McLean IW and Nakane PK. Periodate-lysine-paraformaldehyde fixative. A new fixation for immunoelectron microscopy. *J Histochem Cytochem* 22: 1077-1083, 1974.

McVicar AJ. Influence of surgical approach on the renal vascular effects of pressor doses of vasopressin in anaesthetised laparotomized rats. *J Physiol* 403: 26P, 1988.

Meerson NR, Delautier D, Durand-Schneider AM, Moreau A, Schilsky ML, Sternlieb I, Feldmann G and Maurice M. Identification of B10, an alkaline phosphodiesterase of the apical plasma membrane of hepatocytes and biliary cells, in rat serum: increased levels following bile duct ligation and during the development of cholangiocarcinoma. *Hepatology* 27: 563-568, 1998.

Meerson NR, Bello V, Delaunay JL, Slimane TA, Delautier D, Lenoir C, Trugnan G and Maurice M. Intracellular traffic of the ecto-nucleotide pyrophosphatase/phosphodiesterase NPP3 to the apical plasma membrane of MDCK and Caco-2 cells: apical targeting occurs in the absence of N-glycosylation. *J Cell Sci* 113: 4193-4202, 2000.

Mercer PF and Kline RL. Renal function in rats with innervated and denervated kidneys before and during sodium pentobarbital anesthesia. *Can J Physiol Pharmacol* 62: 683-688, 1984.

Mihaylova-Todorova ST, Todorov LD and Westfall DP. Enzyme kinetics and pharmacological characterization of nucleotidases released from the guinea pig isolated vas deferens during nerve stimulation: Evidence for a soluble ecto-nucleoside triphosphate diphosphohydrolases-like ATPase and a soluble ecto-5'-nucleotidase-like AMPase. *J. Pharm Exp Ther.* 302: 992-1001, 2002.

Mitchell CH, Carre DA, McGlinn AM, Stone RA and Civan MM. A release mechanism for stored ATP in ocular ciliary epithelial cells. *Proc Natl Acad Sci U S A* 95: 7174-7178, 1998.

Mo J and Fisher MJ. Uridine nucleotide-induced stimulation of gluconeogenesis in isolated rat proximal tubules. *Naunyn Schmiedebergs Arch Pharmacol* 366: 151-157, 2002.

Moe OW, Ujiie K, Star RA, Miller RT, Widell J, Alpern RJ and Henrich WL. Renin expression in renal proximal tubule. *J Clin Invest* 91: 774-779, 1993.

Morales MM, Falkenstein D and Lopes AG. The cystic fibrosis transmembrane regulator (CFTR) in the kidney. *An Acad Bras Cienc* 72: 399-406, 2000.

Moran WH, Jr., Miltenberger FW, Shuayb WA and Zimmermann B. The relationship of antidiuretic hormone secretion to surgical stress. *Surgery* 56: 99-108, 1964.

Mui KW, van Son WJ, Tiebosch AT, Van Goor H and Bakker WW. Clinical relevance of immunohistochemical staining for ecto-AMPase and ecto-ATPase in chronic allograft nephropathy (CAN). *Nephrol Dial Transplant* 18: 158-163, 2003.

Mulero JJ, Yeung G, Nelken ST and Ford JE. CD39-L4 is a secreted human apyrase, specific for the hydrolysis of nucleoside diphosphates. *J Biol Chem* 274: 20064-20067, 1999.

Navar LG, Burke TJ, Robinson RR, Clapp JR. Distal tubular feedback in the autoregulation of single nephron glomerular filtration rate. *J Clin Invest.* 53: 516-525, 1974.

Neer EJ. Heterotrimeric G proteins: organizers of transmembrane signals. *Cell* 80: 249-257, 1995.

Nishiyama A, Majid DS, Walker M, III, Miyatake A and Navar LG. Renal interstitial ATP responses to changes in arterial pressure during alterations in tubuloglomerular feedback activity. *Hypertension* 37: 753-759, 2001.

North RA. Molecular physiology of P2X receptors. *Physiol Rev* 82: 1013-1067, 2002.

Okada SF, O'Neal WK, Huang P, Nicholas RA, Ostrowski LE, Craigen WJ, Lazarowski ER and Boucher RC. Voltage-dependent anion channel-1 (VDAC-1) contributes to ATP release and cell volume regulation in murine cells. *J Gen Physiol* 124: 513-526, 2004.

Okada S, Paradiso AM, Lazarowski ER and Boucher RC. A calcium-dependent pathway in swelling-induced ATP release from airway epithelial cells. *J Physiol* 567P: C53, 2005.

Okusa MD. A_{2A} adenosine receptor: a novel therapeutic target in renal disease. *Am J Physiol Renal Physiol* 282: F10-F18, 2002.

Osswald H, Muhlbauer B and Schenk F. Adenosine mediates tubuloglomerular feedback response: an element of metabolic control of kidney function. *Kidney Int Suppl* 32: S128-S131, 1991.

Ostrom RS, Gregorian C and Insel PA. Cellular release of and response to ATP as key determinants of the set-point of signal transduction pathways. *J Biol Chem* 275: 11735-11739, 2000.

Oyama T. Endocrine responses to anaesthetic agents. *Br J Anaesth* 45: 276-281, 1973.

Oyama T, Taniguchi K, Jin T, Satone T and Kudo T. Effects of anaesthesia and surgery on plasma aldosterone concentration and renin activity in man. *Br J Anaesth* 51: 747-752, 1979.

Paller MS, Schnaith EJ and Rosenberg ME. Purinergic receptors mediate cell proliferation and enhanced recovery from renal ischemia by adenosine triphosphate. *J Lab Clin Med* 131: 174-183, 1998.

Pawelczyk T, Grden M, Rzepko R, Sakowicz M and Szutowicz A. Region-specific alterations of adenosine receptors expression level in kidney of diabetic rat. *Am J Pathol* 167: 315-325, 2005.

Pellegatti P, Falzoni S, Pinton P, Rizzuto R and Di VF. A novel recombinant plasma membrane-targeted luciferase reveals a new pathway for ATP secretion. *Mol Biol Cell* 16: 3659-3665, 2005.

Peti-Peterdi J, Fintha A, Fuson AL, Tousson A and Chow RH. Real-time imaging of renin release in vitro. *Am J Physiol Renal Physiol* 287: F329-F335, 2004.

Pettinger WA, Marchelle M and Augusto L. Renin suppression by DOC and NaCl in the rat. *Am J Physiol* 221: 1071-1074, 1971.

Pettinger WA, Tanaka K, Keeton K, Campbell WB and Brooks SN. Renin release, an artifact of anesthesia and its implications in rats. *Proc Soc Exp Biol Med* 148: 625-630, 1975.

Philbin DM and Coggins CH. Plasma vasopressin levels during cardiopulmonary bypass with and without profound haemodilution. *Can Anaesth Soc J* 25: 282-285, 1978.

Poelstra K, Baller JF, Hardonk MJ and Bakker WW. Intraglomerular thrombotic tendency and glomerular ADPase. Unilateral impairment of ADPase elicits a proaggregatory microenvironment in experimental glomerulonephritis. *Lab Invest* 64: 520-526, 1991.

Poelstra K, Heynen ER, Baller JF, Hardonk MJ and Bakker WW. Modulation of anti-Thy1 nephritis in the rat by adenine nucleotides. Evidence for an anti-inflammatory role for nucleotidases. *Lab Invest* 66: 555-563, 1992.

Radford KM, Virginio C, Surprenant A, North RA and Kawashima E. Baculovirus expression provides direct evidence for heteromeric assembly of $P2X_2$ and $P2X_3$ receptors. *J Neurosci* 17: 6529-6533, 1997.

Reddy MM, Quinton PM, Haws C, Wine JJ, Grygorczyk R, Tabcharani JA, Hanrahan JW, Gunderson KL and Kopito RR. Failure of the cystic fibrosis transmembrane conductance regulator to conduct ATP. *Science* 271: 1876-1879, 1996.

Reisin IL, Prat AG, Abraham EH, Amara JF, Gregory RJ, Ausiello DA and Cantiello HF. The cystic fibrosis transmembrane conductance regulator is a dual ATP and chloride channel. *J Biol Chem* 269: 20584-20591, 1994.

Reymann S, Florke H, Heiden M, Jakob C, Stadtmuller U, Steinacker P, Lalk VE, Pardowitz I and Thinnes FP. Further evidence for multitopological localization of mammalian porin (VDAC) in the plasmalemma forming part of a chloride channel complex affected in cystic fibrosis and encephalomyopathy. *Biochem Mol Med* 54: 75-87, 1995.

Rogenes PR and Gottschalk CW. Renal function in conscious rats with chronic unilateral renal denervation. *Am J Physiol* 242: F140-F148, 1982.

Roman RM, Lomri N, Braunstein G, Feranchak AP, Simeoni LA, Davison AK, Mechetner E, Schwiebert EM and Fitz JG . Evidence for multidrug resistance-1 P-glycoprotein-dependent regulation of cellular ATP permeability. *J Membr Biol* 183: 165-173, 2001.

Ronco P, Pollard H, Galceran M, Delauche M, Schwartz JC and Verroust P. Distribution of enkephalinase (membrane metalloendopeptidase, E.C. 3.4.24.11) in rat organs. Detection using a monoclonal antibody. *Lab Invest* 58: 210-217, 1988.

Rouse D, Leite M and Suki WN. ATP inhibits the hydrosmotic effect of AVP in rabbit CCT: evidence for a nucleotide P2u receptor. *Am J Physiol* 267: F289-F295, 1994.

Rubera I, Tauc M, Bidet M, Verheecke-Mauze C, Poujeol C, Cuiller B and Poujeol P. Extracellular ATP increases $[Ca^{2+}]_{(i)}$ in distal tubule cells. II. Activation of a Ca^{2+}-dependent Cl^- conductance. *Am J Physiol Renal Physiol* 279: F102-F111, 2000.

Sabirov RZ, Dutta AK and Okada Y. Volume-dependent ATP-conductive large-conductance anion channel as a pathway for swelling-induced ATP release. *J Gen Physiol* 118: 251-266, 2001.

Sabirov RZ and Okada Y. Wide nanoscopic pore of maxi-anion channel suits its function as an ATP-conductive pathway. *Biophys J* 87: 1672-1685, 2004.

Sands JM. Micropuncture: unlocking the secrets of renal function. *Am J Physiol Renal Physiol* 287: F866-F867, 2004.

Schnermann JB, Traynor T, Yang T, Huang YG, Oliverio MI, Coffman T and Briggs JP. Absence of tubuloglomerular feedback responses in AT_{1A} receptor-deficient mice. *Am J Physiol* 273: F315-F320, 1997.

Schulze-Lohoff E, Hugo C, Rost S, Arnold S, Gruber A, Brune B and Sterzel RB. Extracellular ATP causes apoptosis and necrosis of cultured mesangial cells via P2Z/$P2X_7$ receptors. *Am J Physiol* 275: F962-F971, 1998.

Schwiebert EM. ATP release mechanisms, ATP receptors and purinergic signalling along the nephron. *Clin Exp Pharmacol Physiol* 28: 340-350, 2001.

Schwiebert EM Extracellular nucleotide and nucleoside signaling: First principles. Purinergic receptors and signaling (Current Topics in Membranes 54), edited by EM Schwiebert. Academic Press. 2003, p. xvii – xxii.

Schwiebert EM, Wallace DP, Braunstein GM, King SR, Peti-Peterdi J, Hanaoka K, Guggino WB, Guay-Woodford LM, Bell PD, Sullivan LP, Grantham JJ and Taylor AL. Autocrine extracellular purinergic signaling in epithelial cells derived from polycystic kidneys. *Am J Physiol Renal Physiol* 282: F763-F775, 2002.

Schwiebert EM, Zsembery A and Geibel JP. Cellular mechanisms and physiology of nucleotide and nucleoside release from cells: Current knowledge, novel assays to detect purinergic agonists, and future directions. Purinergic receptors and signaling (Current Topics in Membranes 54), edited by EM Schwiebert. Academic Press. 2003, p. 31-58.

Sévigny J, Sundberg C, Braun N, Guckelberger O, Csizmadia E, Qawi I, Imai M, Zimmermann H and Robson SC. Differential catalytic properties and vascular topography of murine nucleoside triphosphate diphosphohydrolase 1 (NTPDase1) and NTPDase2 have implications for thromboregulation. *Blood* 99: 2801-2809, 2002.

Shi JD, Kukar T, Wang CY, Li QZ, Cruz PE, voodi-Semiromi A, Yang P, Gu Y, Lian W, Wu DH and She JX. Molecular cloning and characterization of a novel mammalian endo-apyrase (LALP1). *J Biol Chem* 276: 17474-17478, 2001.

Shirley DG, Bailey MA and Unwin RJ. In vivo stimulation of apical P2 receptors in collecting ducts: evidence for inhibition of sodium reabsorption. *Am J Physiol Renal Physiol* 288: F1243-F1248, 2005.

Shirley DG, Walter MF, Walter SJ, Thewles A and Lote CJ. Renal aluminium handling in the rat: a micropuncture assessment. *Clin Sci* 107: 159-165, 2004.

Shirley DG and Walter SJ. A micropuncture study of the renal response to haemorrhage in rats: assessment of the role of vasopressin. *Exp Physiol* 80: 619-630, 1995.

Shirley DG, Zewde T and Walter SJ. Renal function in normal and potassium-depleted rats before and after preparation for micropuncture experimentation. *Pflügers Arch* 416: 74-79, 1990.

Silinsky EM and Redman RS. Synchronous release of ATP and neurotransmitter within milliseconds of a motor nerve impulse in the frog. *J Physiol* 492: 815-822, 1996.

Simmons NL. Stimulation of Cl^- secretion by exogenous ATP in cultured MDCK epithelial monolayers. *Biochim Biophys Acta* 646: 231-242, 1981.

Simpson P and Forsling M. The influence of halothane on plasma vasopressin concentrations during cardiopulmonary bypass. *Br J Anaesth* 48: 265-266, 1976.

Skøtt O and Taugner R. Effects of extracellular osmolality on renin release and on the ultrastructure of the juxtaglomerular epithelioid cell granules. *Cell Tissue Res* 249: 325-329, 1987.

Smith JA, Sivaprasadarao A, Munsey TS, Bowmer CJ and Yates MS. Immunolocalisation of adenosine A_1 receptors in the rat kidney. *Biochem Pharmacol* 61: 237-244, 2001.

Solini A, Iacobini C, Ricci C, Chiozzi P, Amadio L, Pricci F, Di MU, Di VF and Pugliese G. Purinergic modulation of mesangial extracellular matrix production: role in diabetic and other glomerular diseases. *Kidney Int* 67: 875-885, 2005.

Sorensen CE and Novak I. Visualization of ATP release in pancreatic acini in response to cholinergic stimulus. Use of fluorescent probes and confocal microscopy. *J Biol Chem* 276: 32925-32932, 2001.

Srinivas SP, Mutharasan R and Fleiszig S. Shear-induced ATP release by cultured rabbit corneal epithelial cells. *Adv Exp Med Biol* 506: 677-685, 2002.

Steinhausen M. [A method for the differentiation of proximal and distal tubuli in the renal cortes in vivo and its use in determining tubular flow rates.] *Pflügers Arch* 277: 22-35, 1963.

Stout C, Goodenough DA and Paul DL. Connexins: functions without junctions. *Curr Opin Cell Biol* 16: 507-512, 2004.

Sugita M, Yue Y and Foskett JK. CFTR Cl^- channel and CFTR-associated ATP channel: distinct pores regulated by common gates. *EMBO J* 17: 898-908, 1998.

Sun D, Samuelson LC, Yang T, Huang Y, Paliege A, Saunders T, Briggs J and Schnermann J. Mediation of tubuloglomerular feedback by adenosine: evidence from mice lacking adenosine 1 receptors. *Proc Natl Acad Sci U S A* 98: 9983-9988, 2001.

Suzuki H, Ikeda K, Furukawa M and Takasaka T. P2 purinoceptor of the globular substance in the otoconial membrane of the guinea pig inner ear. *Am J Physiol* 273: C1533-C1540, 1997.

Takeda M, Yoshitomi K and Imai M. Regulation of Na^+-$3HCO_3^-$ cotransport in rabbit proximal convoluted tubule via adensosine A_1 receptor. *Am J Physiol* 265: F511-F519, 1993.

Tanaka K and Pettinger WA. Renin release and ketamine-induced cardiovascular stimulation in the rat. *J Pharmacol Exp Ther* 188: 229-233, 1974.

Ternovsky VI, Okada Y and Sabirov RZ. Sizing the pore of the volume-sensitive anion channel by differential polymer partitioning. *FEBS Lett* 576: 433-436, 2004.

Thomsen K and Olesen OV. Effect of anaesthesia and surgery on urine flow and electrolyte excretion in different rat strains. *Ren Physiol* 4: 165-172, 1981.

Thomsen K and Shirley DG. The validity of lithium clearance as an index of sodium and water delivery from the proximal tubules. *Nephron* 77: 125-138, 1997.

Thomson S, Bao D, Deng A and Vallon V. Adenosine formed by 5'-nucleotidase mediates tubuloglomerular feedback. *J Clin Invest* 106: 289-298, 2000.

Thorn JA and Jarvis SM. Adenosine transporters. *Gen Pharmacol* 27: 613-620, 1996.

Tisher CC and Madsen KM. Anatomy of the kidney. In: The kidney. 4th Edition, edited by Brenner BM and Rector FC. Philadelphia: W.B. Saunders Company, 1991, p. 3-75.

Todorov LD, Mihaylova-Todorova S, Westfall TD, Sneddon P, Kennedy C, Bjur RA and Westfall DP. Neuronal release of soluble nucleotidases and their role in neurotransmitter inactivation. *Nature* 387: 76-79, 1997.

Torres GE, Egan TM and Voigt MM. Hetero-oligomeric assembly of P2X receptor subunits. Specificities exist with regard to possible partners. *J Biol Chem* 274: 6653-6659, 1999.

Turner CM, Ramesh B, Srai SK, Burnstock G and Unwin RJ. Altered ATP-sensitive P2 receptor subtype expression in the Han:SPRD cy/+ rat, a model of autosomal dominant polycystic kidney disease. *Cells Tissues Organs* 178: 168-179, 2004.

Turner CM, Vonend O, Chan C, Burnstock G and Unwin RJ. The pattern of distribution of selected ATP-sensitive P2 receptor subtypes in normal rat kidney: an immunohistological study. *Cells Tissues Organs* 175: 105-117, 2003.

Turner CM, Ramesh B, Srai SK, Burnstock G and Unwin RJ. Altered ATP-sensitive P2 receptor subtype expression in the Han:SPRD cy/+ rat, a model of autosomal dominant polycystic kidney disease. *Cells Tissues Organs* 178: 168-179, 2004.

Udaka N, Ito T, Sato Y, Satoh S and Kanisawa M. Expression of connexin 32 gap junction protein in the kidneys during fetal development of the hamster (*Mesocricetus auratus*). *Anat Embryol (Berl)* 192: 399-406, 1995.

Unwin RJ, Bailey MA and Burnstock G. Purinergic signaling along the renal tubule: the current state of play. *News Physiol Sci* 18: 237-241, 2003.

Van der Kloot W. Loading and recycling of synaptic vesicles in the Torpedo electric organ and the vertebrate neuromuscular junction. *Prog Neurobiol* 71: 269-303, 2003.

Verhoef PA, Estacion M, Schilling W and Dubyak GR. $P2X_7$ receptor-dependent blebbing and the activation of Rho-effector kinases, caspases, and IL-1 beta release. *J Immunol* 170: 5728-5738, 2003.

Vieira VP, Rocha JB, Stefanello FM, Balz D, Morsch VM and Schetinger MR. Heparin and chondroitin sulfate inhibit adenine nucleotide hydrolysis in liver and kidney membrane enriched fractions. *Int J Biochem Cell Biol* 33: 1193-1201, 2001.

Vielhauer V, Stavrakis G and Mayadas TN. Renal cell-expressed TNF receptor 2, not receptor 1, is essential for the development of glomerulonephritis. *J Clin Invest* 115: 1199-1209, 2005.

Vitzthum H, Weiss B, Bachleitner W, Kramer BK and Kurtz A. Gene expression of adenosine receptors along the nephron. *Kidney Int* 65: 1180-1190, 2004.

Walker LA, Buscemi-Bergin M and Gellai M. Renal hemodynamics in conscious rats: effects of anesthesia, surgery, and recovery. *Am J Physiol* 245: F67-F74, 1983.

Walker LA, Gellai M and Valtin H. Renal response to pentobarbital anesthesia in rats: effect of interrupting the renin-angiotensin system. *J Pharmacol Exp Ther* 236: 721-728, 1986.

Walter SJ, Zewde T and Shirley DG. The effect of anaesthesia and standard clearance procedures on renal function in the rat. *Q J Exp Physiol* 74: 805-812, 1989.

Wang Q, Wang L, Feng YH, Li X, Zeng R and Gorodeski GI. $P2X_7$ receptor-mediated apoptosis of human cervical epithelial cells. *Am J Physiol Cell Physiol* 287: C1349-C1358, 2004.

Wang TF and Guidotti G. Golgi localization and functional expression of human uridine diphosphatase. *J Biol Chem* 273: 11392-11399, 1998.

Wang Y, Roman R, Lidofsky SD and Fitz JG. Autocrine signaling through ATP release represents a novel mechanism for cell volume regulation. *Proc Natl Acad Sci U S A* 93: 12020-12025, 1996.

Weisman GA, Wang M, Kong Q, Chorna NE, Neary JT, Sun GY, Gonzalez FA, Seye CI and Erb L. Molecular determinants of $P2Y_2$ nucleotide receptor function: implications for proliferative and inflammatory pathways in astrocytes. *Mol Neurobiol* 31: 169-183, 2005.

Westfall DP, Todorov LD and Mihaylova-Todorova ST. ATP as a cotransmitter in sympathetic nerves and its inactivation by releasable enzymes. *J Pharmacol Exp Ther* 303: 439-444, 2002.

Wilcox CS, Welch WJ, Schreiner GF and Belardinelli L. Natriuretic and diuretic actions of a highly selective adenosine A_1 receptor antagonist. *J Am Soc Nephrol* 10: 714-720, 1999.

Wildman SS, Marks J, Churchill LJ, Peppiatt CM, Chraibi A, Shirley DG, Horisberger JD, King BF and Unwin RJ. Regulatory interdependence of cloned epithelial Na^+ channels and P2X receptors. *J Am Soc Nephrol* 16: 2586-2597, 2005.

Wildman SS, Peppiatt CM, Boone M, Konings I, Marks J, Churchill LJ, Turner CM, Shirley DG and King BF. Possible role of apical P2 receptors in modulating aquaporin-2-mediated water reabsorption in the collecting duct. *Proc Physiol Soc.* April, 2006.

Wilson PD, Hovater JS, Casey CC, Fortenberry JA and Schwiebert EM. ATP release mechanisms in primary cultures of epithelia derived from the cysts of polycystic kidneys. *J Am Soc Nephrol* 10: 218-229, 1999.

Wolff SC, Qi AD, Harden TK and Nicholas RA. Polarized expression of human P2Y receptors in epithelial cells from kidney, lung, and colon. *Am J Physiol Cell Physiol* 288: C624-C632, 2005.

Woost PG, Orosz DE, Jin W, Frisa PS, Jacobberger JW, Douglas JG and Hopfer U. Immortalization and characterization of proximal tubule cells derived from kidneys of spontaneously hypertensive and normotensive rats. *Kidney Int* 50: 125-134, 1996.

Yagil C, Katni G and Yagil Y. The effects of adenosine on transepithelial resistance and sodium uptake in the inner medullary collecting duct. *Pflügers Arch* 427: 225-232, 1994.

Yamaguchi S, Umemura S, Tamura K, Iwamoto T, Nyui N, Ishigami T and Ishii M. Adenosine A_1 receptor mRNA in microdissected rat nephron segments. *Hypertension* 26: 1181-1185, 1995.

Yegutkin G, Bodin P and Burnstock G. Effect of shear stress on the release of soluble ecto-enzymes ATPase and 5'-nucleotidase along with endogenous ATP from vascular endothelial cells. *Br J Pharmacol* 129: 921-926, 2000.

Yoshioka K, Hosoda R, Kuroda Y and Nakata H. Hetero-oligomerization of adenosine A_1 receptors with $P2Y_1$ receptors in rat brains. *FEBS Lett* 531: 299-303, 2002.

Zhao Z, Kapoian T, Shepard M and Lianos EA. Adenosine-induced apoptosis in glomerular mesangial cells. *Kidney Int* 61: 1276-1285, 2002.

Zimmermann H. Extracellular metabolism of ATP and other nucleotides. *Naunyn Schmiedebergs Arch Pharmacol* 362: 299-309, 2000.

Zimmermann H. Ecto-nucleotidases. In: Handbook of Experimental Pharamacology, Purinergic and Pyrimidinergic Signalling 1, edited by MP Abbracchio and M Williams. Berlin: Springer-Verlag, 2001a, p. 209-250.

Zimmermann H. Ectonucleotidases: Some recent developments and a note on nomenclature. *Drug Development Research* 52: 44-56, 2001b.